



Sea Breeze Power Projects Inc.

A wholly owned subsidiary of Sea Breeze Power Corp.

info@SeaBreezePower.com
www.SeaBreezePower.com
Voice (604) 689-2991

Lobby Box 91, Suite 1400 - 333 Seymour Street
Vancouver, British Columbia V6B 5A6 Canada
Fax (604) 689-2990

Wind Resource Assessment Storm Hills, NWT

Report prepared by Adrian Matangi
Wind Resource Assessment - Sea Breeze Power Corp.
May 9, 2014

1 Contents

2	Executive Summary	4
2.1	Analysis Conclusions	7
2.2	Recommendations and Next Steps	11
3	Site Description	13
3.1	General Regional Geography and Climatology	13
3.2	The Data Set	20
3.3	Sensor Models and the Data Format	20
4	Quality Control (QC).....	22
4.1	Data Flagging and Inspection Process	22
4.2	Data Range Flagging	23
4.2.1	Invalidating Physically Unreasonable Measurements	23
4.2.2	Wind Speed Standard Deviation	23
4.2.3	Gust Factor.....	23
4.2.4	Wind Vane Standard Deviation.....	23
4.2.5	Wind Vane Standard Deviation II: Obvious Sensor Degradation	25
4.3	Sensor Relational Flagging	29
4.4	Data Trend Flagging	29
4.5	Icing Part I: Obvious Anemometer Stalling and Slow-Down	29
4.6	Icing Part II: Vane Stalling at Low Temperatures	31
4.7	Tower Distortion Effects & Comparative Underperformance	32
4.8	Sensor Integrity	34
5	Data Selection	35
6	Post-QC Data Recovery	37
6.1	Physical Sensor Recovery Rates	37
6.2	Derived Variable Calculable Rates.....	41
7	Preliminary Characterization of the Observed Wind Speeds.....	43
8	Wind Shear and Vertical Extrapolation.....	48
8.1	The Approach to Wind Shear	49
8.2	The Regional Terrain	50
8.3	Shear Characteristics – All Valid Data between 2012-Oct-05 and 2013-Oct-04	53
8.3.1	Shear Calculated Using Derived Variables UT & UB.....	54
8.4	Extrapolation to Hub Height	60

9	Turbulence Intensity (TI)	64
9.1	Mean and Representative TI Characteristics	65
9.2	TI at the Hub Height	68
10	Climatological Adjustment	71
10.1	The Long-Term Reference Data Set	71
10.2	Comparison of the Concurrent Target and Raw Reference Data Sets	74
10.3	Quality Control of the Reference Data	77
10.4	Measure-Correlate-Predict (MCP) Process	79
10.5	Characterizing the Long-Term Wind Climate	82
10.5.1	3-Hour Time-Step MCP Climatological Adjustment Results	86
11	Appendices.....	89
11.1	Data Recovery Rates By Month and Hour of Day	89
11.1.1	Physical Sensors (data to 2013-Dec-12)	89
11.1.2	Derived Variables (data to 2013-Dec-12)	91
11.2	Wind Roses - Validated Sensor Data	93
11.2.1	Frequency of Wind Occurrence by Sector, and Month (data to 2013-Dec-12).....	93
11.2.2	Frequency of Wind Occurrence by Sector, and Hour (data to 2013-Dec-12).....	93
11.2.3	Frequency of Wind Occurrence by Sector, Month, and Hour (data to 2013-Dec-12).....	94
11.3	Wind Shear: The Physical Sensors.....	102
11.3.1	Shear: South-Southwest-Oriented Sensors U1 & U3	102
11.3.2	Shear:North-Northeast-Oriented Sensors U2 & U4	106
11.4	Measure-Correlate-Predict Data	110

2 Executive Summary

There is growing interest in finding an alternative energy solution to displace diesel generated power in the Northwest Territories community of Inuvik. Following the Inuvik wind energy pre-feasibility analysis prepared in March, 2012, by J.P. Pinard and J.F. Maissan¹, which suggested that wind energy projects for Inuvik, NWT have the potential to be developed at a lower cost than diesel², a wind monitoring campaign was undertaken to measure the wind resource available in the region. Three specific sites (Inuvik, Caribou Hills, and Storm Hills) were considered in that pre-feasibility study, and an initial project size of 1.5-1.8 MW was suggested.

Direct measurements were taken near the Storm Hills Distant Early Warning (DEW) Line radar station, 60 km north and slightly west of Inuvik (Figure 2-1 and Figure 2-3). The meteorological measurements were taken at the New North Networks communications tower (herein referred to as the Storm Hills met mast) located about 1 km south of the DEW site and 3 km South of Environment Canada's (EC) Storm Hills climate monitoring station (Figure 2-2 and Figure 2-4).

This wind resource analysis is a comprehensive review of the data collected at the Storm Hills met mast from October 4, 2012 to March 7, 2014, and is intended to be used as guidance for any proposed wind energy development in the region. The process and rationale behind data quality control measures are documented in this report, as are analysis of the results. The assessment does not attach an uncertainty to its findings, though that would be a logical next step, required in annual energy production analysis. One caveat to the results is that data recovery rates after quality control were low for most sensors, but reasonable efforts were made to work with the available data.

¹Jean-Paul Pinard, John F. Maissan, Inuvik Wind Energy Pre-Feasibility Analysis (March 28, 2012)

² Pinard & Maissan



Figure 2-1 - Storm Hills met mast relative to Inuvik, and Environment Canada's Trail Valley climate station



Figure 2-2 - Storm Hills met mast relative to Environment Canada's Storm Hills climate station, and the Storm Hills DEW

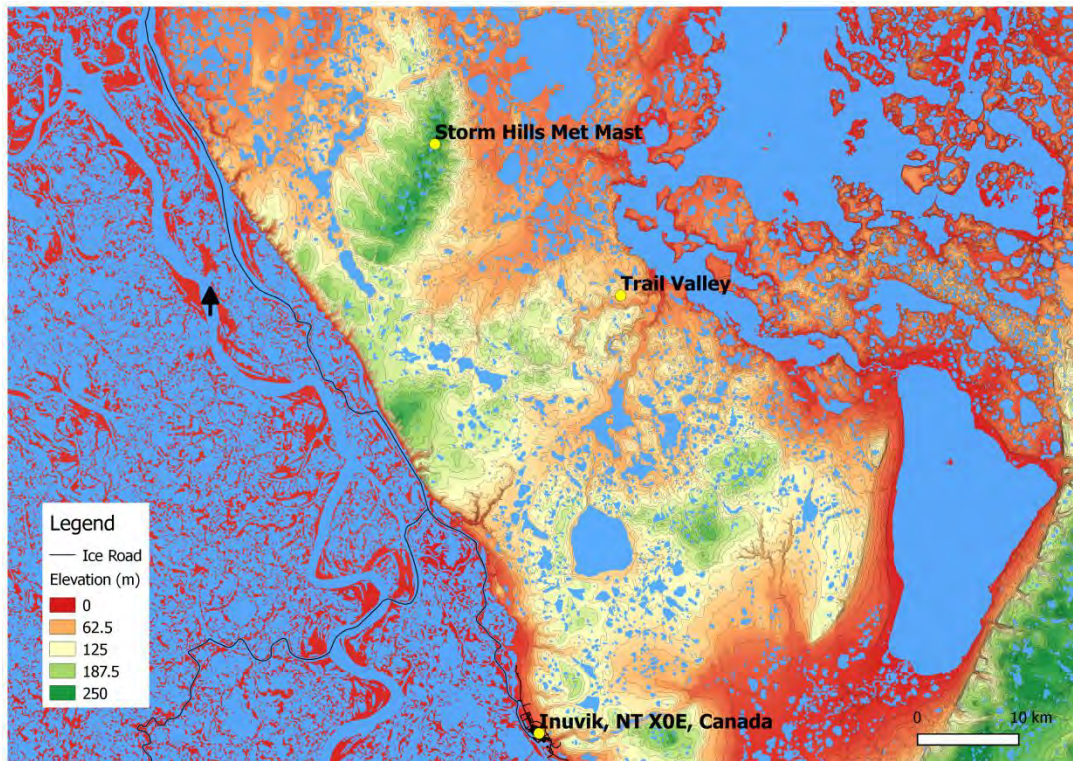


Figure 2-3 - Regional terrain map north of Inuvik, to Storm Hills

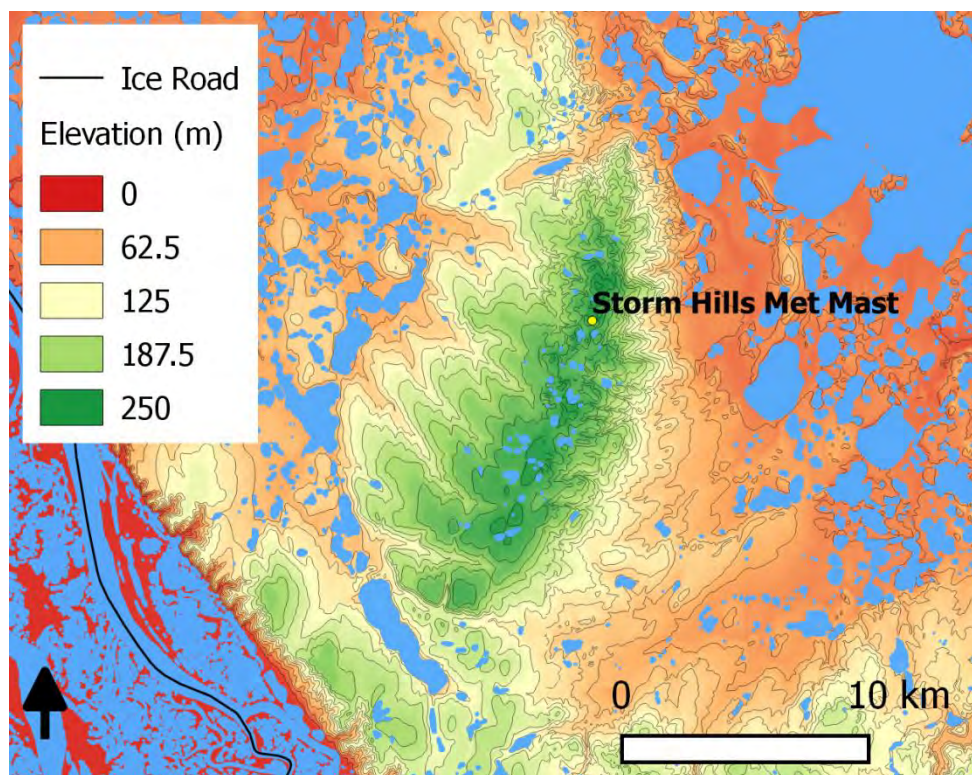


Figure 2-4 - Storm Hills terrain map

2.1 Analysis Conclusions

The Storm Hills data was recorded at 16.5 m and 39 m above ground level (a.g.l.) and so can reliably be extrapolated to at least 60 m. When correlated with a concurrent data set from the Trail Valley climate station (EC) and back-predicted using historical records, the data implies a reasonably strong 60 m wind regime with an annual average wind speed of around 7.8 m/s. This regime is well-suited to a design-class III wind turbine under the International Electrotechnical Commission (IEC) standard 61400-1. Further extrapolation to 78 m a.g.l. (the hub height of a turbine model known to be suitable for use in cold climates) predicts a mean speed of about 8.1 m/s, and is also suitable to design-class III machines.

More importantly, because of the relatively low mean air temperature and low elevation (256 m) at the site, air density is high and so the 50 m a.g.l. mean wind power density is also high, at around 520 W/m². This is generally categorized as class 5 (out of 7), which reflects an excellent wind resource³.

Tower coordinates	68° 53.013' N, 133° 56.893' W
Tower base elevation	256 m
Anemometer measurement heights	39 m, 16.5 m
Measurement period	October 4, 2012 - March 7, 2014
Data recovery rate at 39 m	51.4%
Observed annual wind speed at 39 m (measured)	7.3 m/s
Observed Weibull <i>k</i> (shape) parameter at 39 m	2.05
Observed Weibull <i>c</i> (scale) parameter at 39 m	8.3 m/s
Predicted annual wind speed at 60 m (long-term)	~7.8 m/s
Weibull <i>k</i> parameter at 60 m	2.19
Weibull <i>c</i> parameter at 60 m	8.7 m/s
Predicted annual wind speed at 78 m (long-term)	~8.1 m/s
Weibull <i>k</i> parameter at 78 m	2.17
Weibull <i>c</i> parameter at 78 m	9.1 m/s
Mean air density	1.314 kg/m ³
Mean turbulence intensity at 15 m/s	0.061
IEC 3rd edition turbine turbulence design class	C (site has low turbulence)
Mean surface roughness length	0.0001 m
Mean power law shear exponent	0.08
Wind power density at 39 m (measured)	505 W/m ²
Wind power density at 60 m (long-term)	~520 W/m ²
Wind power density at 78 m (long-term)	~580 W/m ²
Wind power class (based on 50m a.g.l.)	5 (of 7 - excellent)
IEC 3rd edition turbine design class	III

Figure 2-5 - Statistics from the measured data, and the long-term prediction using a correlation with Trail Valley (EC) data

Wind shear, the change in wind speed with height a.g.l., is generally very low. This is as would be expected for a site with few surface roughness elements (such as tall trees or buildings) and a winter snow pack; the mean power law shear exponent was found to be around 0.08 (a typical value would be 0.2). Low shear implies that the selection of a suitable wind turbine may not require the developer to accept the costs associated with purchasing and installing machines with taller hub heights.

The typical turbulence intensity (TI) at the site is low, with mean TI of 0.061 under 15 m/s wind conditions (TI-15), while the 90th percentile, representative TI-15 is 0.084. These characteristics describe a turbulence regime suitable to a turbine of IEC 61400-1 turbulence design class C (or A, or B).

³<http://rredc.nrel.gov/wind/pubs/atlas/tables/A-8T.html>

The wind regime is directionally bi-polar (Figure 2-6), with winds most frequently coming from the west-northwest and the east, with a slight southerly component.

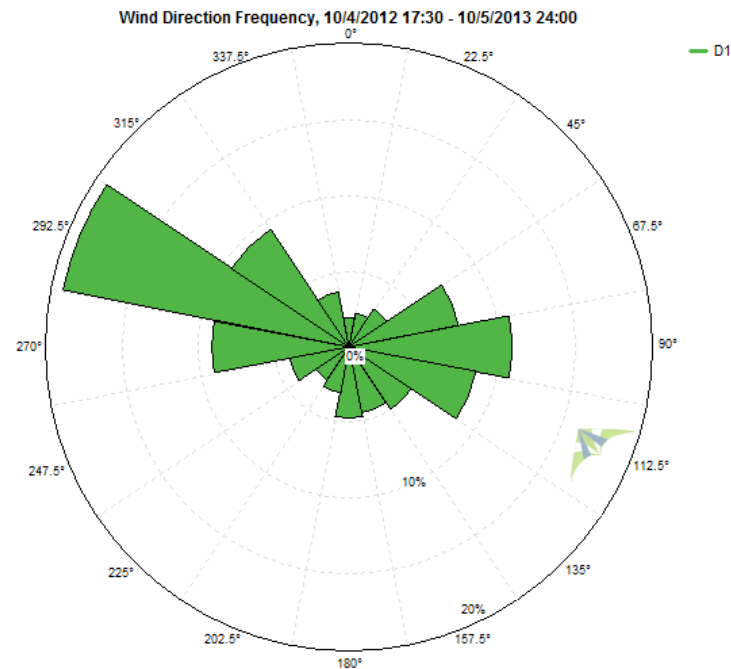


Figure 2-6 - Storm Hills measured data wind frequency rose - 1 full year

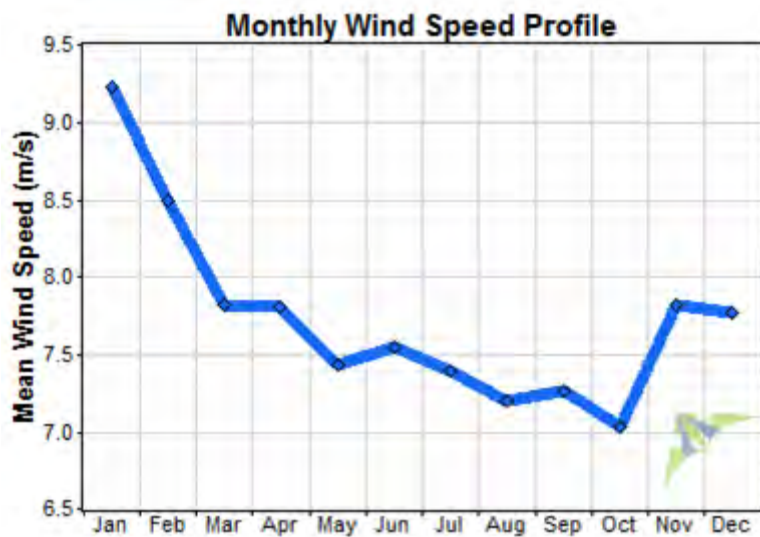


Figure 2-7 - Long term annual wind speed profile is winter-peaking

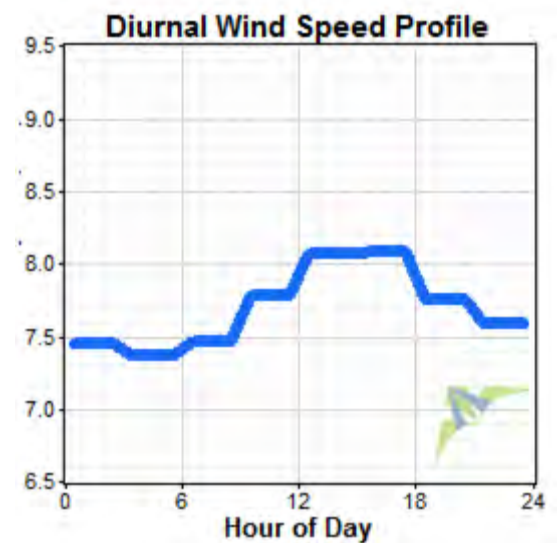


Figure 2-8 - Long term diurnal wind speed profile is afternoon-peaking

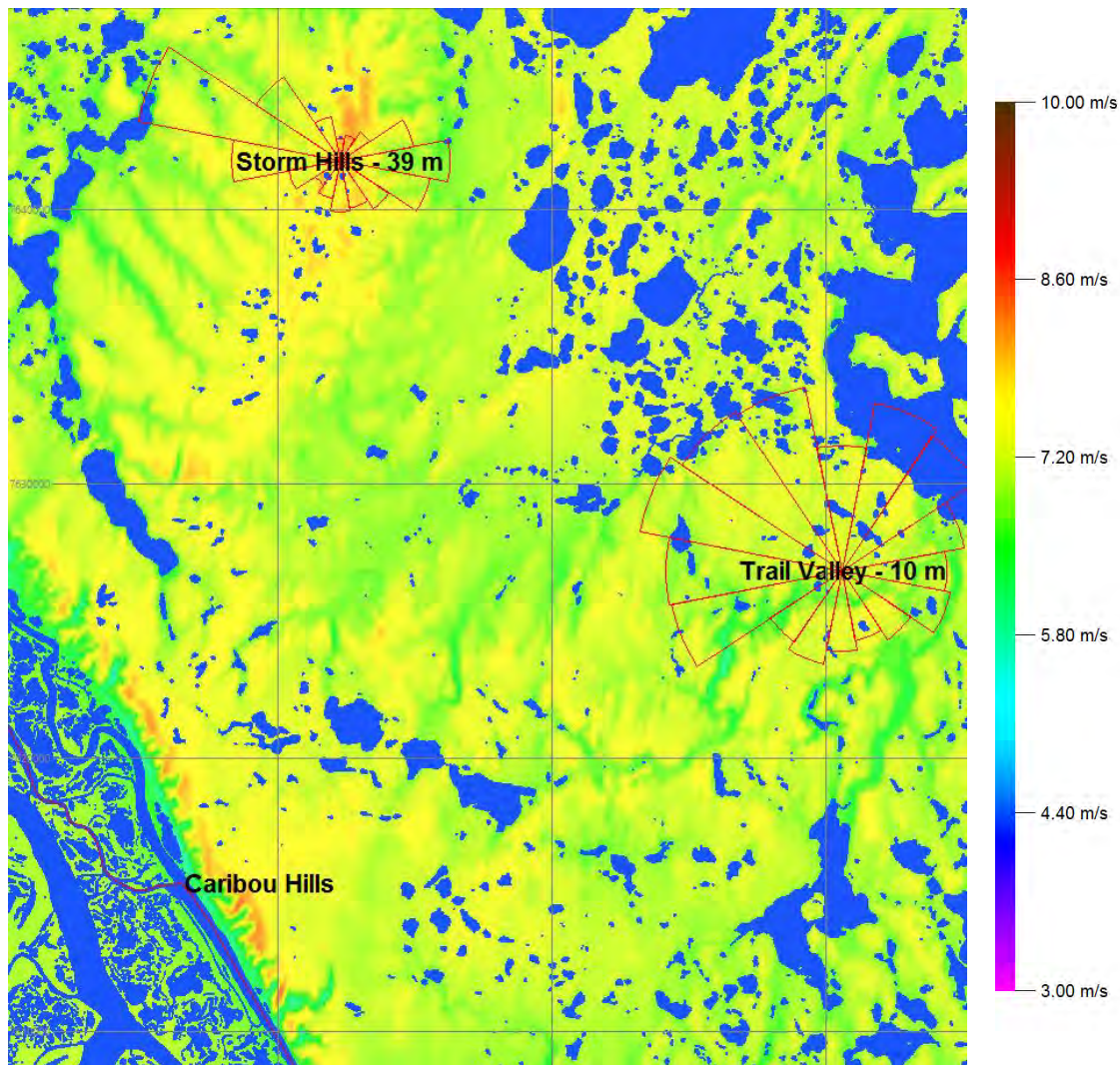


Figure 2-9 - Modelled regional wind resource map at 78 m a.g.l. (likely turbine hub height). Grid lines represent 10 km.

The wind map in Figure 2-9 was generated in Openwind using a simple wind flow model called NOABL. The model is driven by a long-term data set at Storm Hills which was created by correlation with data from Environment Canada's Trail Valley climate station (10 m a.g.l.). The "wind roses" represent the frequency of wind events by direction sector (16 sectors in all). The EC Trail Valley site is only at 10 m a.g.l., which is close to the ground and so the wind frequency rose in Figure 2-9 shows heavy influence from frictional drag near the surface, particularly when wind speeds are low. The roses in Figure 2-10 compare concurrent-period data collected at Storm Hills and Trail Valley, but only when wind speeds exceed 5 m/s at the respective locations. The wind roses are much more similar (radial scale is up to 35% frequency of occurrence).

The wind map is generated on a larger scale than would normally be done using a simple flow model driven by a single met mast, but it shows that there may be sufficient wind resource along the ridges at Caribou Hills to pursue further wind resource assessment there. Caribou Hills may also be more accessible than Storm Hills, from a project construction perspective.

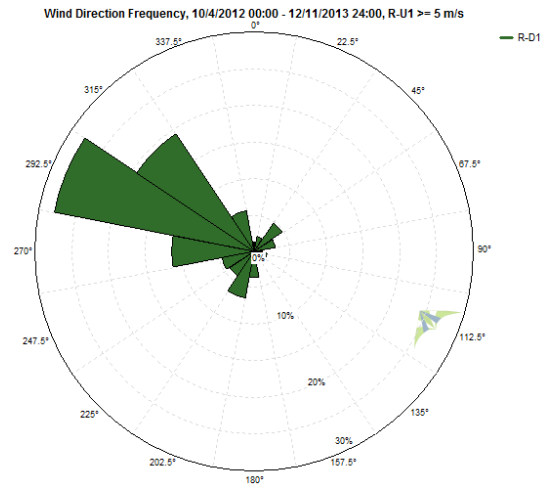
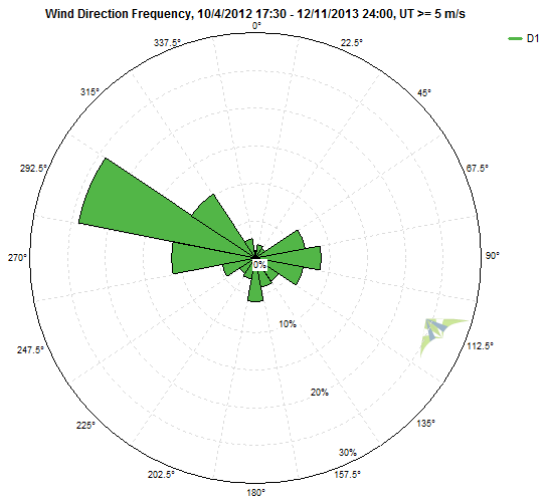


Figure 2-10 - Wind roses at Storm Hills and Trail Valley when wind speeds exceed 5 m/s (just above turbine cut-in)

2.2 Recommendations and Next Steps

Suggestions for any further wind resource campaign at the Storm Hills site include the following (refer to the bulk of the assessment report for context):

- the wind direction vane needs to be replaced as it is damaged - at present all new data is unusable without corresponding direction data;
- consider mounting at least one heated sensor on the tower at the 39 m level to mitigate data losses due to icing;
- boom angles could be changed so that co-levelled sensors are not directly opposite one another (this helps with quality control procedures);
- boom lengths should be extended significantly so as to remove tower distortion affects on the wind measured (this is critical because there can be unnecessary data loss as a result of booms being too short)

It is the author's opinion that continuing to take measurements at Storm Hills is a good idea so as to provide a longer-term high-quality data set for future reference; the use of 10 m a.g.l. Environment Canada data sets as references is not ideal. The recommendations bulleted above will add cost to the existing measurement campaign, but as a reasonable resource has been indicated, it may prove worthwhile. The addition of a new wind direction vane is absolutely critical to maintain the present site.

Although erecting a new met tower will be a significant expense, it may be worthwhile from a project-cost perspective to pursue a concurrent measurement campaign at Caribou Hills (considering little has been spent on apparatus to-date). A sturdy 50 m winter-rated met tower could be installed in a region free from tall trees and outfitted with a robust wind resource assessment tower layout:

- three sensor levels (20 m, 35 m, 50 m), with boom angles between 45° and 60° about 290°;
- six cup anemometers, of which at least one is class 1, and one is heated (requiring a power system);
- three wind direction vanes, one at each sensor level, of which one is an RM Young Alpine model;
- a pressure sensor;
- a relative humidity sensor;
- two temperature sensors (top and bottom sensor levels);
- and a solar radiation sensor.

The purpose of taking solar and humidity data is to provide information streams to assist turbine manufacturers in anticipating the likelihood and persistence of ice build-up on their machines; this affects annual energy production analyses. The purpose of a pressure sensor is to better track air density and therefore better compute wind power density, and the purpose of having two temperature sensors is to better understand anemometer icing events, as well as to interpret the any effects owing to summer-time thermal instability.

Wind turbines and cup anemometers are very different things, but there is enough icing and cold temperature data recorded at the Storm Hills met mast to warrant the consideration of heated blades as a desirable characteristic for any turbine chosen to be installed in the area around Inuvik. Regardless, the turbine manufacturers should be engaged to provide information on their most robust cold-weather packages, and a qualified engineering firm should be consulted to recommend one of the options.

Going forward, high-quality long-term data sets for correlation purposes can be purchased from a number of industry consulting groups; again, the Environment Canada data set can mislead correlation analyses because of the influence of the ground on their measurements (including temperature).

3 Site Description

3.1 General Regional Geography and Climatology

The climate in this region is generally classified as subarctic. According to the 1981-2010 climate data measured at the Environment Canada climate station Inuvik A (Climate ID 2202570, 66° 18'15.000" N, 133° 28'58.000" W), the coldest daily average air temperature was -29.9° C in January and the warmest daily average was 14.1° C in July. From 1981-2010, the region received 158.6 cm of snowfall on average annually, with heaviest snows in October (30.1 cm). August is the rainiest month with 36.4 mm of precipitation, on average.

From 1981-2010, measured wind speeds at 10 m above ground level at the Inuvik weather station were highest during summer (May-August) and the highest monthly average was in June (3.4 m/s). Lowest average monthly wind speeds were during the winter (December-January, 2.0 m/s average). Throughout the year, wind directions were most frequently from the east, and the annual average wind speed was 2.6 m/s. These statistics generally don't match closely with measurements taken at the Storm Hills site.

The Canadian Wind Energy Atlas, based on results from the Environment Canada (EC) Wind Energy Simulation Toolkit (WEST) suggests that wind speeds in the region might resemble those in Figure 3-1⁴.

Numerical Values at 50m

Latitude = 68.893, longitude = -133.968

Period	Mean Wind Speed	Mean Wind Energy	Weibull shape parameter (k)	Weibull scale parameter (A)
Annual	6.23 m/s	231.13 W/m ²	2.00	7.04 m/s
Winter (DJF)	6.67 m/s	276.50 W/m ²	2.05	7.53 m/s
Spring (MAM)	5.80 m/s	181.63 W/m ²	2.06	6.55 m/s
Summer (JJA)	5.28 m/s	133.75 W/m ²	2.10	5.96 m/s
Fall (SON)	6.14 m/s	215.63 W/m ²	2.05	6.93 m/s

Figure 3-1 – Canadian Wind Energy Atlas: WEST model predicted wind regime near Storm Hills

The following Google Earth imagery has been provided to give a general physical overview of the Storm Hills wind project site.

⁴<http://www.windatlas.ca/en/index.php>



Figure 3-2 - Google Earth Imagery of Storm Hills location in North America

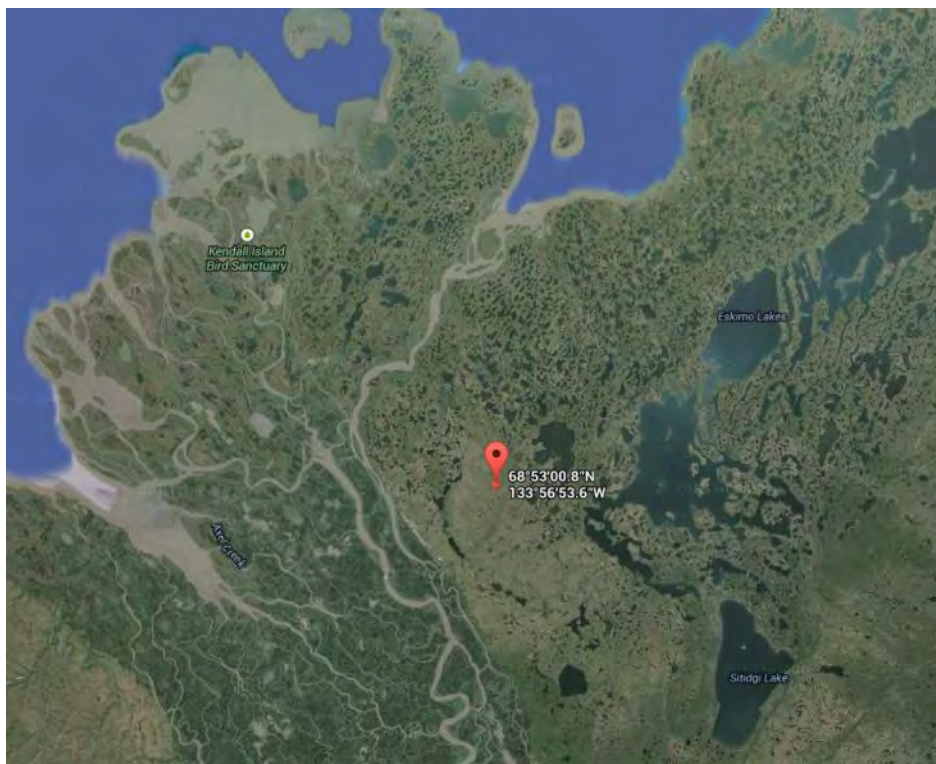


Figure 3-3 - Storm Hills location in northern Northwest Territories

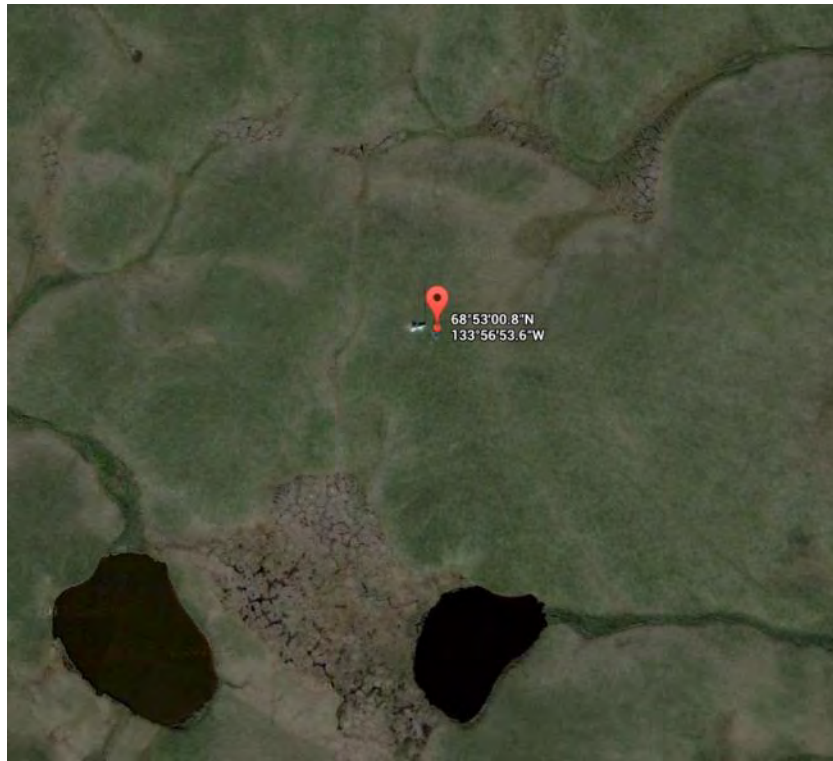


Figure 3-4 - Google Earth satellite image of Storm Hills site from above

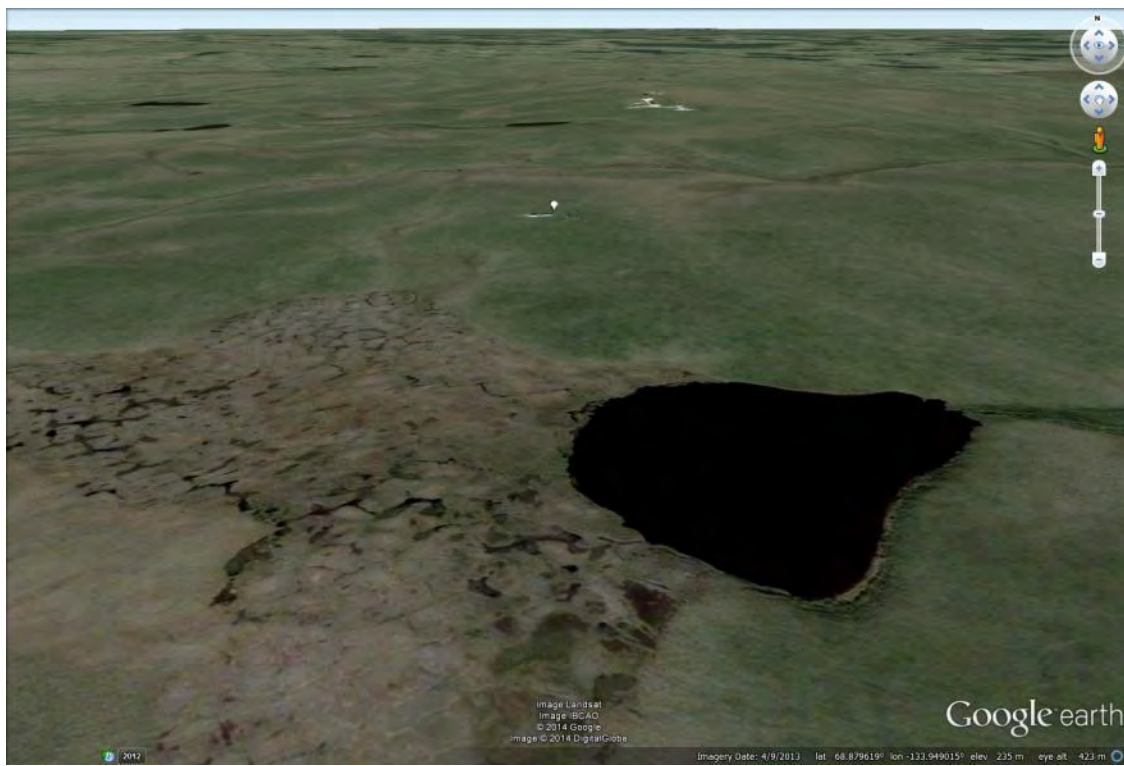


Figure 3-5 - Google Earth image of the site, looking north



Figure 3-6 - Google Earth image of the site, looking east



Figure 3-7 - Google Earth image of the site, looking south



Figure 3-8 - Google Earth image of the site, looking west

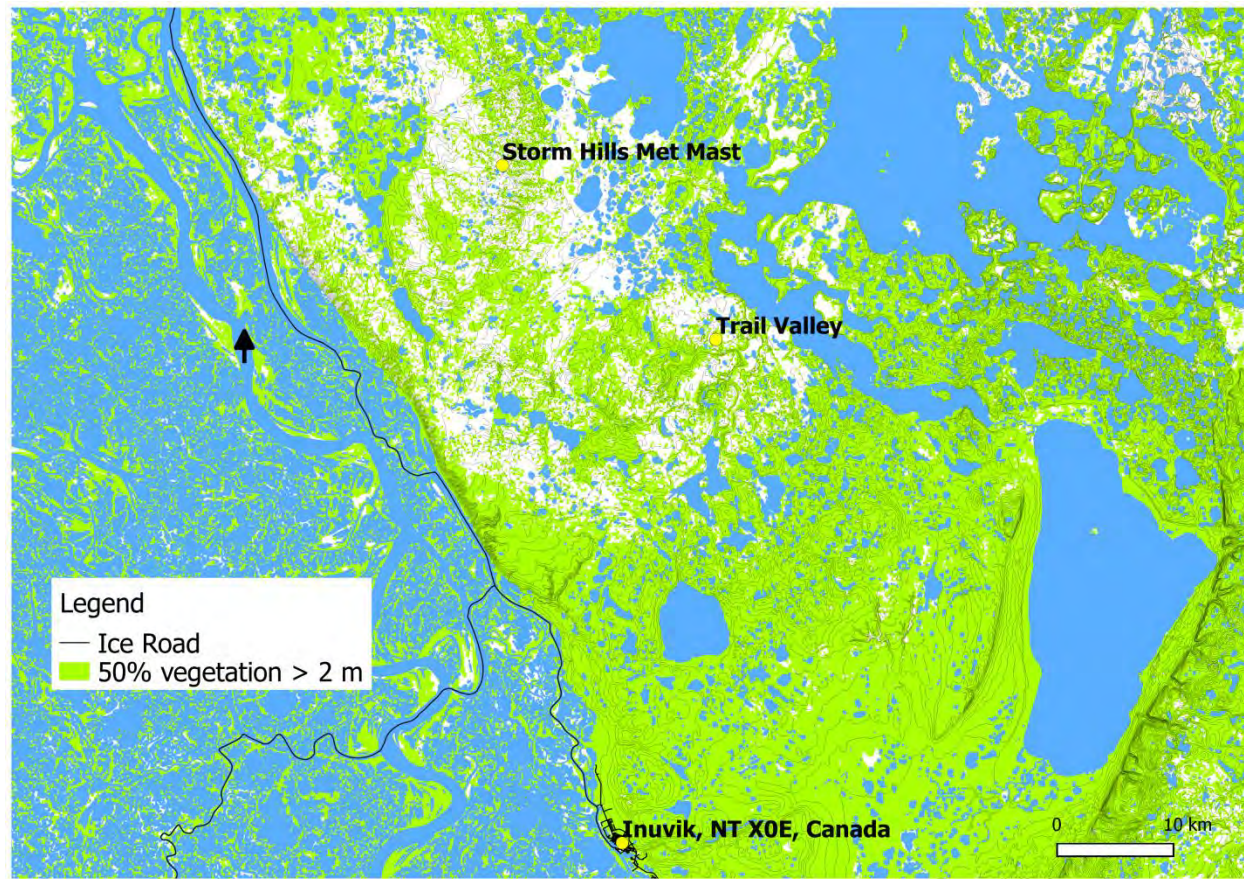


Figure 3-9 - Green indicates where at least 50% of the vegetation is taller than 2 m in height - Canadian Vector Database



Figure 3-10 - The Storm Hills meteorological mast at the New North Networks communications station, looking southeast

3.2 The Data Set

The raw logger data was scaled and interpreted as per the instrument and tower layout specifications described in the site installation log, and by using the NRG Symphonie Data Retriever 7.03.15 software. As with any field data, the sensor measurements inevitably contained faulty or questionable readings that required special scrutiny to determine what was to be filtered out prior to the final site resource analysis.

A number of industry-standard data flagging routines⁵ were modified to suit the site and applied to the data using the Windographer 3.2.5 analysis software. Final data removal was completed by visual inspection and interpretation by the analyst, taking into consideration the flagging. Reasonable leniency was given in some cases to retain useful data recovery rates without drastically affecting the final analysis.

3.3 Sensor Models and the Data Format

The meteorological tower at Storm Hills is a lattice mast with a 2' distance between the legs. It is equipped with anemometer pairs at two altitudes, 39m and 16.5 m, as well as a vane at 39 m and a temperature sensor 2 m off the ground.

39m up the tower is one NRG Class-1 cup anemometer mounted on a boom, 40" away from the nearest lattice leg. The mounting boom is pointing north-northeast, away from the tower. Pairing that cup is an R.M. Young Alpine Wind Monitor horizontal-propeller anemometer. The propeller sensor is also the wind direction vane and is mounted 40" from a mast leg, on the same boom, which is oriented towards the south-southwest with the vane dead-band aligned with true north. Figure 3-10 is a view looking southeast towards the Storm Hills station, with the building to the west of the tower and the booms set so that the instruments are relatively clear of the existing communications equipment.

There are two NRG Class-1 cup anemometers at 16.5 m with similar bearings and boom mountings to the two sensors at 39 m.

Variable	Altitude (m)	Sensor Type	Model	Boom Orientation	Boom Length (")	Response Offset	Response Slope (scale factor)
U1	39	propeller anemometer	R.M.Young Alpine	~SSW	40	0 m/s cut-in	0.098 m/s/Hz
U2	39	cup anemometer	NRG Class 1	~NNE	40	0.2 m/s cut-in	0.766 m/s/Hz
U3	16.5	cup anemometer	NRG Class 1	~SSW	40	0.18 m/s cut-in	0.768 m/s/Hz
U4	16.5	cup anemometer	NRG Class 1	~NNE	40	0.21 m/s cut-in	0.766 m/s/Hz
D1	39	wind vane	R.M. Young Alpine	~SSW	40	0° (true) dead-band alignment	0.351
T1	2	temperature sensor	NRG 110S	-	-	-86.383 °C	0.136

**Table 1– Summary of the sensors and variable naming convention;
The R.M. Young Alpine Wind Monitor vane has a response threshold of 1.1 m/s**

The data was collected in a raw format by an NRG Symphonie logger, which samples sensor signals once every two seconds and records statistical values (average, standard deviation, maximum and minimum) over ten-minute time steps.

⁵ AWS Truepower, *Wind Resource Assessment Handbook: Final report* (Albany, New York, USA: State of New York Energy Research and Development Authority, 2010) Section 9 – Data Validation, 9-1 to 9-11

This averaging period is the industry standard as it minimizes remote data storage requirements while maximizing relevant data collection within the boundary between mesoscale (1 to 100 km) and microscale (< 1 km) weather events. Mesoscale meteorological phenomena, like cyclones, pass over minutes to days, while microscale phenomena, like turbulence or gusts, last seconds to minutes⁶. This averaging period represents part of an energy gap in the standard near-to-ground wind intensity spectrum over which speeds can be studied statistically because of the low prevalence of noise due to atmospheric eddies⁷. Those eddies which do arise on this time scale are the larger of the micro-scale turbulent ones which are important because they impact wind turbine performance and can cause gradual wear and tear on the machines. 10 minutes is also a time scale relevant to energy off-takers like power utilities.

The recorded variables in this analysis are referred to as: U_i , U_i -SD, U_i -max, and U_i -min for the individual anemometers; D1 and D1-SD for the direction vane; and T1 for the temperature sensor.

The full data collection period was 2012-Oct-04 to 2014-Mar-07.

⁶Janardan S. Rohatgi & Vaughn Nelson, *Wind Characteristics: An Analysis For The Generation Of Wind Power* (Canyon, Texas, USA: Alternative Energy Institute, West Texas A&M University, 1994) 11

⁷Roland B. Stull, *An Introduction to Boundary Layer Meteorology* (Dordrecht, The Netherlands: Kluwer Academic Publishers, 1988) 32-33

4 Quality Control (QC)

4.1 Data Flagging and Inspection Process

The following is a generalized description of the process used to exclude data or flag it for special scrutiny.

1. Apply data range flags⁸:

Data records outside the reasonable site-specific ranges for each sensor variable and their important derivatives were flagged for later scrutiny.

2. Apply sensor relational flags⁹:

A sequence of standard criteria examining the relationships between the different sensors was used to flag data for later scrutiny.

3. Apply data trend flags¹⁰:

A series of standard criteria examining how the data changed over given periods were used to flag for later scrutiny.

4. Remove obvious icing events:

- a. Anemometer data revealing obvious stalling or slow-down due to icing was excluded using screening tests and manual examination of the data as a time-series.
- b. Vane data revealing obvious stalling due to icing was excluded using screening tests and manual examination of the data as a time-series. All corresponding anemometer data was also removed.

5. Examine tower distortion:

- a. Ratios and differences between co-levelled anemometer data were plotted against wind direction to infer the normal wind speed distortion characteristics of the met mast.
- b. Remove tower shading:

Data was excluded when the wind direction likely placed anemometers within the met mast's wind shadow. Slower co-levelled anemometer data was also discarded.

- c. Flag acceleration zones:

Data was flagged when the wind direction implied anemometers might have experienced higher-than free-stream wind speeds as a result of the presence of the met mast.

6. Detect sensor underperformance:

All flags from steps 1-3 and 5c were used to identify and manually exclude data from underperforming sensors. This was done by visual inspection of the time-series data.

⁸ AWS Truepower, *Wind Resource Assessment Handbook: Final report*, 9-4

⁹ AWS Truepower, *Wind Resource Assessment Handbook: Final report*, 9-5

¹⁰ AWS Truepower, *Wind Resource Assessment Handbook: Final report*, 9-5

4.2 Data Range Flagging

4.2.1 Invalidating Physically Unreasonable Measurements

Wind speed U_i and maximum 2-second gust U_{i-max} data for all anemometers fell within the reasonable ranges. The U_i data was all between the sensor offset (cut-in wind speed) and 30 m/s. All 2-second gusts fell within the range spanning from the offsets to 35 m/s.

Wind direction $D1$ data were within the 0° to 359° range, as referenced to true north (the dead-band alignment).

Temperature $T1$ data were within the range -37.4°C to 30.1°C , which is reasonable for an arctic environment over the course of a full year or longer.

4.2.2 Wind Speed Standard Deviation

The standard deviation of the wind speed U_i -SD of a 10-minute anemometer data step was flagged if it exceeded 3.0 m/s. These events typically happen when an anemometer is freezing or thawing at the periphery of an icing event, or during events of severe underperformance.

4.2.3 Gust Factor

The ratio of the maximum recorded 2-second wind gust to the 10-minute average wind speed is the gust factor¹¹:

$$GF = U_{\max,i}/U_i$$

Anemometer data segments containing time steps with gust factors exceeding 2.5 were flagged¹². Time steps reporting extreme gust factors often occur at the beginning or end of anemometer icing periods.

4.2.4 Wind Vane Standard Deviation

It was important to determine the normal performance characteristics for the wind vane at the site. The standard deviation of wind direction $D1$ -SD should fall within reasonable ranges, but those ranges are site-specific. When $D1$ -SD was very low there was a good chance the vane was partly frozen in place or was not responding correctly because the wind speeds were low, and perhaps below the sensor threshold; the R.M. Young Alpine Wind Monitor vane has a threshold sensitivity of 1.1 m/s. Stalling due to icing is dealt with later, so this section deals with excessively high $D1$ -SD values.

Elevated $D1$ -SD can indicate the passage of a front, where changes in wind direction and temperature can be sudden and genuinely erratic. It can also be indicative of a lull, where low wind speeds fail to meet the vane threshold, producing an intermittent response to the wind direction. High $D1$ -SD is indicative of unusually erratic behaviour in a wind vane if it occurs for an extended period of time. Erratic vane behaviour can have a number of different causes, which may include damage or icing-related obstruction to the sensor. Typically vane standard deviation values require scrutiny when they exceed 75° in a single time step¹³, though that measure is site specific.

¹¹Windographer 3.2.5 documentation: Gust Factor

¹²AWS Truepower, *Wind Resource Assessment Handbook: Final report*, section 9-5

¹³AWS Truepower, *Wind Resource Assessment Handbook: Final report*, section 9-4

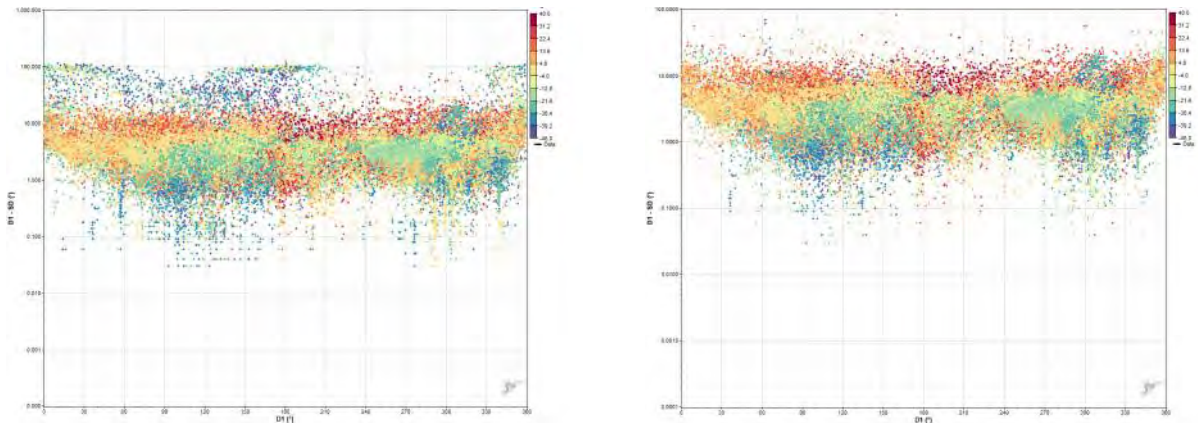


Figure 4-1- log (D1-SD) vs. D1 before and after full quality control
Coloured by T1

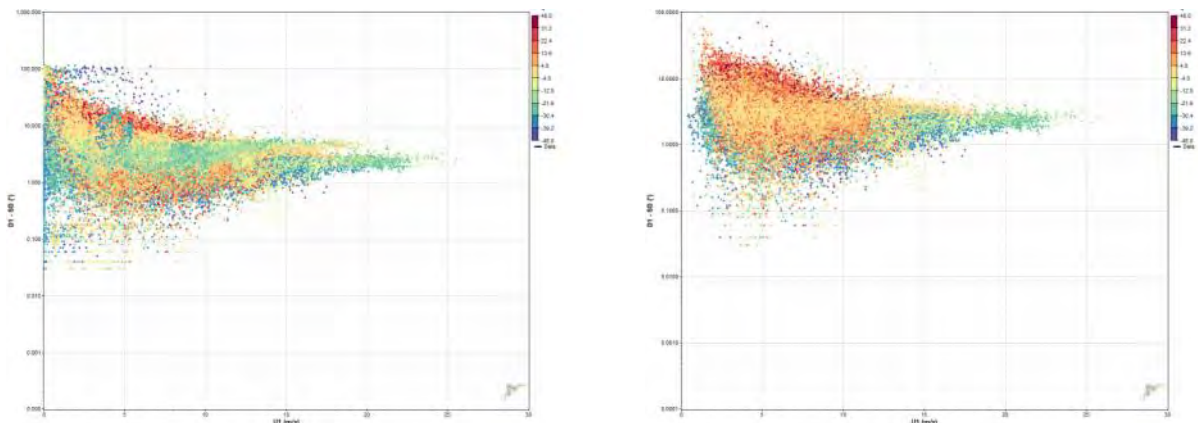


Figure 4-2 - log (D1-SD) vs. U1 before and after full quality control
Coloured by T1

For this site D1-SD data was initially flagged based on the left-hand frames of Figure 4-1 and Figure 4-2, then eliminated by visual inspection of the time-series. Vane data was eliminated when reporting extreme D1-SD if it was felt that the actual wind direction could not reasonably be known. All anemometer data was also eliminated in these events under the assumption that the R.M. Young vane was the most robust sensor on the tower. Inspection of the data set confirmed this was not too conservative an approach.

Figure 4-3 shows a period during which the wind vane was erratic and U1 was experiencing an icing event.

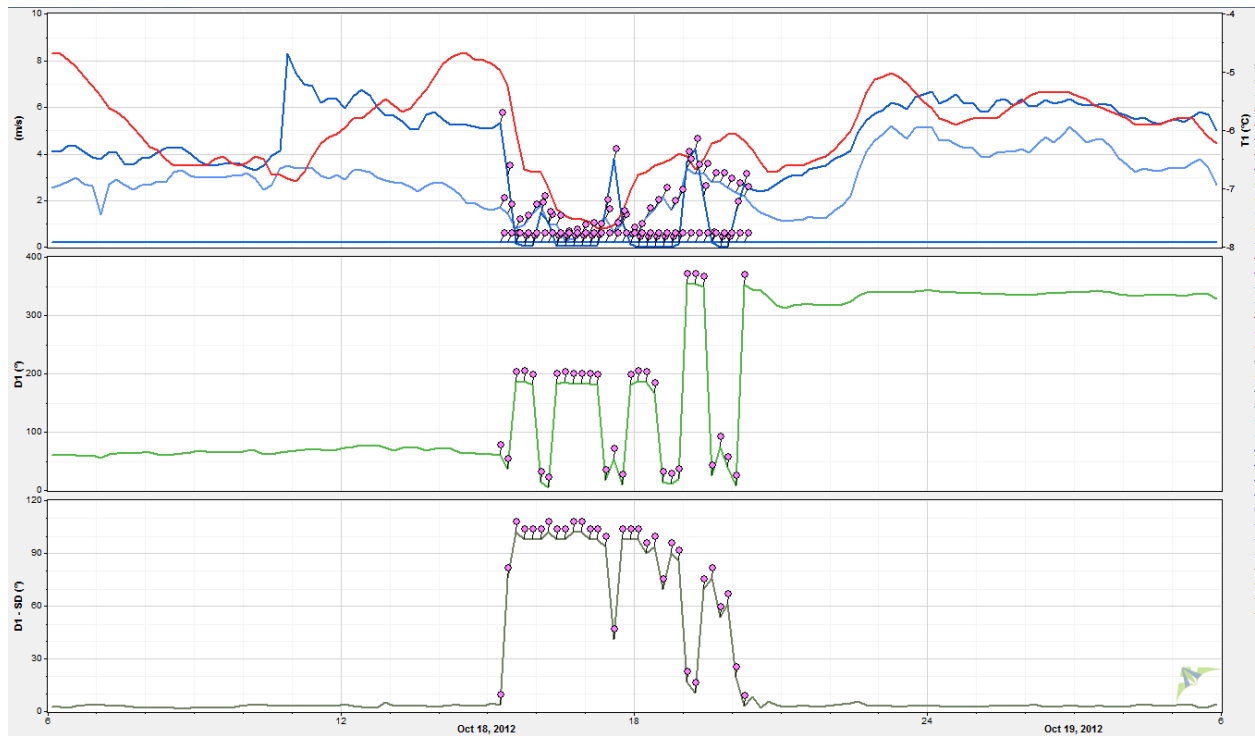


Figure 4-3 - High D1-SD and extended erratic vane behaviour with anemometers also flagged

4.2.5 Wind Vane Standard Deviation II: Obvious Sensor Degradation

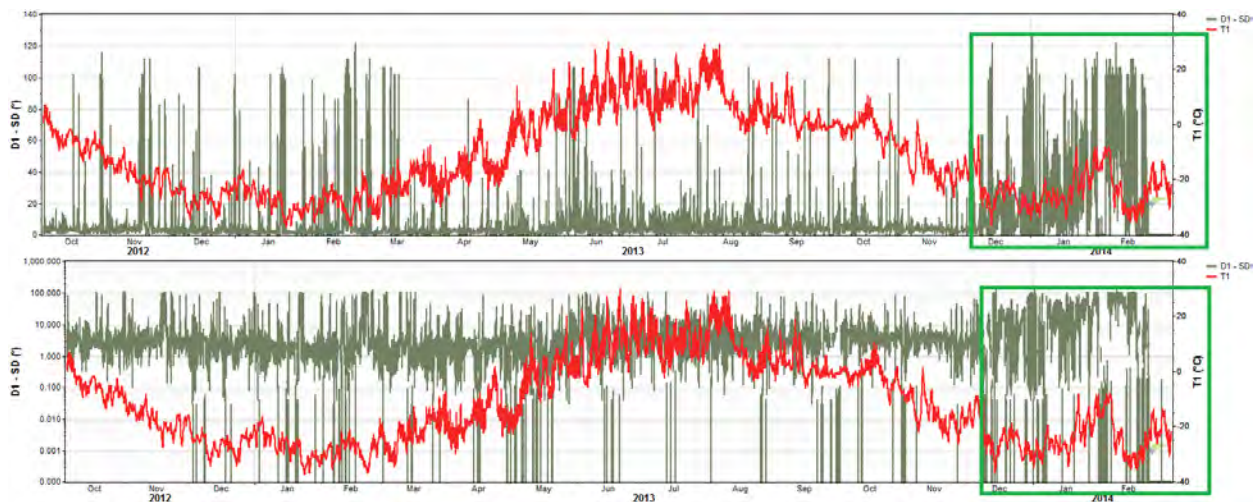


Figure 4-4 - D1-SD above, log(D1-SD) below, with T1, all prior to quality control
Erratic D1-SD time steps roughly marked in green

On 2013-Dec-12 anemometer U1 was stalled in an icing event. From that point until the end of the data set on 2014-Dec-12, the wind vane D1 behaved in an abnormal and erratic fashion. When compared to the same time period a year earlier, and to the majority of the data set, the vane was biased northwards and behaved erratically, frequently reporting excessively high D1-SD values when not pointing northwards.

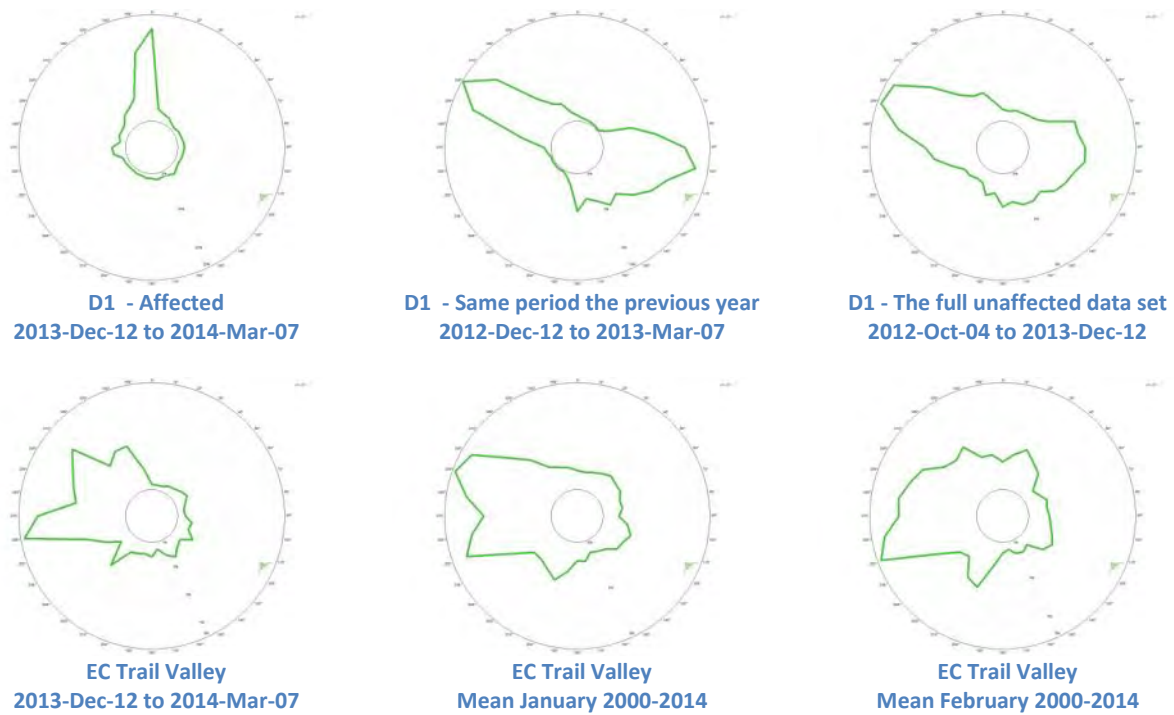


Figure 4-5 - Wind direction frequency of occurrence prior to quality control

A northerly wind regime between December and March is inconsistent with both historical data at the tower and with reference data from a nearby Environment Canada station at Trail Valley, where there is a sonic anemometer mounted 10 m above the ground. Figure 4-5 illustrates the northerly bias issue comparatively, using wind frequency roses over time periods of interest.

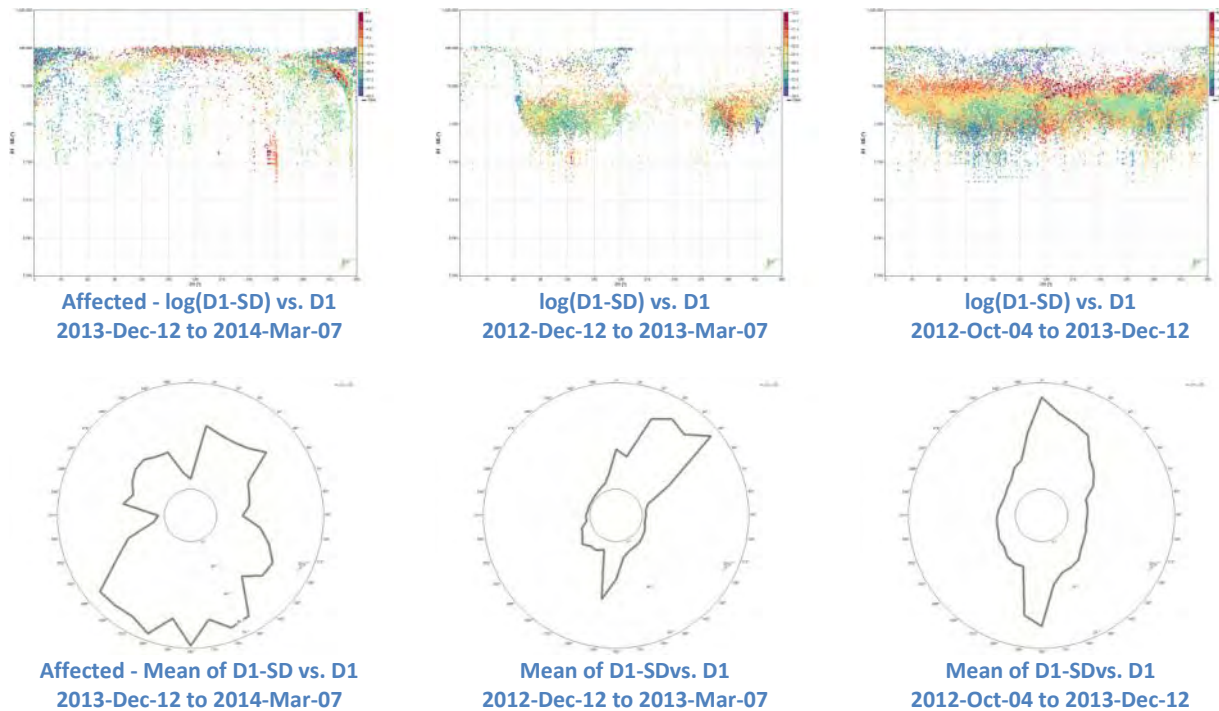


Figure 4-6 - Prior to quality control
 Left Panels: $D1-SD$ frequently high, especially when non-northerly
 Center Panels: $D1-SD$ same period the previous year
 Right Panels: $D1-SD$ the full unaffected data set

After 2013-Dec-12, $D1-SD$ was reported too frequently outside the reasonable range of values. Earlier data showed the value was consistently between 0.5° and 10° for a typical time step. Figure 4-6 shows how $D1-SD$ varied across relevant time periods and the top-left panel demonstrates that after 2013-Dec-12 the vane response characteristics were unusually erratic and biased northwards. The comparison is made to both: the same period one year earlier (center panels); and to all of the prior data (right panels). The vane data suggests that abnormal vane behaviour may have begun to occur as early as 2013-Dec-05.

All the sensor data after 22:40 on 2013-Dec-12 was marked as invalid and excluded from the analysis, because without vane data a full quality control regime could not be implemented.



Figure 4-7 - After 2013-Dec-12, while $D1$ was erratic, $U1$ consistently underperformed and was flagged invalid

The issue with the R.M. Young anemometer may have extended further back in the data set. U1 began performing poorly when compared to U2 after coming out of a 24-hour period of icing-related slow-down on 2013-Sep-24. It was also underperforming when compared to U3, which was directly below it, even while U3 performed acceptably against U4. For the majority of the affected time period the winds were from a direction in which U2 was expected to experience tower-induced flow acceleration (from the free-stream wind speed). This complicated the analysis; however examination of the time-series data suggested that U1 was indeed underperforming against U2 in an uncharacteristic fashion which was more than just a result of tower distortion. See Figure 4-8 and Figure 4-9.

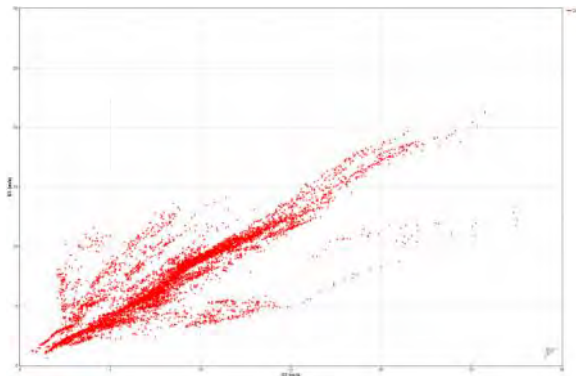


Figure 4-8 - U1 vs. U2
2013-Sep-23 to 2013-Dec-12
U1 consistently underperforming against U2

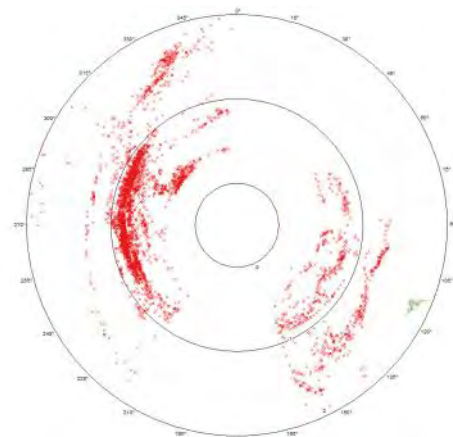


Figure 4-9 - U1/U2 vs. D1
2013-Sep-23 to 2013-Dec-12
Tower distortion signal exacerbated by U1 underperformance

All of the U1 data after 2013-Sep-24 was labelled as subject to the effects of icing and therefore excluded from the analysis, though it was used to help flag obvious icing-related underperformance in U2 before being discarded.

Assumed damage to the R.M. Young wind direction sensor resulted in a recovery loss of 16.2% of the original U1 and D1 data sets. U1 probably suffered greater losses in relation to this damage, though that was removed later as possibly icing-related.

As of the final data segment available (2014-Mar-07), the R.M. Young sensor was unreliable in its functions as both a propeller anemometer and as a wind direction vane. It is recommended that it be replaced.

4.3 Sensor Relational Flagging

A set of standard criteria was employed to flag data showing odd comparative values between co-levelled anemometers, and between measurements at different heights. The purpose of these flags was to indicate periods likely to be reporting: underperformance due to icing; excessive and incorrect shear values; and acceleration or slow-down of the free-stream wind speed due to the presence of the met mast.

As will be discussed shortly, the tower configuration suffered heavily from tower distortion effects and icing. This rendered blanket tests between co-levelled anemometers relatively ineffective as the distortion was sector-wise ubiquitous and extremely non-uniform.

Climate-related anemometer slow-down and stalling rendered attempts to verify characteristic shear scenarios was difficult as there were relatively few time steps where both anemometers at 16.5 m could be used to confirm the actual free-stream wind speed at that level. The site itself should have low shear, being an arctic tundra location with a winter snow blanket at the ground, however there were several instances where relatively high shear scenarios could neither be confirmed reasonably valid, nor rejected as impossible. There was no sensor at the 16.5 m level which could be relied upon as being the primary anemometer under all circumstances.

4.4 Data Trend Flagging

Standard anemometer 1-hour performance trend tests ultimately revealed nothing unusual which was not later flagged for some other, more-obvious reason. Anemometer data segments flagged for sudden changes were found to be consistent across the set of sensors and so were considered legitimate phenomena, often occurring at high wind speeds and concurrent with significant valid changes in wind direction.

Temperature sensor data flagged by 1-hour change tests were considered reasonable for an arctic climate, happening primarily in the warmer months, early in the morning and late in the evening, and often coinciding with sudden and significant changes in wind direction and speed. These events were most likely related to the diurnal solar cycle.

4.5 Icing Part I: Obvious Anemometer Stalling and Slow-Down

Some standard icing-related tests were used to flag the data, then the full anemometer time-series was examined manually and segments were excluded from the analysis when determined to be experiencing extended periods of stalling and/or obvious slow-down as a result of variable-temperature and cold-temperature events. Co-levelled anemometers were examined independently, with all statistical variables considered (U_i , U_i -SD, U_i -max, U_i -min) for each time step. D1, D1-SD and T1 data was also used to determine meteorological conditions when periods of stalling were found. Anemometer data determined independently of other sensors to be affected by obvious icing was excluded from the analysis.

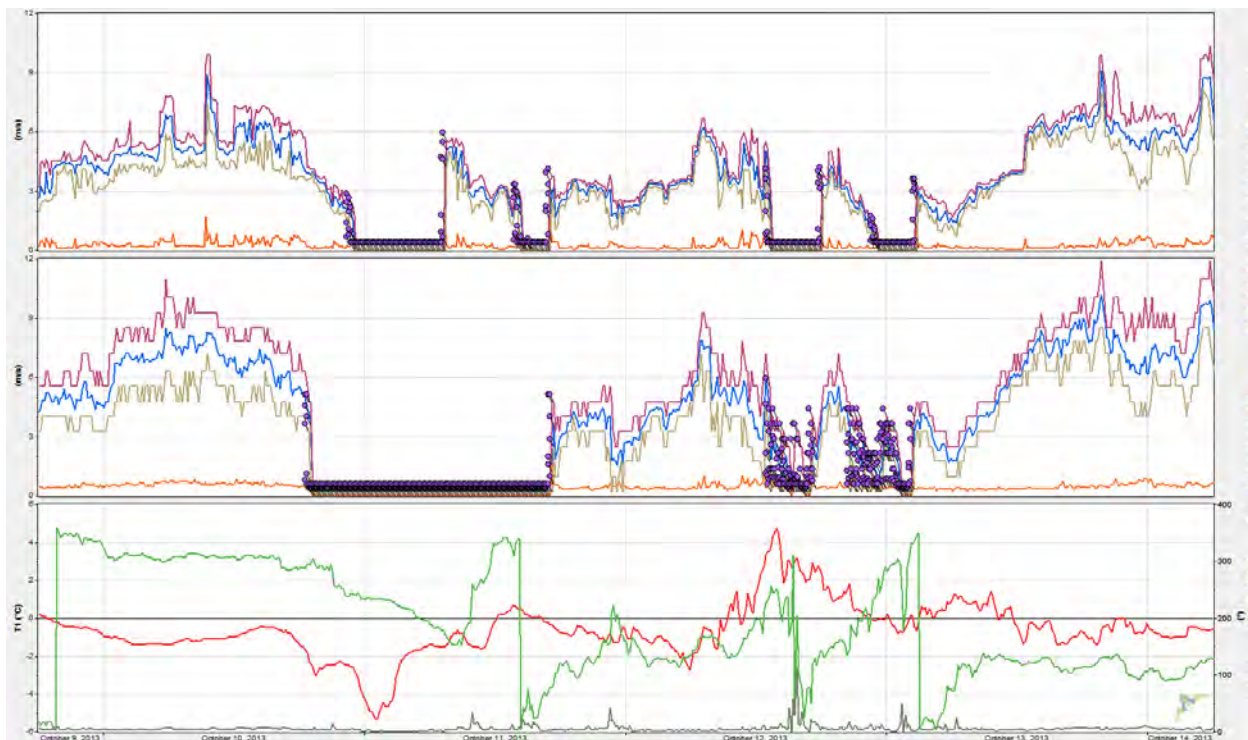


Figure 4-10 - Obvious icing-related stalling and slow-down flagged in U1 (top) and U2 (middle)
 U, Ui-SD, Ui-max, Ui-min used to identify anemometer icing
 D1, D1-SD, T1 used to identify changing weather conditions

4.6 Icing Part II: Vane Stalling at Low Temperatures

The wind vane data time-series was examined and flagged as being likely affected by icing when the sensor experienced extended periods of flat-lining, with D1-SDat or near zero, and with T1 near or below 1°C or changing significantly. Short data periods (one time step, or so) with similar characteristics were ignored if it appeared that the vane data was consistent with what would have been expected at that time, especially if the anemometers were reading reasonable wind speeds.

The vane was a robust alpine model designed for harsh winter climates. Whenever the vane was affected by icing all the anemometers were also assumed to be affected and the data was excluded from the analysis. This conservative approach was found to be consistent with the time-series data.



Figure 4-11 - Obvious case of an extended period of D1 icing and corresponding anemometer stalling
Top: all anemometers stalled or slow (was also independently flagged)
Middle: D1 flat-line indicating vane stalling, T1 low
Bottom: D1-SD very low

4.7 Tower Distortion Effects & Comparative Underperformance

The presence of the meteorological mast influences wind speeds around the tower which can cause an anemometer to encounter a wind speed other than the actual free stream one. This effect is described in the IEC documentation¹⁴ and is dependent on the type of mast, length of the anemometer mounting boom, and the wind direction relative to the mast and sensor.

An anemometer downwind of the mast is effectively shaded and reads below the actual free stream wind speed, often also reporting increased turbulence intensity. To a lesser degree a similar slow-down is measured when an anemometer is mounted upwind of the mast. Tower shading can be graphically examined by polar-plotting the ratio and/or difference of co-levelled sensors against the corresponding wind vane direction readings.

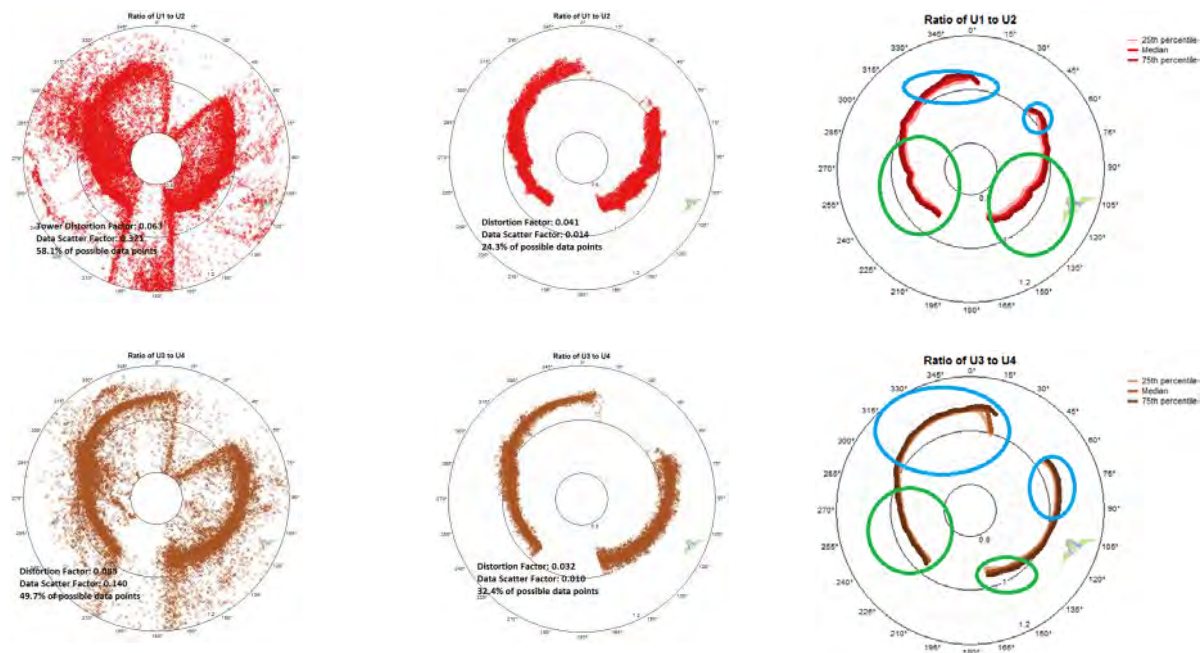


Figure 4-12 - Tower Distortion Polar Plots

Top: U1/U2vs.D1 scatter polar plots prior to and after data validation; and statistically, after data validation

Bottom: U3/U4vs. D1scatter and statistical polar plots

Sectors of higher-than free-stream wind speed marked: U1 and U3 in blue, U2 and U4in green

Figure 4-12 plots the wind speed ratios U1/U2 and U3/U4 vs. D1 after: only obvious icing data has been removed (left); and after full quality control (centre and right). The shading of anemometers U1 and U3 is clear when the winds are from the north-northeast, and the shading of U2 and U4 occurs from the south-southwest.

There remained considerable scatter in the representations of the data sets where only obvious icing had been removed (left panels). Tower shading is clear, but most of the noise was a result of co-levelled anemometers underperforming relative to one another in the severe arctic conditions. That faulty data was excluded by: examination of the data streams together in a time-series, making reference to flags and looking for clear co-levelled anemometer relative underperformance or excessive shear between sensor levels; and by examination of various scatter plot presentations of the data to determine general validation patterns.

¹⁴ IEC 64100-121-1, Annex G.6, 70

Absolute sensor underperformance, in a general sense, was suspected but difficult to quantify as none of the sensors was deemed of high enough quality to be taken as a benchmark for comparison.

Once the data showing obvious icing, tower shading, relative underperformance, or excessive shear were excluded from the analysis, the data scatter factor of the wind speed ratio vs. wind direction polar plot at the 39 m level changed from 0.321 to 0.014. This factor is the weighted mean of the standard deviation of the wind speed ratios when binned into 72 direction sectors¹⁵. At the 16.5 m level, the scatter factor dropped from 0.140 to 0.010. At both levels these changes are indicative of a significant improvement in the general agreement in wind speed readings between co-levelled sensors for data time steps included in the final analysis. However, in both cases the percent of possible data time steps with valid paired readings and concurrent valid vane data dropped significantly: 58.1% to 24.3% at the 39 m level; and 49.7% to 32.4% at the 16.5 m level.

The plots in Figure 4-12 demonstrate significant tower-induced distortion of the free-stream wind speed in one of the anemometers at both sensor heights, almost all the way around the met mast. In the case of the 39 m anemometers, the two sensors are different makes and models so such a ratio could be expected to show some deviation from unity, however in this case the distortion is extreme.

The free-stream wind speed distortion appears primarily because the sensors were mounted on short anemometer booms on a lattice-type tower. Ideally the speed ratio plots in Figure 4-12 would cluster around the unity ratio circle, but the tower distortion factors were high: 0.041 at 39 m; and 0.032 at 16.5 m. These distortion factors quantify the weighted non-unity of the median values of the wind speed ratios when binned by sector¹⁶.

Ideally, met mast booms should be long enough and oriented in such a way as to ensure the horizontal wind speeds encountered by a sensor are within 99.5% to 100.5% of the actual free-stream speed during the most frequently occurring events, as well as during the most energetic wind events (if possible). For a three-legged lattice mast the wind speed near to the tower can be expected to deviate from the free-stream value as described in the IEC documentation¹⁷. Effects seen in the measured wind speed due to upwind speed deficits or around-tower acceleration are exacerbated the closer the sensor is mounted to the tower. Interpretation of the documentation suggests the value of R/L , where R is the distance from the geometric center of the tower to the anemometer and L is the distance between the lattice legs, should be higher than 5.0 in order for the sensors to experience wind speeds that are at least 99% of the free stream wind speed when sited upwind of the mast.

The value of R/L for this met mast configuration was around 1.5 (low) for all anemometers. Distortion on this mast was fairly high for that reason; severe deficits occurred upwind of the mast, and beyond-free-stream speed-ups were seen at anemometer locations around the mast from the upwind direction.

In Figure 4-12 the regions of tower distortion have been marked; the blue ovals highlight wind directions where the odd numbered sensors, mounted to the south-southwest of the tower, measured higher than free-stream wind speeds, while the green circles highlight the same for the even numbered sensors mounted north-northeast. Very little of the data in this data set was free from tower distortion effects.

¹⁵Windographer 3.2.5 documentation: Scatter Factor, $f_{scatter} = \sum_{i=1}^n \sigma_i m_i / \sum_{i=1}^n m_i$; n is the number of direction sectors in the polar plot; σ_i is the standard deviation of the sensor speed ratios in sector i ; m_i is the number of records in sector i

¹⁶Windographer 3.2.5 documentation: Tower Distortion Factor, $f_{td} = \sum_{i=1}^n |1 - \mu_i| m_i / \sum_{i=1}^n m_i$; n is the number of direction sectors in the polar plot; μ_i is the median value of the ratios of wind speeds in sector i ; m_i is the number of records in sector i

¹⁷ IEC 61400-12-1, G.6.2

4.8 Sensor Integrity

Sector			0			45			90			135			180			225			270			315		
			Valid	U1/U2	R ²	Valid	U1/U2	R ²	Valid	U1/U2	R ²	Valid	U1/U2	R ²	Valid	U1/U2	R ²	Valid	U1/U2	R ²	Valid	U1/U2	R ²	Valid	U1/U2	R ²
2012	Oct	Mar	117	1.058	0.998				134	0.948	0.989	569	0.932	0.996				342	0.916	0.999	1605	0.951	0.998	540	0.999	0.996
	Dec	May	144	1.046	0.997	206	1.012	0.997	1065	0.981	0.992	1090	0.93	0.997				152	0.919	0.999	2151	0.97	0.998	845	1.002	0.999
	Feb	Jul	420	1.045	0.998	510	1.013	0.998	2717	0.978	0.994	1607	0.928	0.997				475	0.917	0.999	3355	0.967	0.998	1838	1.001	0.999
	Apr	Sep	651	1.046	0.997	694	1.013	0.998	4068	0.979	0.995	1722	0.922	0.997				730	0.92	0.998	4206	0.966	0.998	2629	1.001	0.999
	Jun	Nov	508	1.046	0.998	508	1.014	0.998	3067	0.978	0.996	1060	0.922	0.998				611	0.92	0.998	2402	0.957	0.997	1882	0.999	0.998
	Aug	Jan	232	1.047	0.996	204	1.014	0.998	1394	0.981	0.996	515	0.922	0.998				284	0.924	0.998	1183	0.959	0.997	876	0.998	0.998
	ALL		768	1.048	0.997	726	1.014	0.998	4202	0.979	0.995	2291	0.926	0.997	90	0.896	0.998	1072	0.919	0.998	5811	0.962	0.998	3169	1	0.998

Figure 4-13 - U1 vs. U2 linear best fit
8 direction sector bin centres: # valid data pairs; best-fit slope $m = U1/U2$; R^2
Overlapping 6 month sample periods

Sector			0			45			90			135			180			225			270			315		
			Valid	U3/U4	R ²	Valid	U3/U4	R ²	Valid	U3/U4	R ²	Valid	U3/U4	R ²	Valid	U3/U4	R ²	Valid	U3/U4	R ²	Valid	U3/U4	R ²	Valid	U3/U4	R ²
2012	Oct	Mar	197	1.077	1	107	1.05	0.998	160	1.031	0.996	302	0.971	0.996				219	0.94	1	1576	0.968	0.998	707	1.025	0.995
	Dec	May	636	1.078	1	266	1.048	0.999	1063	1.033	0.995	894	0.974	0.995				102	0.94	1	2156	0.98	0.999	1471	1.024	0.999
	Feb	Jul	968	1.078	0.999	386	1.048	0.999	2897	1.027	0.997	1495	0.974	0.995				361	0.946	1	3463	0.979	0.999	2681	1.025	0.999
	Apr	Sep	788	1.078	0.999	281	1.048	0.999	4460	1.027	0.998	1954	0.97	0.997	250	0.94	0.998	669	0.947	1	4681	0.979	0.999	3811	1.026	0.999
	Jun	Nov	788	1.078	0.999	281	1.048	0.999	3680	1.025	0.998	1813	0.972	0.997	265	0.942	0.997	774	0.947	1	4655	0.97	0.998	2889	1.023	0.998
	Aug	Jan	347	1.076	0.998	122	1.049	0.999	1845	1.025	0.998	1227	0.971	0.996	224	0.942	0.997	519	0.947	1	3451	0.968	0.998	1689	1.02	0.999
	ALL		1069	1.077	0.999	410	1.048	0.999	4880	1.026	0.998	2914	0.972	0.996	335	0.942	0.997	1117	0.946	1	8422	0.979	0.999	5040	1.024	0.998

Figure 4-14 - U3 vs. U4 linear best fit
8 direction sector bin centres: # valid data pairs; best-fit slope $m = U3/U4$; R^2
Overlapping 6 month sample periods

The anemometers on this met tower, being unheated and subjected to arctic conditions had the potential to become damaged or degraded by icing wear-and-tear, even over the brief period of data collection. As pointed out in the quality control, U1 and D1 were affected, possibly in this manner, as of 2013-Dec-12.

To determine if there was any evidence of subtle sensor degradation in the quality controlled data, the time steps containing validated co-levelled anemometer pairs were divided into overlapping 6-month segments and then further separated by eight wind direction sectors to account for tower distortion variations in the relative sensor responses.

Figure 4-13 and Figure 4-14 show the relative performance between U1 and U2 was consistent over the validated dataset, and the same can be said between U3 and U4. For all anemometers the sensor performance did not degrade noticeably over the period of validated data prior to 2013-Dec-12, after which the data could not be binned by direction sector as D1 was invalidated.

5 Data Selection

One common practice in wind resource assessment is to mount co-levelled anemometers on the meteorological mast so that neither sensor need be assumed to be the primary one. This is done by using general knowledge of the regional wind regime to guide in positioning sensor booms in adherence with the IEC orientation recommendations¹⁸.

However, if the sensors are deemed to be of significantly different accuracy or reliability, then a primary might still be identified. In that case data from the secondary sensor would be used to substitute into the primary data set when required.

In this case it was not possible to strictly follow the IEC standards, owing to resource and time constraints, and the ready availability of other infrastructure. It should be noted that the mounting mast was not a standard meteorological mast, but rather a communications station equipped with multiple transmission devices, the effects of which have not been examined in this report.

At this station, and in keeping with good practice, the top measurement level contained at least one class-1 anemometer, as well as a robust R.M. Young winter-weather sensor which doubled as a high-quality vane. In this scenario, given the 180° boom separation and the expected wind regime, the NRG cup anemometer might be selected as the primary sensor because of its independent MEASNET calibration and general certification as a class-1A sensor designed for industrial wind resource assessment. In that case the R.M. Young would be deemed as the secondary as its calibration is simply factory-specified and, being a propeller sensor, it requires that the vane be functioning properly in order to measure the correct upwind speed. Propeller sensors also differ from cup sensors in the degree to which they are sensitive to turbulence; turbulence intensity is an important quantity in wind resource assessment.

In an arctic climate and given the data recovery statistics (section 6) from the months it was functioning properly, the R.M. Young sensor was determined to be the more reliable sensor after initial quality control. Still, in this assessment neither anemometer was deemed to be the primary because of the prevalence of tower distortion effects from all but the most frequent wind directions.

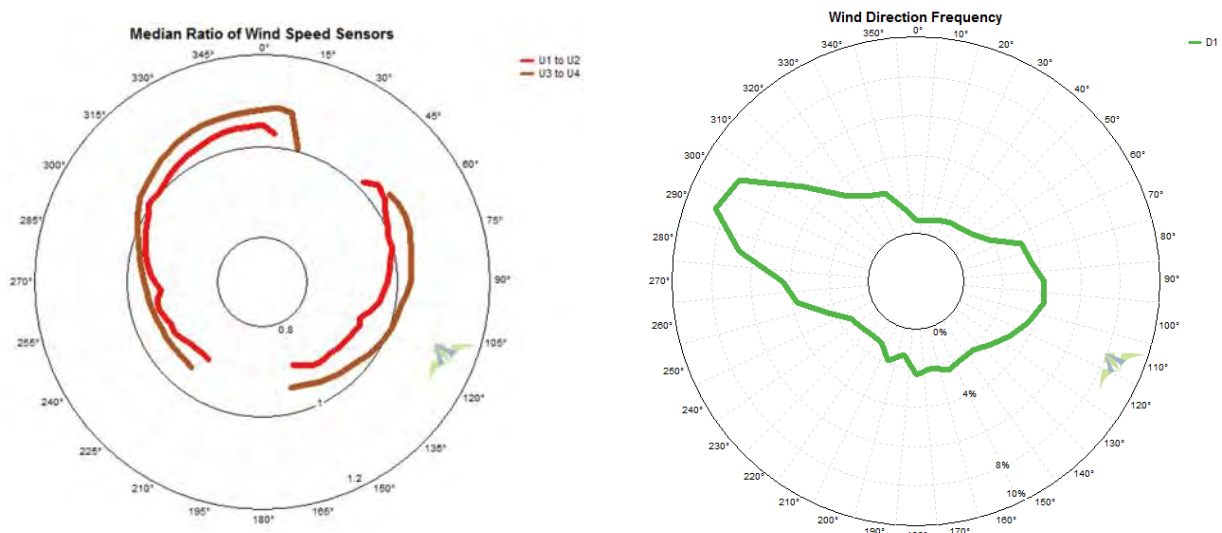


**Figure 5-1 – Winds were of the highest frequency from directions least affected by tower distortion
Distortion was more severe at the 39 m level for southerly and westerly directions and more severe at**

¹⁸ IEC 64100-121-1, Annex G.6.2, 72

16.5 m for northerly and easterly directions
Overall Distortion factors were 0.041 at 39 m, and 0.032 at 16.5 m

All data recorded after 2013-Dec-12 was eliminated from the data set because a proper quality control regime could not be performed without vane data; tower distortion analysis was impossible. As well, taking into consideration the severe distortion described in charts like Figure 5-1, all anemometer readings were removed from the analysis if the charts suggested the sensors were likely to be experiencing higher-than free-stream wind speeds due to tower distortion effects. In sectors where data from both sensors remained for any time step, the average value reported by the two sensors was taken as the free-stream wind speed.

The final data set at each sensor level used in the preliminary assessment (Section 7) consisted of: in most sectors, the validated wind speeds measured by the sensors most likely to be exposed to the free-stream wind; and in some sectors, the average wind speed where both sensors reported valid data. The latter were also the sectors with the highest frequency of wind events. The variables used to label these derived data sets were called UT and UB for the 39 m and 16.5 m sensor levels respectively.

The final selected data sets used in the analysis are displayed graphically in Figure 5-2.

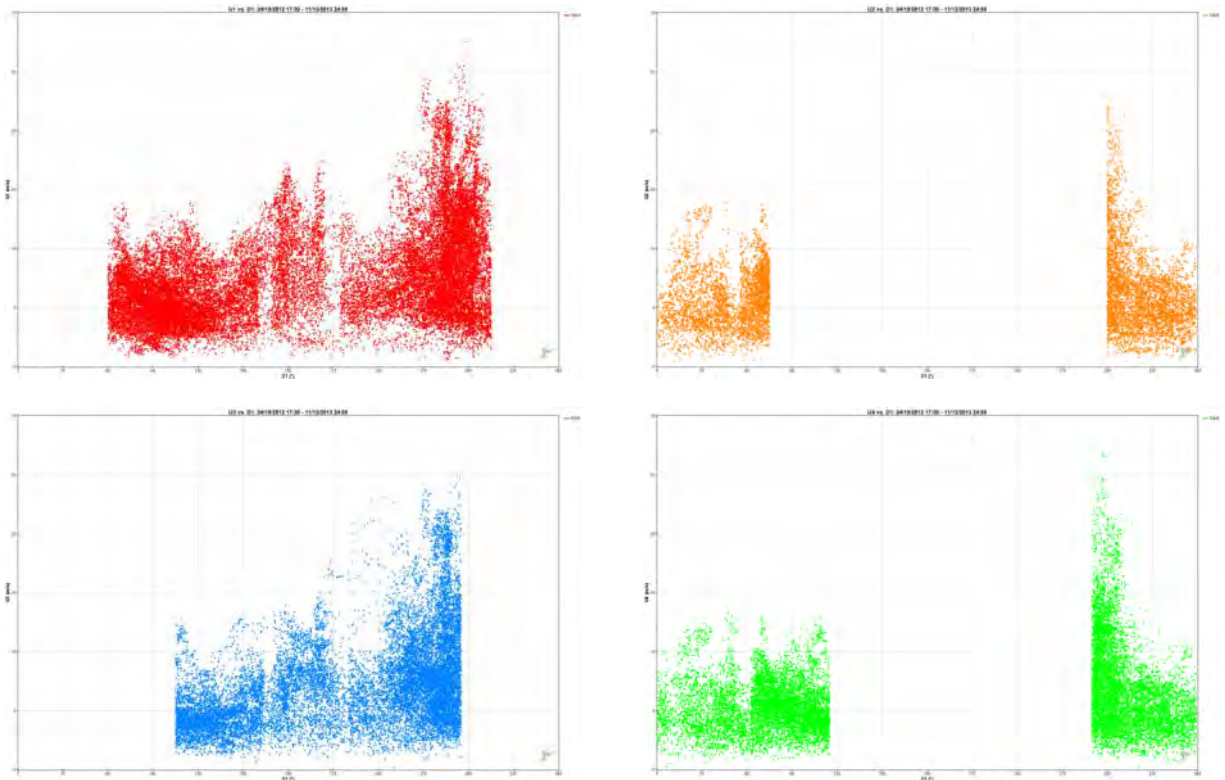


Figure 5-2- All validated wind data, 2012-10-04 to 2013-12-11
Top: U1 vs. D1; U2 vs. D1
Bottom: U3 vs. D1; U4 vs. D1

Of the 62,931 time-steps prior to 2013-Dec-12, there were 1,746 where both U1 and U2 reported valid data and 2,157 where both U3 and U4 were validated. The total number of data points recovered for each sensor were: U1 31,010; U2 8,988; U3 18,129; U4 16,861. The derived variables UT and UB recovered 38,252, and 32,833 data points respectively. Full data recovery statistics are in section 6.

to March being the worst collection periods. This was particularly true for sensors U2, U3, and U4. All the anemometers had data excluded for two primary reasons: stalling or underperformance likely related to icing; and because preferential treatment was given to sensors more likely to be in the free-stream wind flow (i.e. not affected by tower distortion effects).

U1, the R.M. Young sensor, performed well against all three of the NRG Class-1 cup sensors until it became damaged in 2013-Sept and was removed from the analysis.

Generally, when reporting the mean wind speed read by any one sensor over a one month period, that sensor should have a minimum data recovery rate of 80% for that month. In this data set none of the anemometers experienced a full calendar month in which the recovery rate could reliably be said to meet that threshold, and rarely was a threshold of 70% was met. For that reason, where deemed necessary, this wind resource assessment will quote the UT and UB variables derived from combinations of the valid sensor data, and results from a correlation of those with a long-term reference data set.

Figure 6-2 shows that anemometer validation rates were high in wind direction sectors that had the greatest number of occurrences, which was expected given the boom orientation. The low recovery rates for anemometers U1 and U3 when the wind was from the north-east is primarily due to tower shading and distortion, and the same is true for U2 and U4 when the wind was from the south-west.

The heat chart in Figure 6-3 demonstrates the data recovery rates for anemometers U1 and U3, the south-southwest mounted sensors, tended to be higher in the mid-morning to early-afternoon hours than they were overnight. The opposite was true for U2 and U4, the north-northeast mounted sensors. This phenomenon was most prevalent during the summer months (Appendix 11.1.1, Figure 11-1 to Figure 11-4) and appears to be a result of diurnal trends in wind direction and the associated tower shading and distortion validation rules. During the summer months the vane reported more frequent north and north-easterly winds overnight (Figure 6-5), dropping the overall recovery rates for the south-southwest-mounted sensors and boosting them for the north-northeast sensors. This may be a summer nocturnal jet.

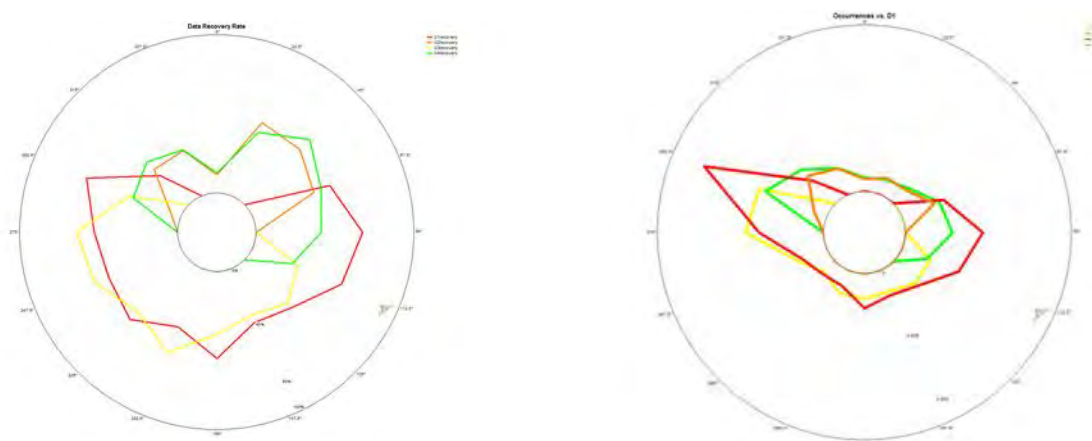


Figure 6-2 - Anemometer validation rates (left) and number of valid occurrences (right), by wind sector U1 (red), U2 (orange), U3 (yellow), U4 (green)

Hour	U1	U2	U3	U4
00:00 - 01:00	41.184	12.548	23.102	22.458
01:00 - 02:00	40.669	11.326	22.973	23.906
02:00 - 03:00	40.734	11.197	23.134	22.876
03:00 - 04:00	41.506	10.94	25.064	22.104
04:00 - 05:00	41.956	11.1	27.317	20.463
05:00 - 06:00	42.6	9.878	27.574	19.337
06:00 - 07:00	42.954	9.878	27.735	18.919
07:00 - 08:00	42.535	9.62	26.448	18.887
08:00 - 09:00	42.632	8.784	27.864	19.144
09:00 - 10:00	42.149	9.459	27.317	19.337
10:00 - 11:00	41.409	10.264	25.161	20.142
11:00 - 12:00	42.664	10.907	25.547	20.914
12:00 - 13:00	42.568	10.811	23.906	21.847
13:00 - 14:00	43.179	11.808	24.743	22.458
14:00 - 15:00	42.535	12.806	24.421	22.201
15:00 - 16:00	42.535	13.481	24.196	24.099
16:00 - 17:00	41.763	14.06	22.072	25.547
17:00 - 18:00	40.791	13.95	21.761	25.972
18:00 - 19:00	41.426	15.061	21.708	25.466
19:00 - 20:00	40.334	15.735	21.066	26.397
20:00 - 21:00	38.6	16.121	21.676	26.429
21:00 - 22:00	39.82	15.639	22.319	25.401
22:00 - 23:00	40.238	14.483	22.704	24.245
23:00 - 24:00	40.462	13.102	23.218	23.635

Figure 6-3 – Mean anemometer hourly recovery rates

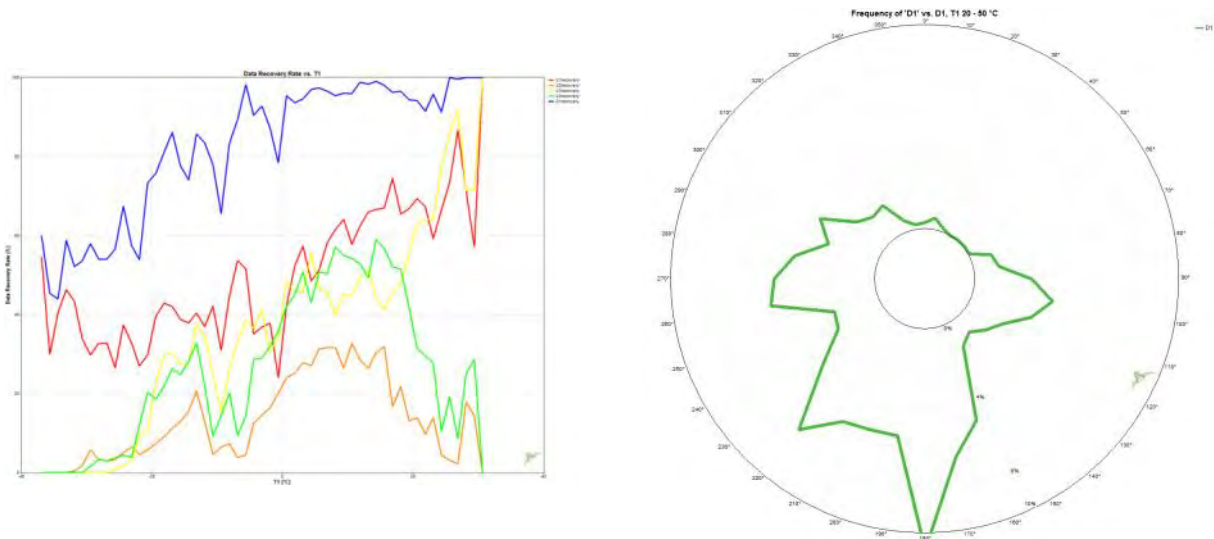


Figure 6-4

Left: Sensor recovery rates D1 (blue), U1 (red), U2 (orange), U3 (yellow), U4 (green), by T1 temperature
Right: Wind frequency rose for T1 > 20°C

The left graphic in Figure 6-4 shows that sensor recovery rates for D1 and the anemometers U1 and U3 all generally increased with temperature. U2 and U4, the north-northeast mounted sensors had weak recovery rates at temperatures above 20°C. When temperatures were warm the winds were generally southerly or south-westerly (Figure 6-4, right), neither of which occurred very often, but when they did U2 and U4 were shaded or distorted by the tower.

It's also clear that U2, U3 and U4 did not generally perform as well as U1 at low temperatures. This is likely owing to the sensor make and model; the R.M. Young Alpine sensor is a more robust and winter-hardy sensor than is the NRG Class-1 cup sensor, though the precision of the NRG is theoretically superior when conditions are favourable.

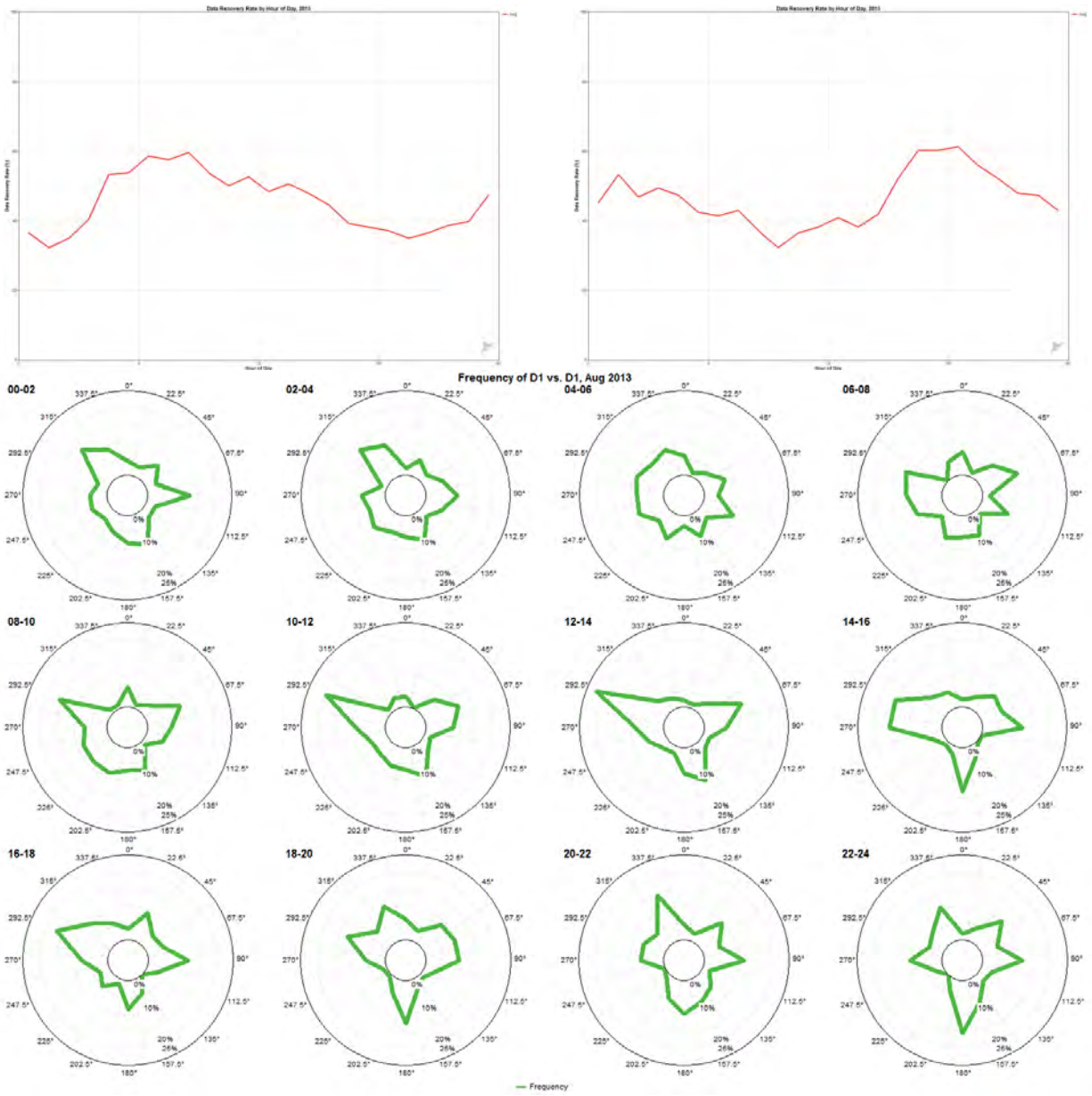


Figure 6-5 – Top: Hourly recovery Rates for U3 (top left) and U4 (top right), for 2013-Aug
Bottom: Bi-hourly wind frequency roses for 2103-Aug

6.2 Derived Variable Calculable Rates

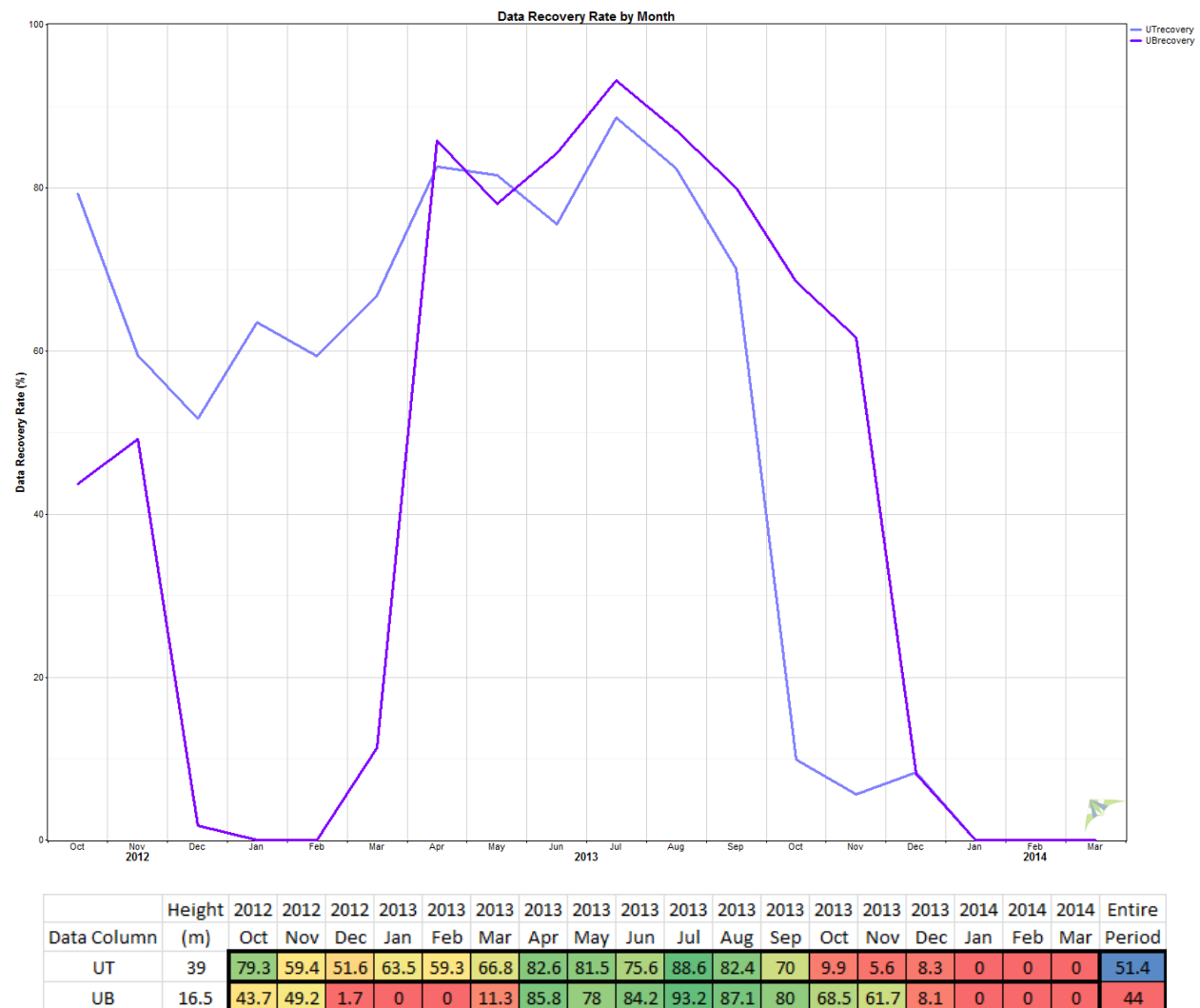


Figure 6-6 - Post-QC derived variable calculable rates by month of data collection

The derived variables UT and UB are the validated wind speeds reported on in section 7 of this wind resource assessment, defining the resource at the 39 m and 16.5 m sensor levels respectively.

The derived variables UT and UB are closer to the free-stream wind speed than are any of the actual physical sensor measurements because of the prevalence of tower distortion effects. Both derived variables have useful data return rates by wind sector (Figure 6-8) and typically had higher rates after noon (Figure 6-8), but the trend was subtle and wasn't consistent across months (Appendix 11.1.2).

As expected, the derived variables had high calculable rates when the temperature was higher. UB had weaker recovery rates than UT at low temperatures as the R.M. Young, mounted at 39 m, was the hardest sensor model (Figure 6-9).

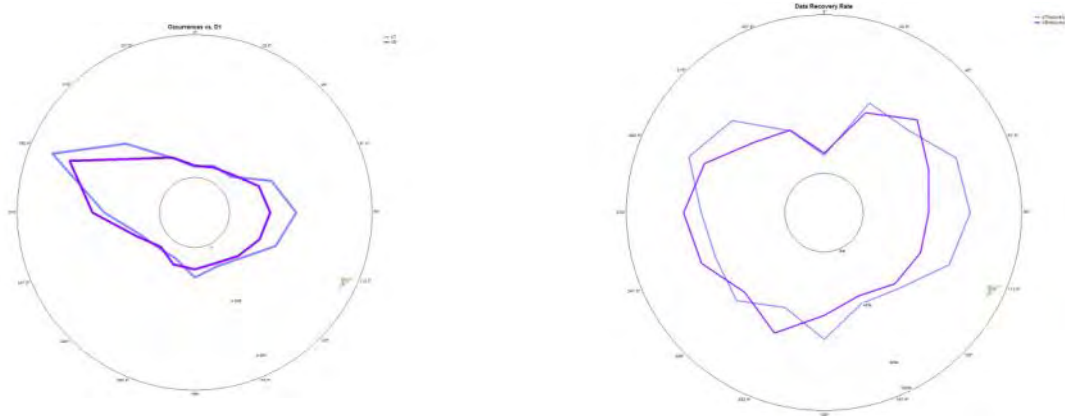


Figure 6-7 - Derived variables: calculable rates (left) and number of valid occurrences (right), by wind sector UT(blue), UB (purple)

Hour	UT	UB
00:00 - 01:00	51.673	43.372
01:00 - 02:00	50.418	43.983
02:00 - 03:00	50.322	43.983
03:00 - 04:00	50.225	44.434
04:00 - 05:00	51.319	44.659
05:00 - 06:00	50.547	44.144
06:00 - 07:00	50.869	43.951
07:00 - 08:00	49.646	43.243
08:00 - 09:00	48.842	43.404
09:00 - 10:00	49.292	43.275
10:00 - 11:00	49.743	42.664
11:00 - 12:00	51.19	43.082
12:00 - 13:00	50.901	42.986
13:00 - 14:00	52.831	43.726
14:00 - 15:00	53.346	43.887
15:00 - 16:00	53.829	44.562
16:00 - 17:00	53.668	44.273
17:00 - 18:00	52.62	44.262
18:00 - 19:00	53.757	44.059
19:00 - 20:00	52.248	44.059
20:00 - 21:00	51.509	45.087
21:00 - 22:00	52.087	45.311
22:00 - 23:00	51.606	44.958
23:00 - 24:00	51.574	44.477

Figure 6-8 - Mean derived variable hourly recovery rates

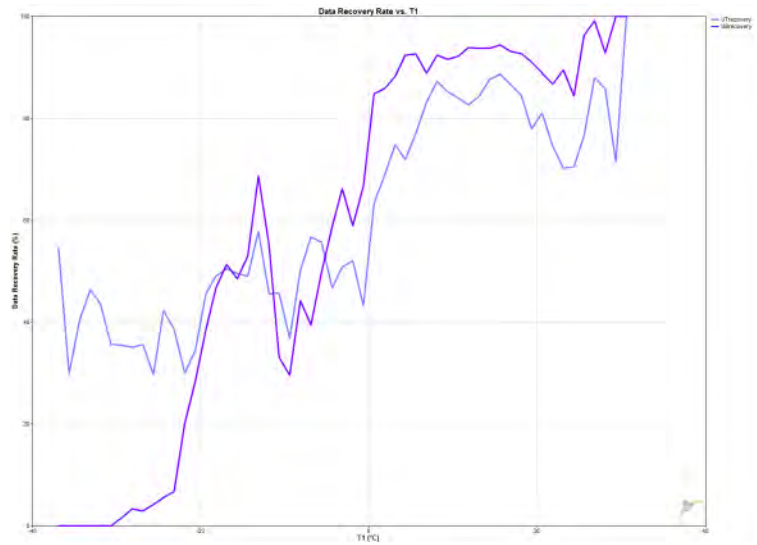


Figure 6-9 - Derived variables calculable rates by temperature

7 Preliminary Characterization of the Observed Wind Speeds

The following wind speed characterizations use the UT and UB data sets. Note that they are fragmented, as shown in Section 6.2, and are biased against low wind speed events coinciding with sensor icing flagged in the quality control process. Of greater interest will be the statistics quoted in section 10 on long-term climatological adjustment of the extrapolated hub-height data set.

Variable	UT	UB
Measurement height (m)	39	16.5
Mean wind speed (m/s)	7.322	6.814
MoMM wind speed (m/s)	7.322	6.79
Median wind speed (m/s)	6.5	6.01
Min wind speed (m/s)	0.21	0.21
Max wind speed (m/s)	27.54	26.85
Weibull k	2.038	1.977
Weibull c (m/s)	8.297	7.723
Mean power density (W/m ²)	512	428
MoMM power density (W/m ²)	512	424
Mean energy content (kWh/m ² /yr)	4,488	3,750
MoMM energy content (kWh/m ² /yr)	4,488	3,716
Energy pattern factor	1.984	2.101
Frequency of calms (%)	0.2	0.13
Possible data points	74,631	74,631
Valid data points	38,375	32,833
Missing data points	36,256	41,798
Data recovery rate (%)	51.42	43.99

Variable	UT	UB
Measurement height (m)	39	16.5
Mean wind speed (m/s)	7.295	6.581
MoMM wind speed (m/s)	7.295	6.581
Median wind speed (m/s)	6.47	5.75
Min wind speed (m/s)	0.3	0.21
Max wind speed (m/s)	27.54	26.51
Weibull k	2.046	1.966
Weibull c (m/s)	8.266	7.458
Mean power density (W/m ²)	505	392
MoMM power density (W/m ²)	505	392
Mean energy content (kWh/m ² /yr)	4,422	3,436
MoMM energy content (kWh/m ² /yr)	4,422	3,436
Energy pattern factor	1.978	2.139
Frequency of calms (%)	0.18	0.1
Possible data points	52,560	52,560
Valid data points	37,420	27,003
Missing data points	15,140	25,557
Data recovery rate (%)	71.19	51.38

Figure 7-1 - Preliminary measured wind summary for derived variables UT and UB
Left: Entire collection period, 2012-10-04 to 2014-03-07 (winter-biased)
Right: One full year with good overall recovery statistics, 2012-10-05 to 2013-10-04



Figure 7-2 - UT and UB monthly wind speed means over the entire data collection period
Recovery threshold for averaging was 60%, 50%, and 40% for each month (top to bottom);
Typical one-month recovery threshold is at least 80% for averaging

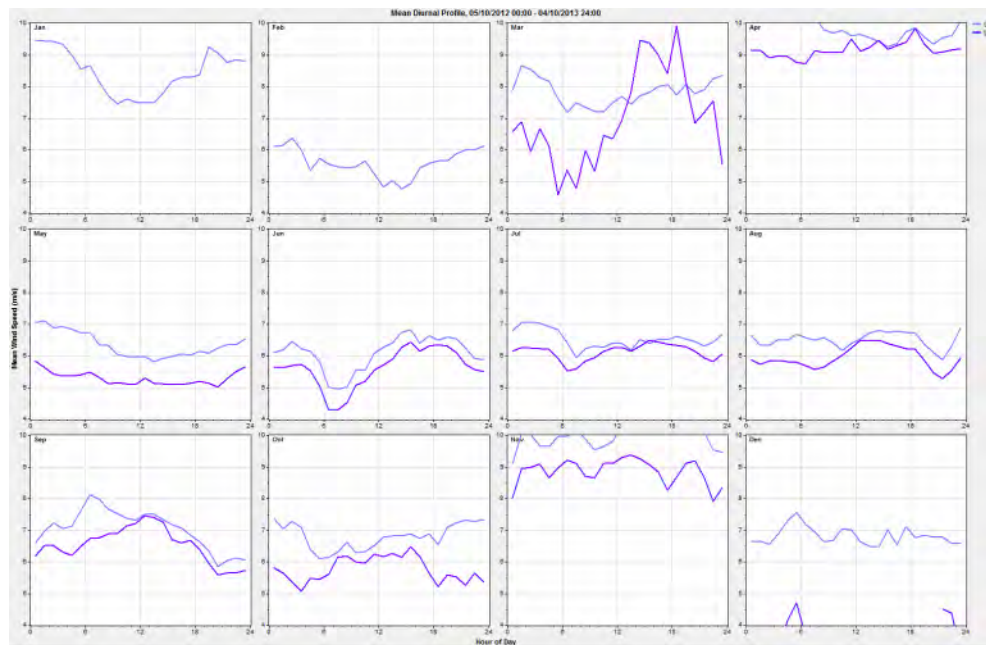


Figure 7-3 - Monthly mean diurnal wind speed profiles, 2012-10-5 to 2013-10-04
 UT blue, UB purple
 Note that recovery rates for UB were very low for 2012-Dec and 2013-Mar

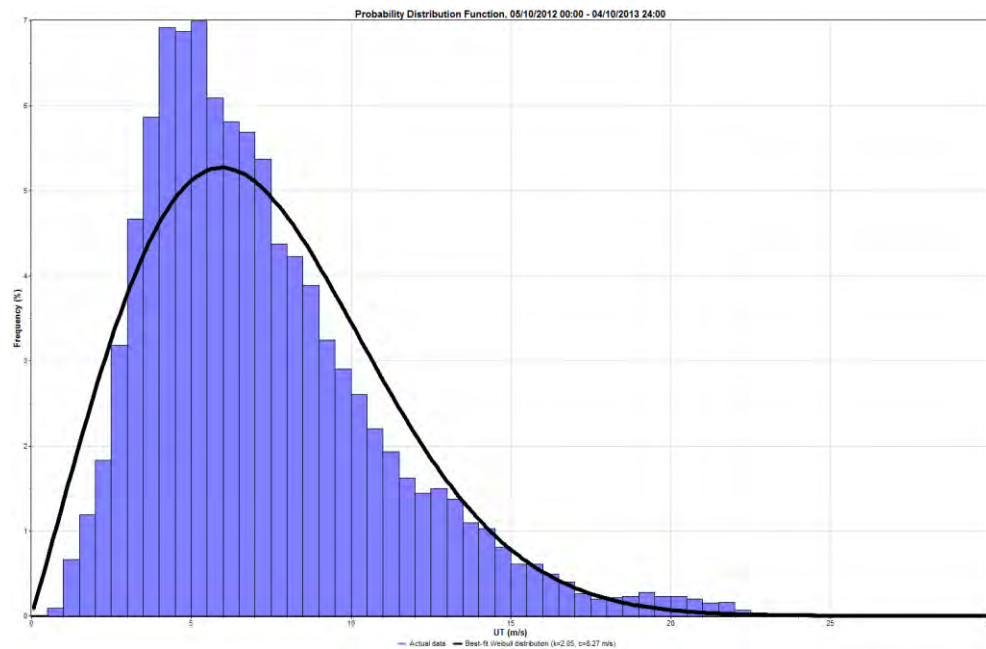


Figure 7-4 - UT wind speed probability distribution, 2012-10-5 to 2013-10-04
 Weibull parameters: shape, $k = 2.05$; scale $c = 8.27$

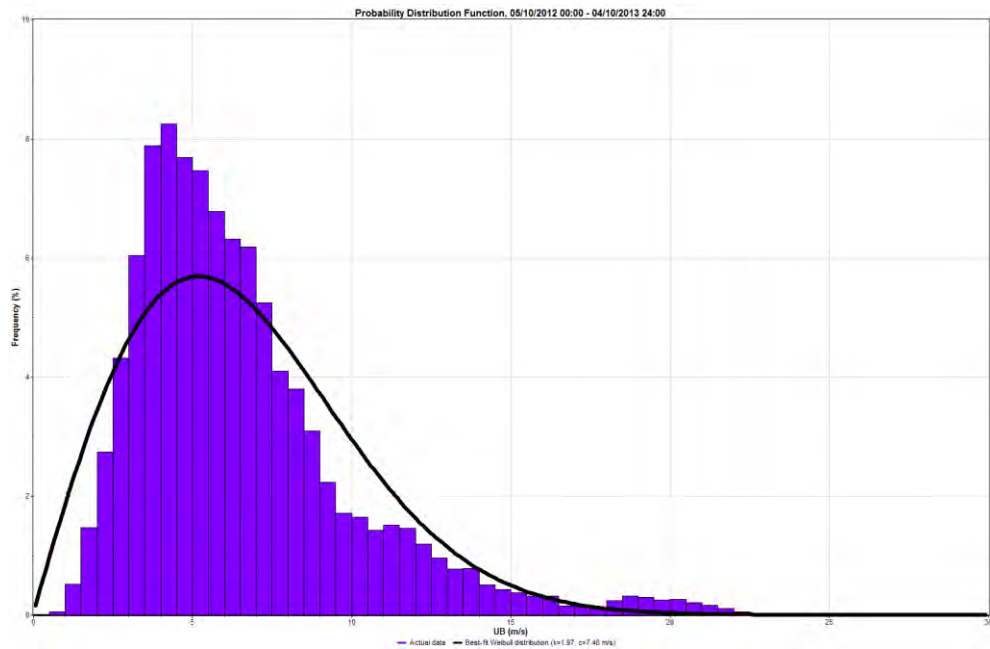


Figure 7-5 - UB wind speed probability distribution, 2012-10-5 to 2013-10-04
Weibull parameters: shape, $k = 1.97$; scale $c = 7.46$

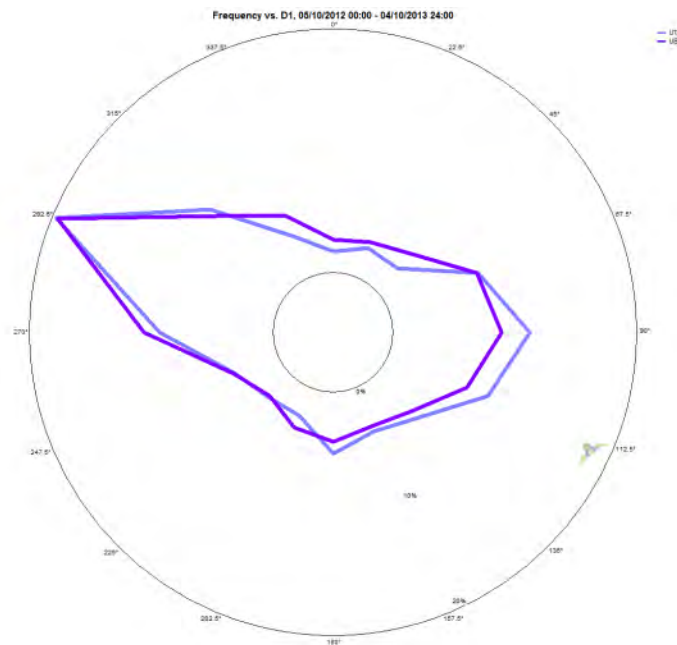


Figure 7-6 - Wind frequency roses, 2012-10-5 to 2013-10-04
UT blue, UB purple



Figure 7-7 - Mean wind speed roses, 2012-10-5 to 2013-10-04
UT blue, UB purple

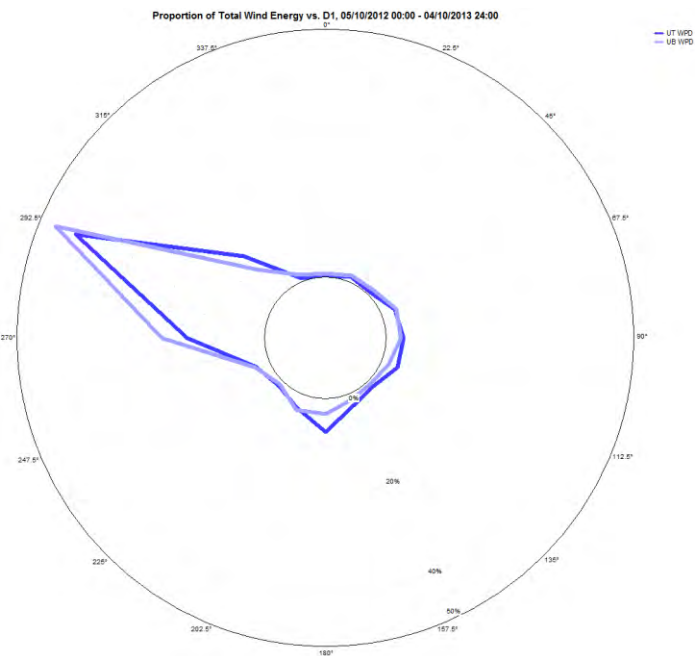


Figure 7-8 - Proportion of total wind energy, 2012-10-5 to 2013-10-04
UT blue, UB purple

8 Wind Shear and Vertical Extrapolation

Wind shear refers to the change in horizontal wind speed with altitude. Typically this results as momentum is transferred downwards from the atmosphere into the ground due to friction between the moving air mass and roughness elements at the surface. In this usual situation the wind speed increases with height above the ground.

In wind regimes with greater shear characteristics wind turbines experience more wear and tear owing to mechanical loading. In cases of high shear wind turbines may need to be installed with higher hub heights, even in strong wind regimes, in order to reduce shear-induced loading.

The shearing effect of surface roughness elements is described quantitatively by a measure known as the roughness length, z_0 . For an arctic tundra site with short grassy vegetation in the summer months and blanket snow cover in the winter months the site characteristic roughness was expected to be around 0.001, which is low¹⁹ and could be characterized as roughness class 0 (zero), which can qualitatively be described as smooth²⁰.

Roughness length is computed from wind speeds measured at different altitudes, and if known can be used to extrapolate the wind to another altitude of interest z via the empirical logarithmic wind profile²¹:

$$\frac{U(z)}{U(z_r)} = \frac{\ln\left(\frac{z}{z_0}\right)}{\ln\left(\frac{z_r}{z_0}\right)}$$

Where z_r is an altitude at which a reference wind speed is known.

When characterizing the wind shear at a site, it is most common to quote the 'shear exponent' in the so-called power-law wind shear profile, commonly referred to as the shear exponent α ²²:

$$U(z)/U(z_r) = (z/z_r)^\alpha$$

¹⁹http://en.wikipedia.org/wiki/Roughness_length

²⁰<http://130.226.56.171/Support/FAQ/WebHelp/TableofRoughnessLengths.htm>

²¹Rohatgi& Nelson 42.

²²Rohatgi& Nelson, 43.

8.1 The Approach to Wind Shear

Though this site has very low wind shear in general, there is evidence of a (likely) stability-related nocturnal increase in wind shear during the summer months when the atmosphere is more affected by diurnal solar heating patterns between May and October. It's possible this is part of a nocturnal jet and there is further suggestion of this in the summer diurnal wind frequency roses in Appendix 11.2.3.

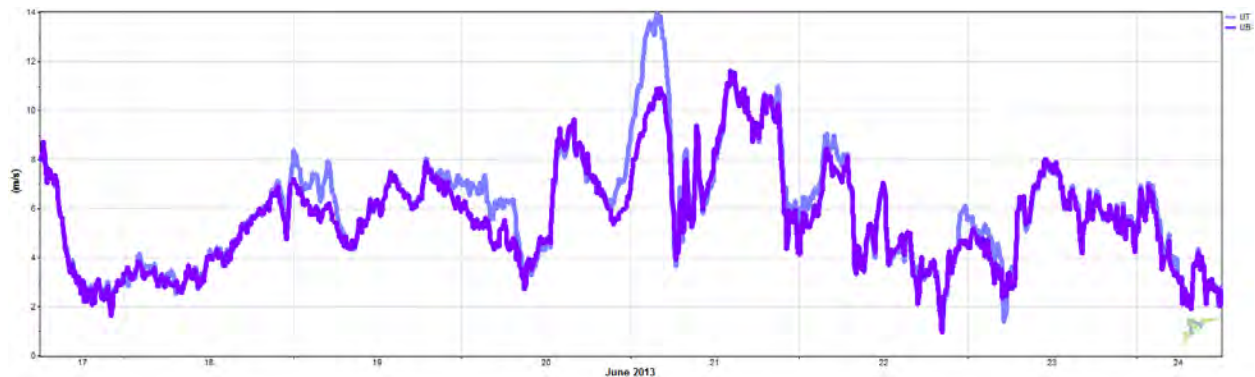


Figure 8-1 - UT and UB in June 2013, with higher nocturnal shear evident

Characteristic shear values used in hub-height calculations are computed using statistics derived from individual time step calculations in such a way that maximizes the use of validated data, while at the same time minimizing the effect of tower distortion on the results.

The two derived wind speed data sets UT and UB (as displayed in Figure 8-1) would not typically be used to derive the primary shear values used in computing the hub-height wind speed, which is discussed in Section 8.4. Those data sets, being comprised of time-steps with mixed sensor orientations, may introduce increased uncertainty into what are already sensitive and assumptive shear calculations. The data selection process outlined in section 5 attempted to account for the effects of tower distortion on the wind speeds reported for each sensor level.

Typically, time step shear values are computed employing coincident data from the actual un-blended anemometer data sets (i.e. U1, U2, U3, and U4). By this standard the shear calculations to hub height are carried out between sensors of similar boom orientations so as to reduce tower distortion influences on the shear uncertainty²³. However, at this site the prevalence of tower distortion in the data set meant that the quality control process eliminated large portions of the data from each sector, reducing overlapping from oppositely-oriented booms on the tower.

Essentially the derived data set is comprised of data from co-oriented sensors at the two different tower heights, so the UT and UB variables were acceptable for use in calculating shear and extrapolating wind speeds to the 60 m hub height, 1.5 times the highest sensor, which is the reasonable limit for shear extrapolations.

²³ AWS Truepower, *Wind Resource Assessment Handbook: Final report*, 10-6

8.2 The Regional Terrain

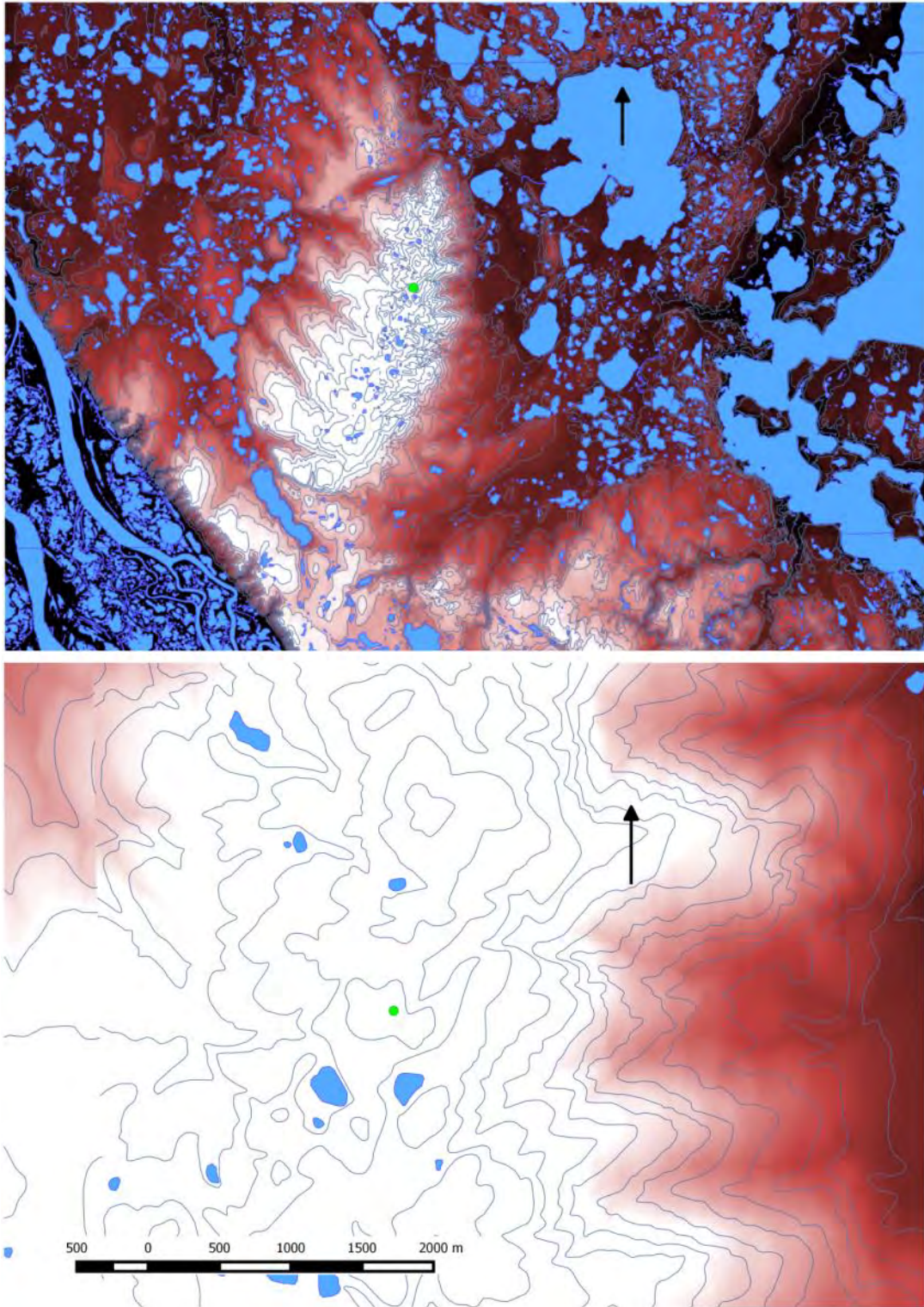


Figure 8-2 - Terrain Maps of Storm Hills Site

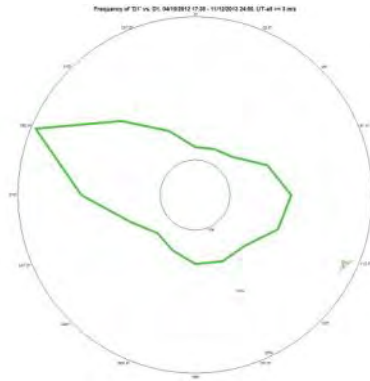


Figure 8-3 - D1 Wind frequency rose

The vane frequency rose in Figure 8-3 shows the majority of the wind events were from west-northwest and east-southeast.

The terrain maps in Figure 8-2 and the gradient profiles in Figure 8-4 and Figure 8-5 reveal gradual slopes immediately to each of those directions. The tower is on a small plateau, at least 150 m from any significant gradient (5%-10%) in the primary wind direction, and 320 m or more from any slope (5%-10%) in the secondary direction.

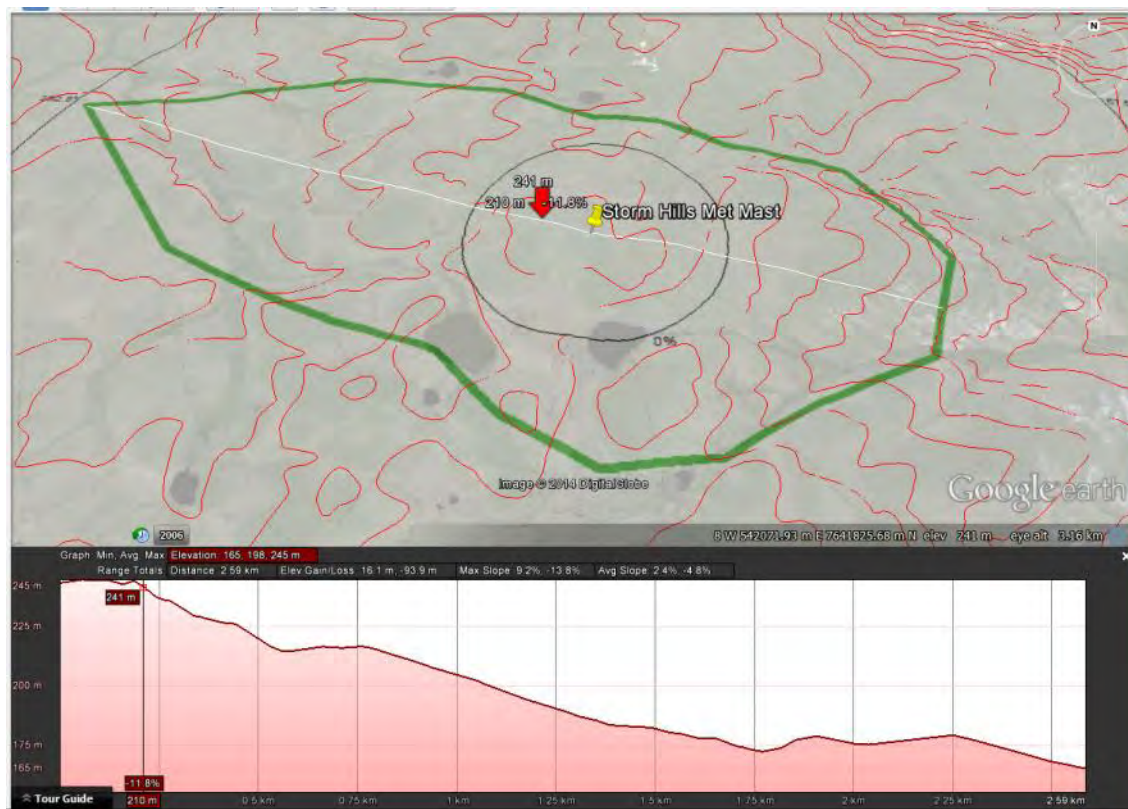


Figure 8-4 - Terrain contours, and Google-Earth terrain profile along the primary, west-northwest wind direction

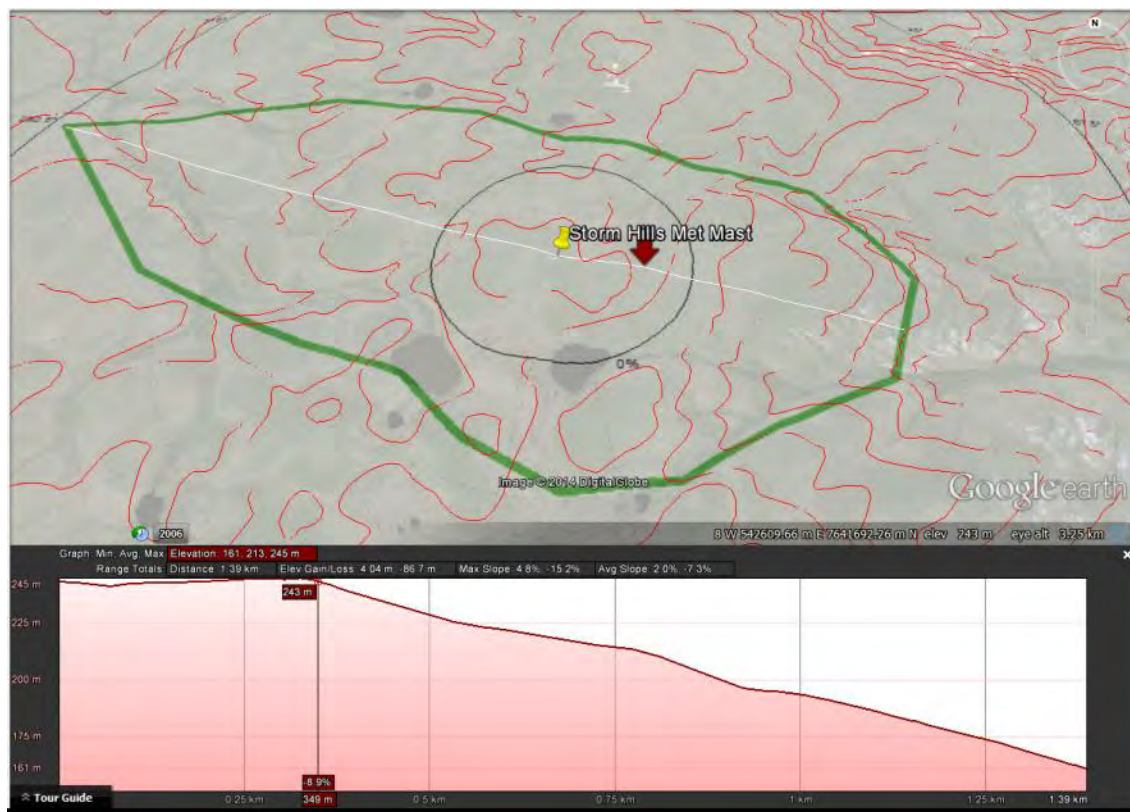


Figure 8-5 - Terrain contours, and Google-Earth terrain profile along the secondary, east-southeast wind direction

8.3 Shear Characteristics – All Valid Data between 2012-Oct-05 and 2013-Oct-04

The charts in this section characterize the wind shear measured at the site taking into account validated data during the one-year period from 2012-Oct-05 to 2013-Oct-04. Shear exponent values were calculated for all time steps reporting concurrent validated data for the derived variables UT and UB, where the 39 m wind speed reported was at least 3 m/s. Over this time period there were 52,560 time steps, and 35,641 of those met the wind speed threshold.

The choice of date range was selected for two main reasons: data recovery rates at the 39 m level were highest for both sensors during this 12-month period (Figure 6-1 and Figure 6-6); and quality control could be carried out thoroughly because all sensors were performing properly, including the vane, allowing for a proper assessment of shading, distortion effects, and weather-related sensor underperformance.

Time steps with light winds, below 3 m/s at the 39 m level, were excluded from the characteristic shear computations as they often reveal either excessively high or false negative wind shear values that may adversely affect the calculations but aren't relevant to turbine power production.

Full shear analysis of the derived UT and UB data sets is carried out in section 8.3.1, measured shear charts for the physical sensor data are shown in Appendix 11.3.1, and 11.3.2.

Figure 8-6 is for reference in the discussions below.



Figure 8-6 - U1, U2, UT number of wind events by D1 wind sector when the 39 m wind speed is at least 3 m/s (up to 9000 events per sector)

8.3.1 Shear Calculated Using Derived Variables UT & UB

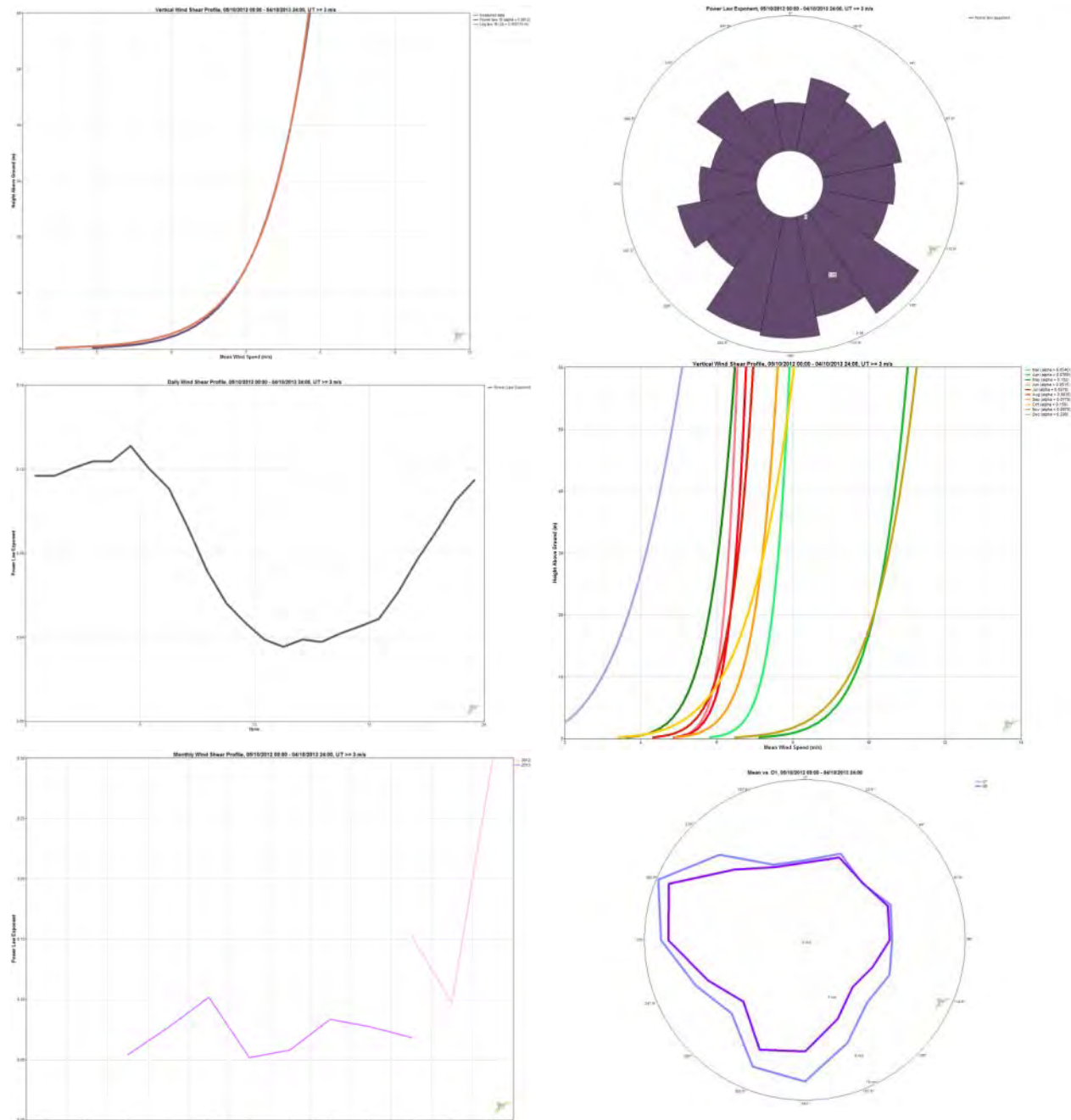


Figure 8-7 - Characteristic shear charts, where $UT > 3\text{m/s}$

$$\alpha = 0.0813, z_0 = 0.00012$$

Top: wind speed profile to 60 m; shear exponent by sector;
 Middle: diurnal shear exponent profile; monthly wind speed profiles;
 Bottom: monthly shear exponent; UT, UB wind speed roses

Wind speeds and shear were generally higher in the winter months, though low data returns from the physical sensors affect those numbers. Figure 8-7 reports an unexpectedly low roughness length for the site; 0.0001 is closer to the roughness length for a water body, such as a lake. The characteristic shear exponent is also low, which is interesting given that shear calculable rates were almost zero during the winter months (Figure 8-8) when

the actual surface roughness would have been expected at its lowest due to snow cover. This suggests that atmospheric stability, which tends to reduce wind shear by transferring horizontal momentum vertically, was an influencing factor on shear during the summer months. June and July reported the lowest shear values, which is evidence of the stability influence. Section 9 on turbulence intensity indicates an increase in TI during the summer months, as expected.

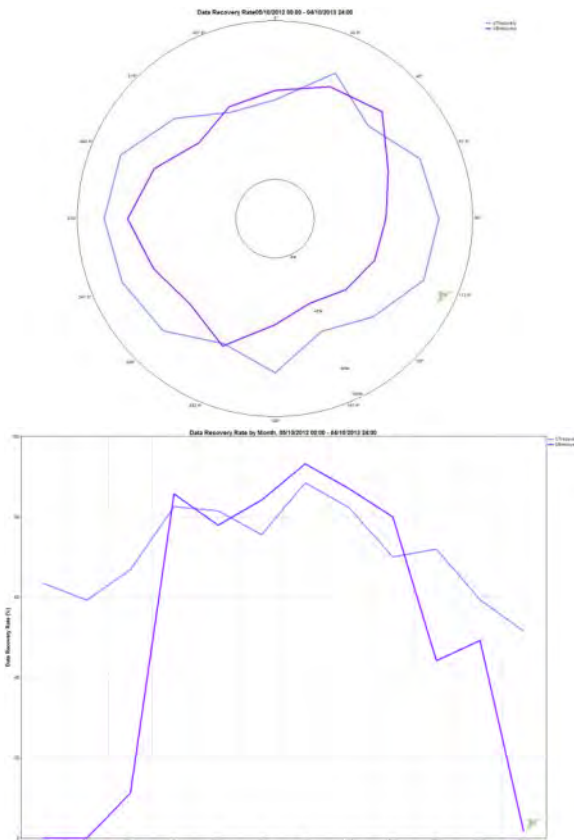


Figure 8-8 - UT (blue) and UB (purple) recovery rates and shear exponent calculable occurrences, by sector and month, where UT > 3 m/s

Direction Sector		Power Law Exp
348.75° - 11.25°	489	0.058
11.25° - 33.75°	766	0.089
33.75° - 56.25°	724	0.079
56.25° - 78.75°	1,858	0.096
78.75° - 101.25°	2,081	0.086
101.25° - 123.75°	1,554	0.08
123.75° - 146.25°	911	0.145
146.25° - 168.75°	501	0.121
168.75° - 191.25°	996	0.143
191.25° - 213.75°	580	0.139
213.75° - 236.25°	542	0.08
236.25° - 258.75°	856	0.097
258.75° - 281.25°	2,594	0.069
281.25° - 303.75°	4,707	0.056
303.75° - 326.25°	1,882	0.093
326.25° - 348.75°	1,167	0.063
	22208	

Month	Time Steps	Power Law Exp
Jan	0	
Feb	0	
Mar	363	0.054
Apr	3,088	0.077
May	2,852	0.102
Jun	2,904	0.051
Jul	3,717	0.058
Aug	3,392	0.083
Sep	2,728	0.077
Oct	1,506	0.15
Nov	1,635	0.097
Dec	23	0.298
	22208	

	Jan	Feb	Mar	Apr	May	Jun	Jul	Aug	Sep	Oct	Nov	Dec	
	0	0	363	3,088	2,852	2,904	3,717	3,392	2,728	1,506	1,635	23	22208
UT			7.732	10.666	6.199	6.398	6.605	6.713	7.356	7.527	10.797	4.473	
UB			7.381	9.984	5.68	6.121	6.285	6.248	6.885	6.614	9.933	3.461	
Power Law Exp			0.054	0.077	0.102	0.051	0.058	0.083	0.077	0.15	0.097	0.298	
													All
00:00 - 01:00			0.046	0.088	0.099	0.118	0.111	0.158	0.106	0.183	0.123		0.117
01:00 - 02:00			0.067	0.101	0.117	0.138	0.11	0.134	0.095	0.167	0.113		0.117
02:00 - 03:00			0.084	0.105	0.13	0.15	0.108	0.128	0.104	0.158	0.117		0.121
03:00 - 04:00			0.125	0.109	0.142	0.129	0.107	0.129	0.109	0.196	0.121	0.517	0.124
04:00 - 05:00			0.163	0.106	0.159	0.121	0.105	0.137	0.1	0.176	0.122	0.192	0.124
05:00 - 06:00			0.261	0.107	0.161	0.123	0.121	0.148	0.12	0.168	0.115	0.236	0.131
06:00 - 07:00			0.102	0.1	0.162	0.087	0.105	0.143	0.119	0.155	0.104	0.324	0.12
07:00 - 08:00			0.116	0.1	0.158	0.058	0.066	0.145	0.112	0.151	0.104		0.111
08:00 - 09:00			0.109	0.085	0.161	0.01	0.025	0.12	0.111	0.169	0.081		0.092
09:00 - 10:00			0.034	0.09	0.115	-0.005	0.018	0.052	0.083	0.158	0.091		0.072
10:00 - 11:00			-0.077	0.089	0.09	-0.017	0.009	0.018	0.059	0.146	0.09		0.056
11:00 - 12:00			0.021	0.078	0.07	-0.021	0.012	0.011	0.047	0.12	0.086	0.427	0.047
12:00 - 13:00			-0.041	0.068	0.05	-0.01	0.01	0.009	0.034	0.109	0.071		0.039
13:00 - 14:00			-0.085	0.058	0.044	-0.01	0.006	0.014	0.022	0.12	0.087		0.035
14:00 - 15:00			0.049	0.039	0.043	-0.005	0.015	0.018	0.022	0.129	0.101		0.039
15:00 - 16:00			0.07	0.031	0.029	0.005	0.007	0.022	0.034	0.117	0.103		0.038
16:00 - 17:00			0.046	0.039	0.053	0.008	0.017	0.03	0.026	0.116	0.092	0.456	0.042
17:00 - 18:00			0.042	0.047	0.078	0.01	0.025	0.033	0.029	0.142	0.07		0.045
18:00 - 19:00			0.023	0.057	0.072	0.009	0.036	0.035	0.042	0.153	0.059		0.049
19:00 - 20:00			0.049	0.069	0.072	0.016	0.034	0.049	0.075	0.17	0.081		0.061
20:00 - 21:00			0.04	0.067	0.095	0.03	0.046	0.093	0.092	0.157	0.101		0.077
21:00 - 22:00			0.106	0.067	0.099	0.067	0.075	0.115	0.109	0.158	0.09	0.181	0.09
22:00 - 23:00			-0.042	0.081	0.117	0.1	0.106	0.143	0.104	0.155	0.09	0.316	0.105
23:00 - 24:00			0.019	0.086	0.124	0.121	0.105	0.151	0.114	0.17	0.097	0.154	0.115

Figure 8-9 - Heat chart of shear exponent by month and hour of day, where UT >3 m/s

The summer stability effect on wind shear is also revealed in the heat plot in Figure 8-11. The lowest wind shear values, indeed negative values, were reported in the afternoons during the summer months. Calculable shear rates were low from 2012-Dec through 2013-Mar, as well as 2013-Oct, primarily due to the absence of data because of low returns at the 16.5 m sensor level.

Figure 8-10 shows that the shear was fairly consistently below 0.2 in most wind sectors throughout the year, and again, low returns in 2012-Nov, 2012-Dec and 2013-Mar suggest outlying vertices in the polar plot are probably not accurate reflections of the monthly shear from a sector.

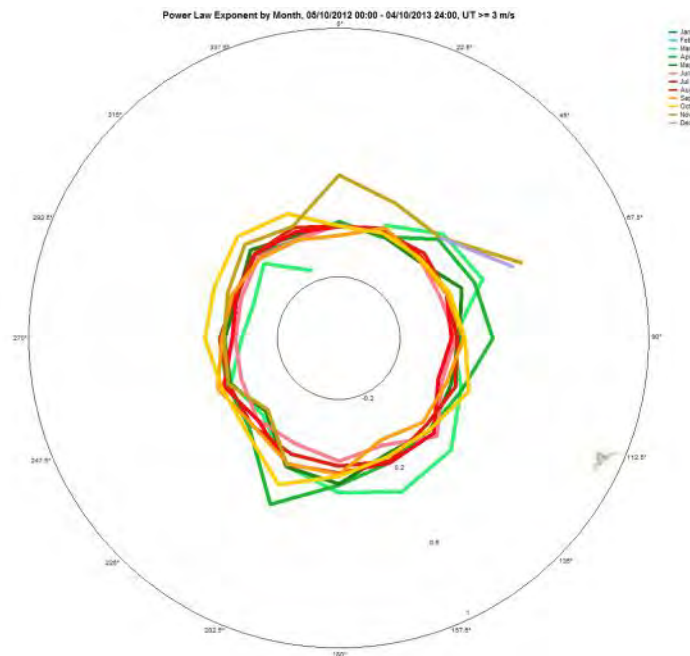


Figure 8-10 - Shear exponent by month and sector, where UT >3 m/s



Figure 8-11 - Shear exponent by month and sector, where $UT > 3$ m/s

Figure 8-11 shows that the wind shear tended to be higher from the southerly sectors when the winds were at their peak for those directions. In these sectors the terrain is slightly more rugged and may have turbulence-inducing characteristics. When a met tower is atop a ridge in significant winds, and upwind of that location is a terrain feature such as a slope, a ridge, or a depression, then if the tower is beyond the mechanical turbulence zone it could report a higher wind shear profile than it would in flat terrain²⁴. Figure 8-12 and Figure 8-13 show the terrain profiles in the 225° and 135° directions respectively; each has a number of potentially important features, but it should be noted that all the gradients along the paths are slight and so are the shear extremes shown above.

²⁴Rohatgi & Nelson 134

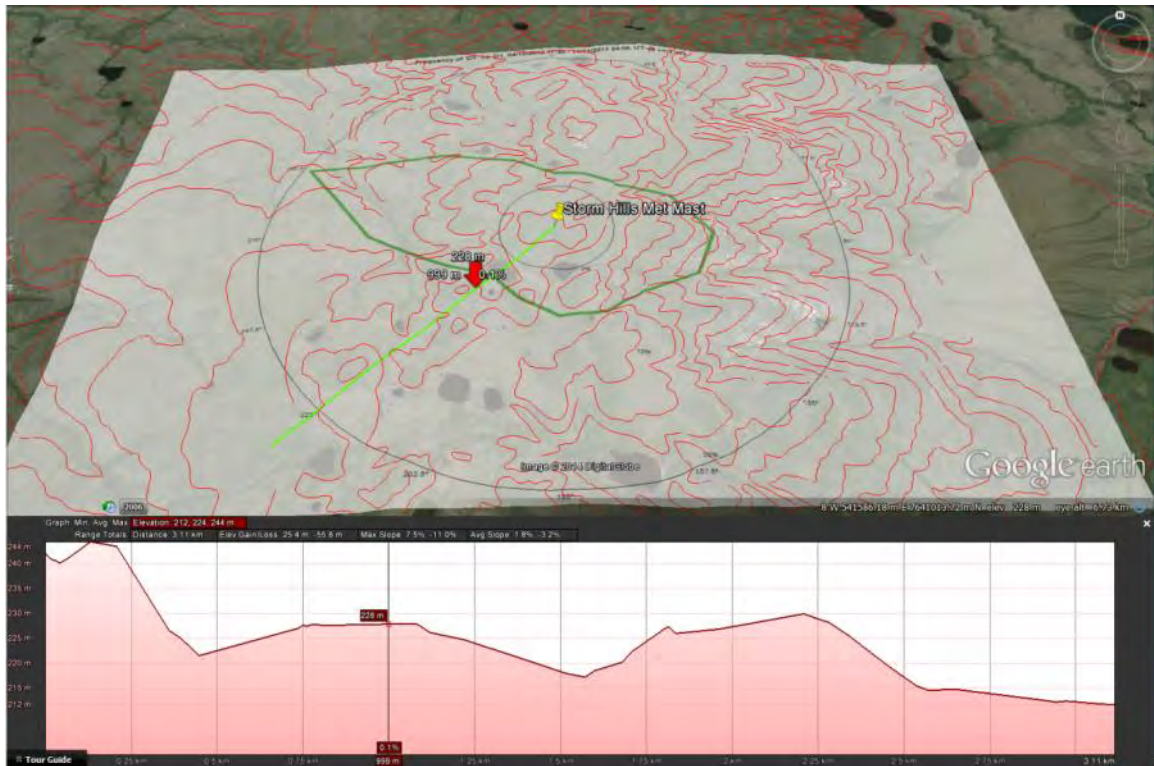


Figure 8-12 - Terrain profile to the southwest of the met mast, maximum slope is 11% or 6°, and the marker is shown at 1000 m from the tower

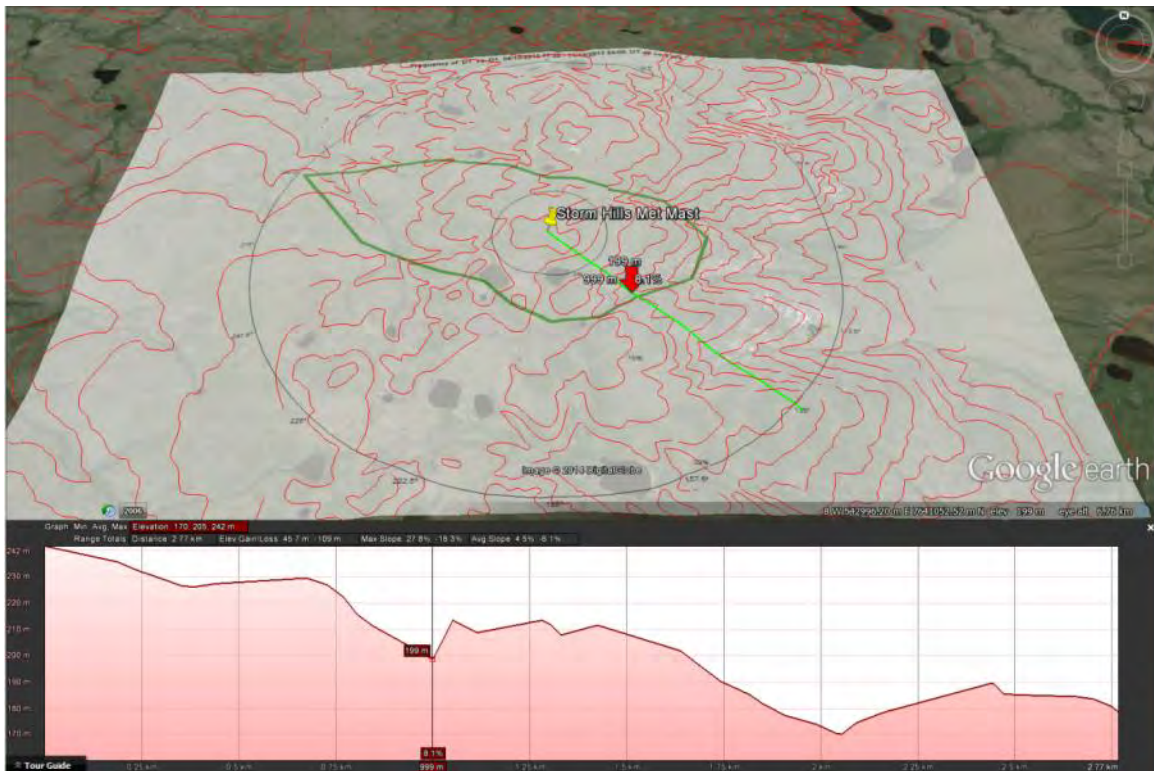


Figure 8-13 - Terrain profile to the southwest of the met mast, maximum slope is 18% or 10°, and the marker is shown at 1000 m from the tower

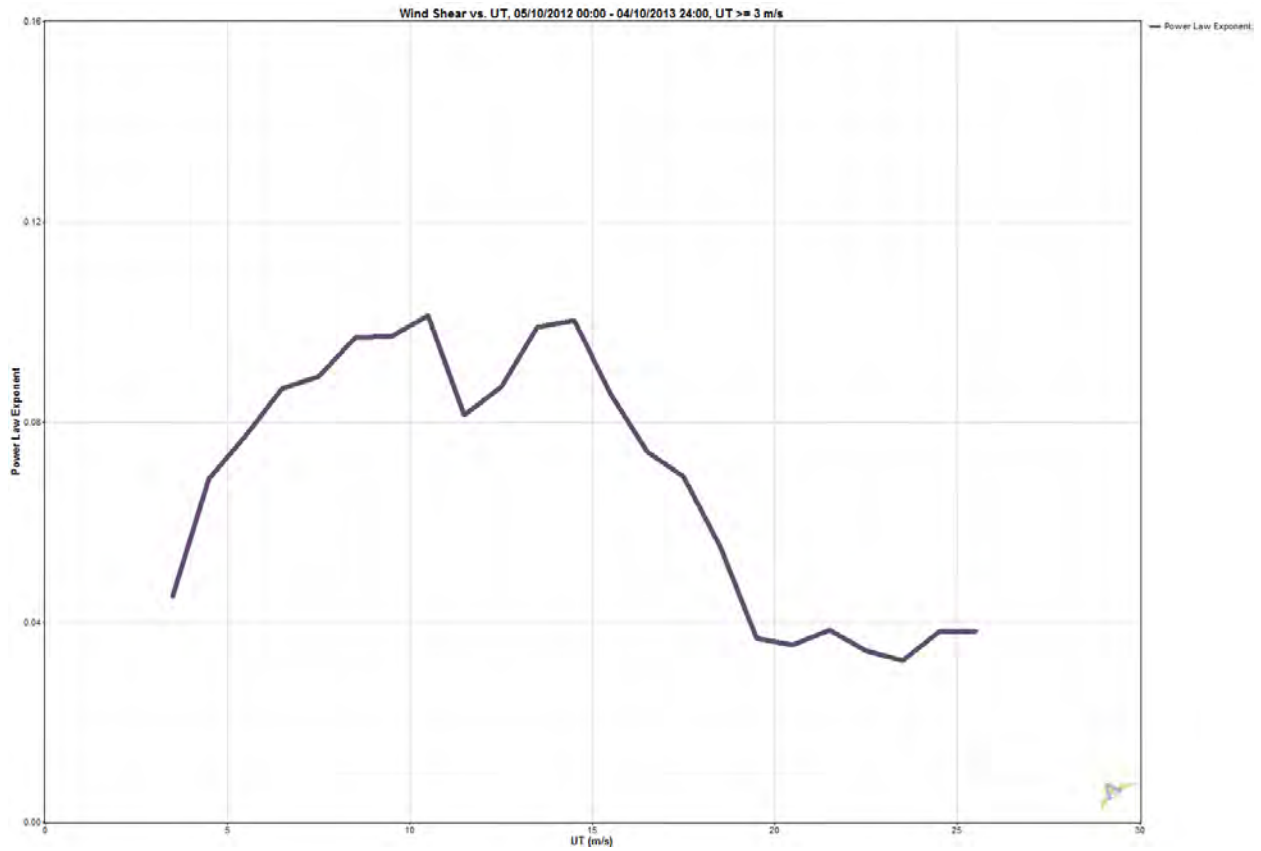


Figure 8-14 - Shear exponent by UT, where UT $>$ 3 m/s

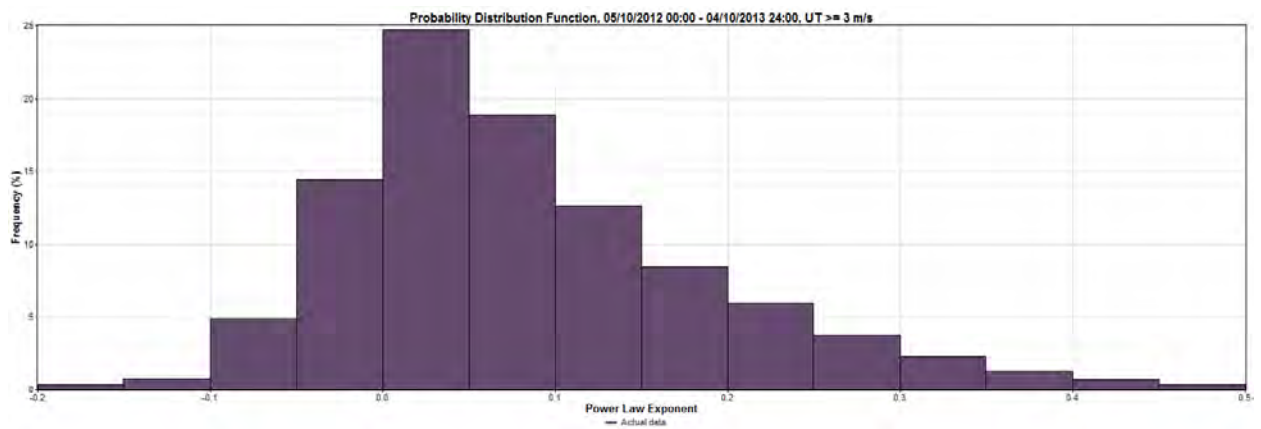


Figure 8-15 - Shear exponent frequency distribution, where UT $>$ 3 m/s

8.4 Extrapolation to Hub Height

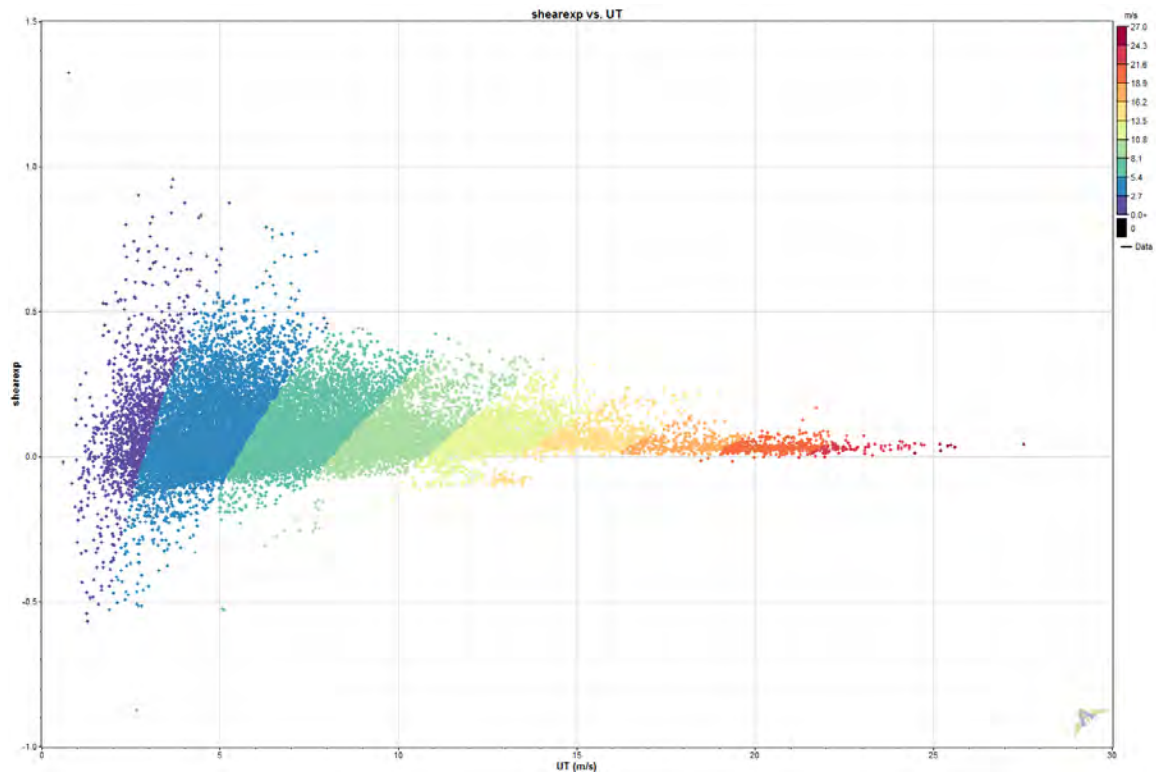


Figure 8-16 - Post-QC wind shear exponent α vs. UT prior to 2013-Dec-12
Colour is scaled by UB

Figure 8-16 shows that the bulk of the extreme shear values occurred when wind speeds were low. When extrapolating the measured wind speeds to the 60 m hub height, the wind shear exponent α was restricted to values between -0.05 and 0.4.

Variable	p60-all	p60-1yr
Measurement height (m)	60	60
Mean wind speed (m/s)	7.725	7.484
MoMM wind speed (m/s)	7.67	7.484
Median wind speed (m/s)	6.89	6.64
Min wind speed (m/s)	0.223	0.252
Max wind speed (m/s)	32.169	28.071
Weibull k	2.02	2.028
Weibull c (m/s)	8.75	8.479
Mean power density (W/m ²)	602	548
MoMM power density (W/m ²)	591	548
Mean energy content (kWh/m ² /yr)	5,271	4,798
MoMM energy content (kWh/m ² /yr)	5,180	4,798
Energy pattern factor	1.993	1.989
Frequency of calms (%)	0.15	0.13
Possible data points	74,631	52,560
Valid data points	47,312	41,073
Missing data points	27,319	11,487
Data recovery rate (%)	63.39	78.14

Figure 8-17– 60 m Hub height wind and recovery statistics
Left: all valid data used; 2012-Oct-05 to 2012-Oct-2013 data only

The data set at the 60 m hub height was referred to as p60 and was generated using Windographer's vertical extrapolation tool, which was set to use the power law to calculate shear exponents for every time step where both UT and UB were valid, and to fill in the gaps using other statistics where required.

The important hub height wind speed charts are shown in Figure 8-18, Figure 8-19, and Figure 8-20

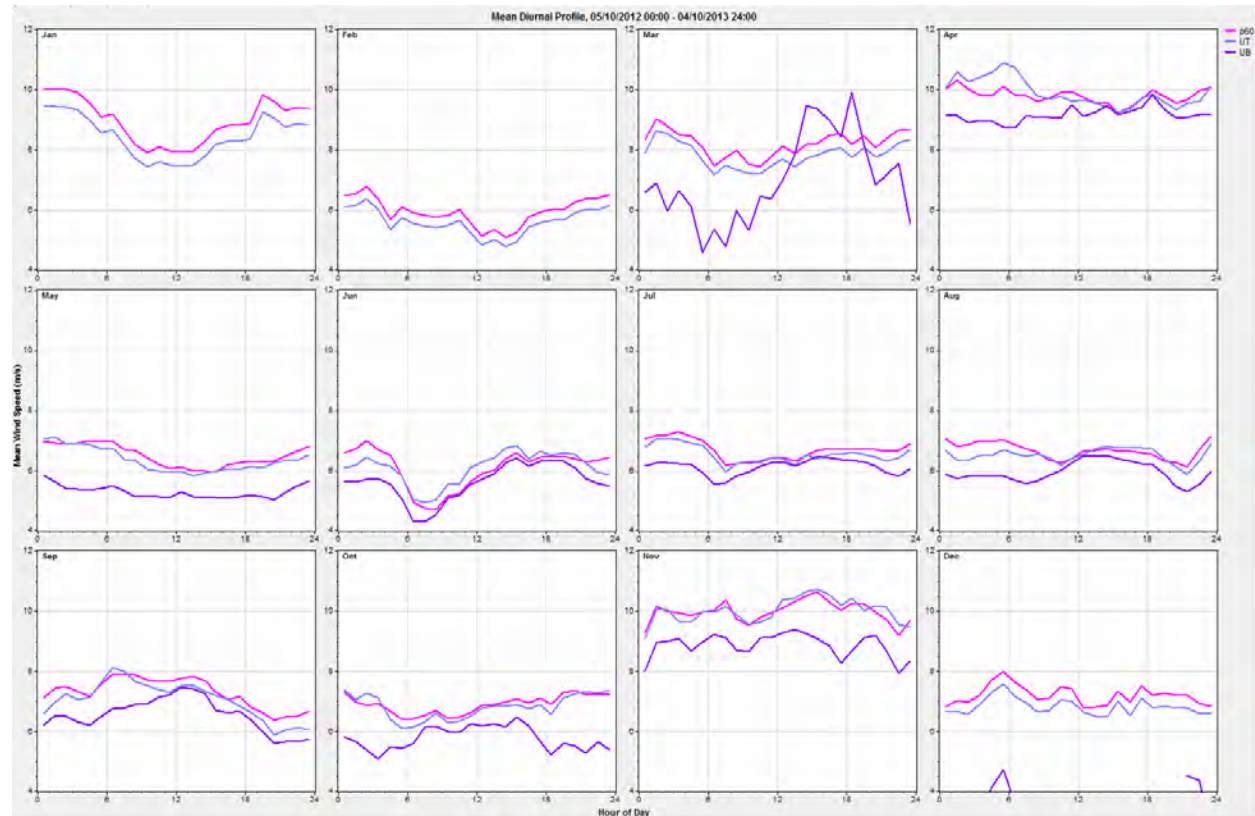


Figure 8-18 – Diurnal Hub height (pink) and UT (blue) and UB (purple) wind speeds



Figure 8-19 - Monthly Hub height (pink) and UT (blue) and UB (purple) wind speeds with recovery threshold for averaging relaxed to 40%

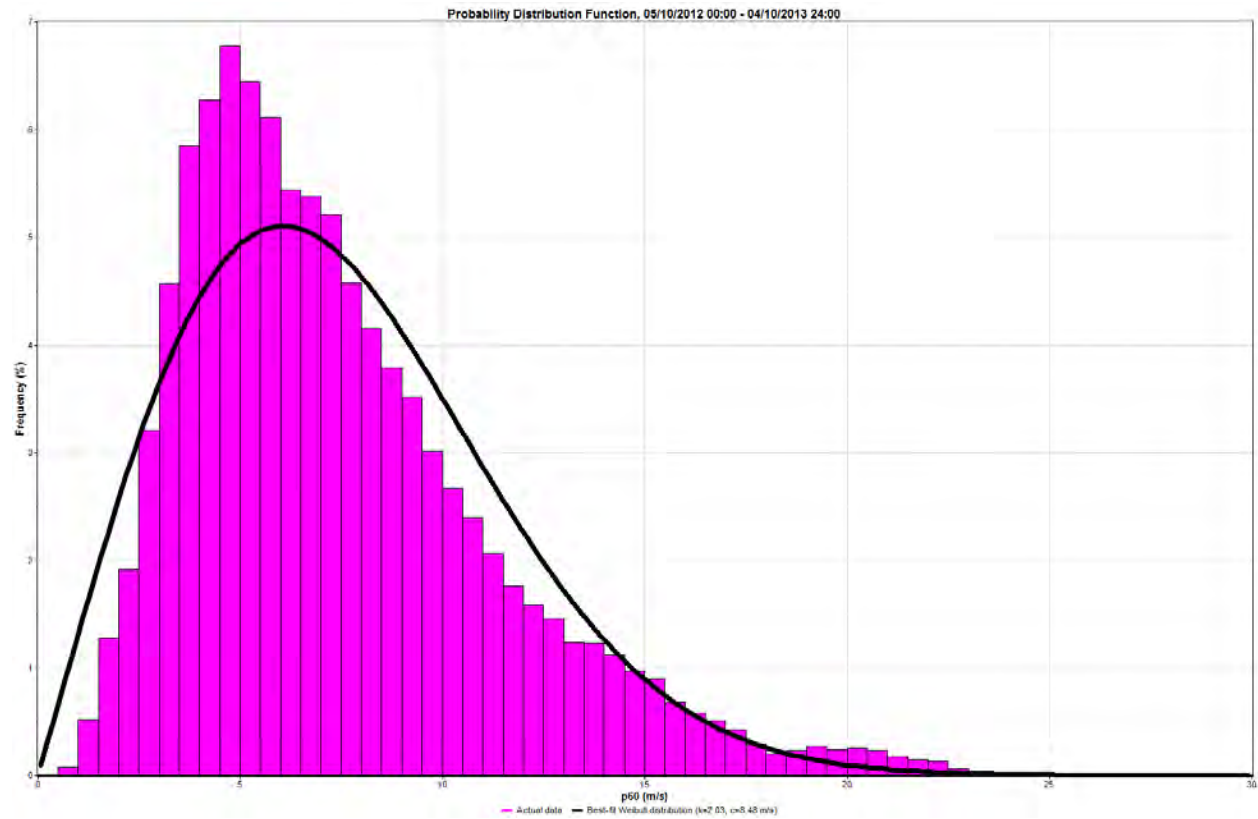


Figure 8-20 – Hub height wind speed histogram
Best-fit Weibull parameters: shape $k=2.03$; scale $c = 8.48$ m/s

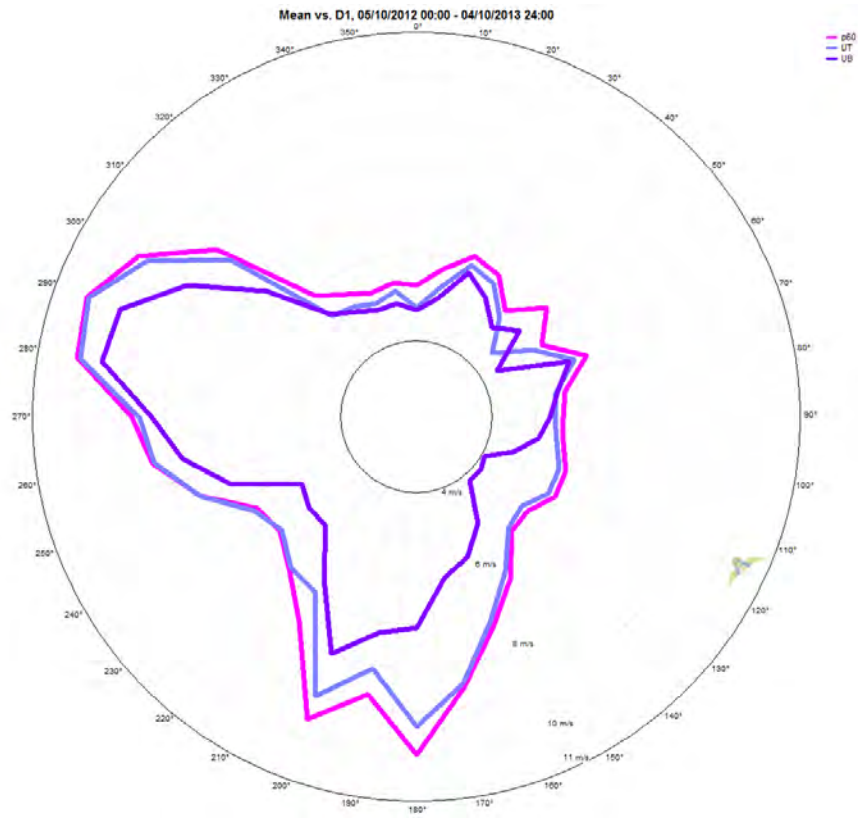


Figure 8-21 -

9 Turbulence Intensity (TI)

Turbulence Intensity (TI) is a dimensionless parameter used to quantify the degree to which the measured wind climate is affected by separated flow or turbulent eddies, which are most commonly caused by flows over rough surface elements or by solar irradiation of the ground creating thermal instability (i.e. turbulent mixing). These types of atmospheric phenomena can put mechanical loads on turbines which will cause wear and tear over time. Turbulence generally reduces wind shear by mixing horizontal momentum vertically.

TI is calculated for a 10-minute data time step as the ratio of standard deviation of the wind speed to the mean wind speed recorded.

$$TI = U_{sd}/U$$

IEC 61400-1 Edition 3 classifies wind turbulence classes with reference to a mean TI-15 value²⁵: the expected mean TI value for wind events falling into the 15 m/s speed bin. The mean TI-15 values for the classifications are: Class S, > 0.16; Class A, 0.14 to 0.16; Class B 0.12 to 0.14; and Class C, 0 to 0.12. The least turbulent class is C.

Other IEC documentation makes reference to so-called representative TI-15. The representative TI of a binned period of wind speed data is the mean of the TI values recorded over that period and in that bin plus 1.28 standard deviations. This report quotes both mean and representative TI statistics, though representative TI-15 is a good benchmark to qualify a turbulence class as it is also the 90th percentile of the TI-15.

As in section 8 on wind shear, this section of the analysis will only use data collected between 2012-Oct-05 and 2013-Oct-04

²⁵IEC 61400-12-1, 22

9.1 Mean and Representative TI Characteristics

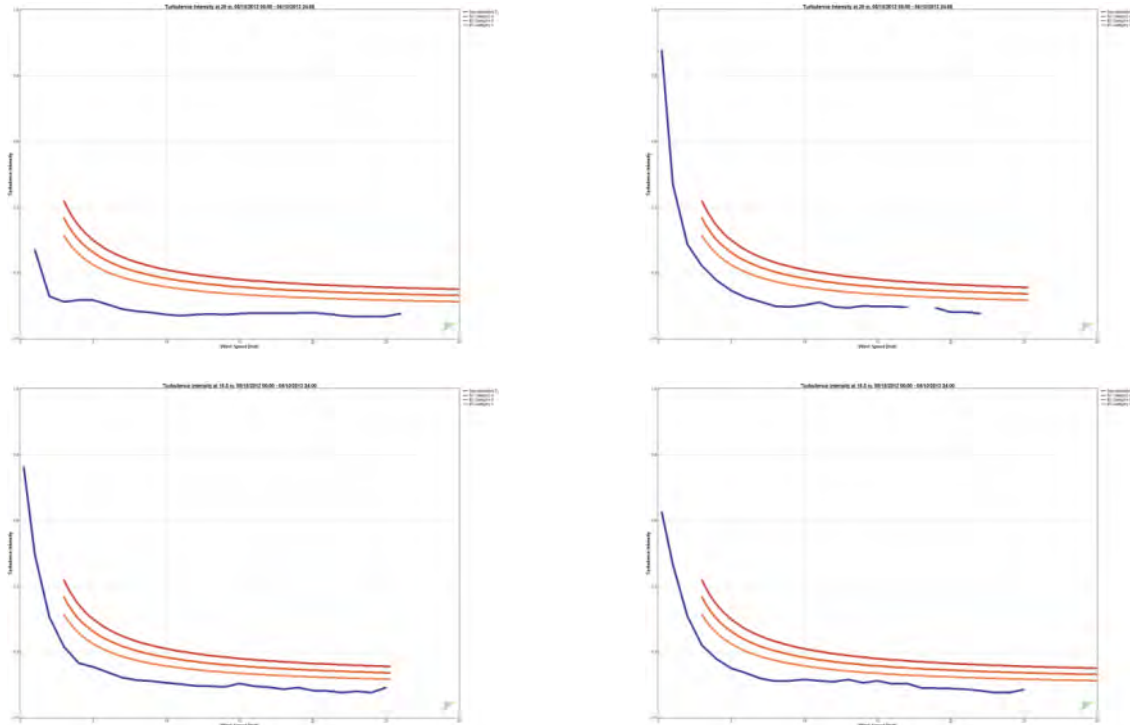


Figure 9-1 – Representative TI and IEC Turbulence Classes A, B and C;
Top: U1, U2 Bottom: U3, U4

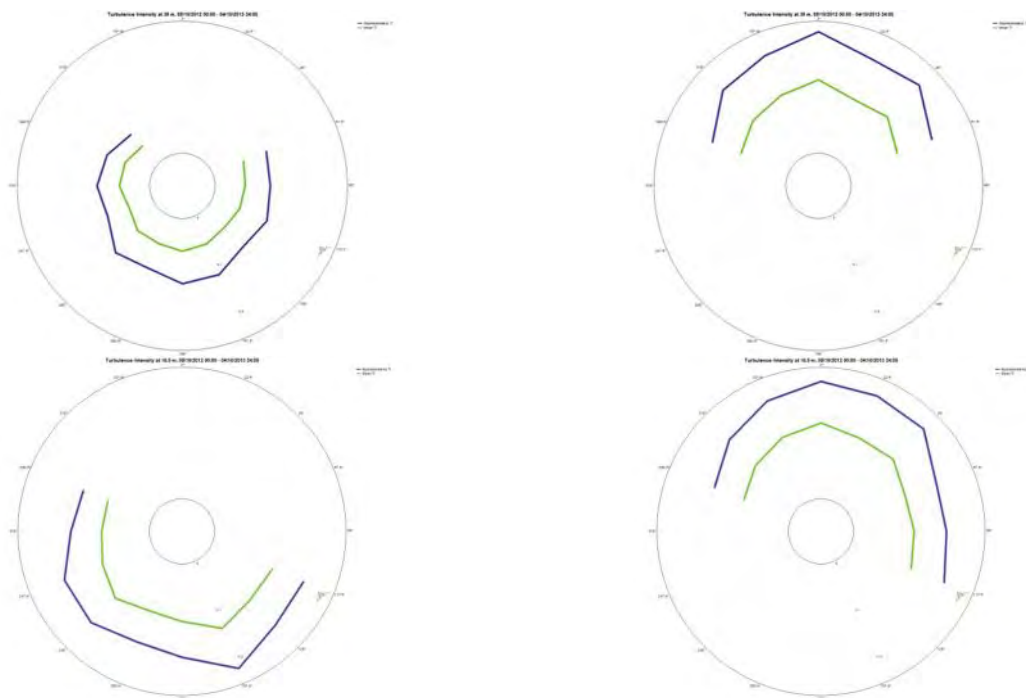


Figure 9-2 Mean (green) and Representative (purple) TI by wind direction

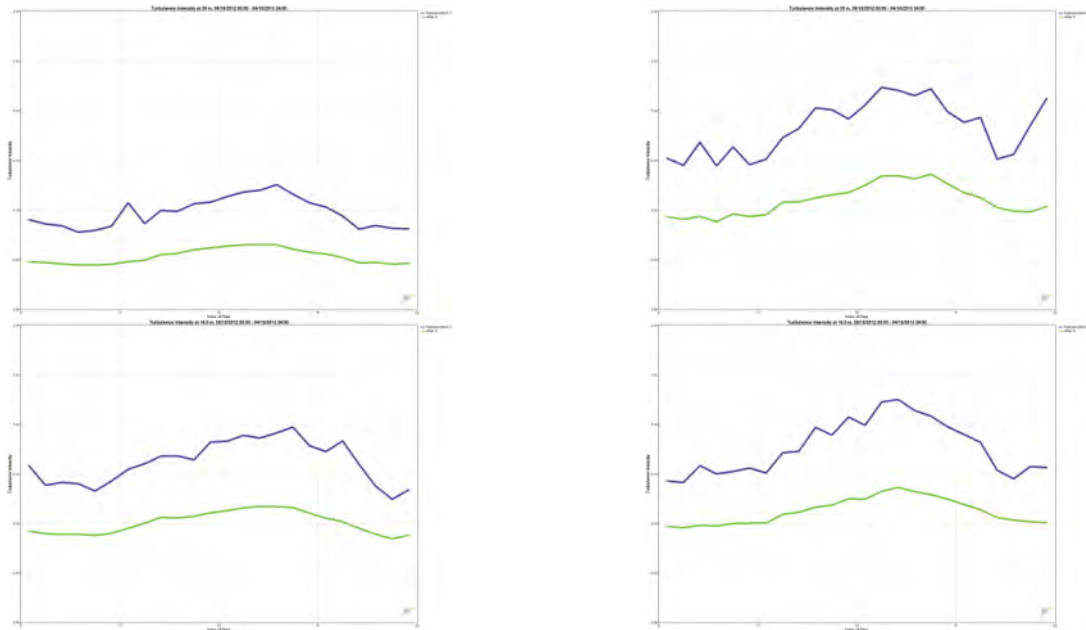


Figure 9-3- Diurnal Mean (green) and Representative (purple) TI

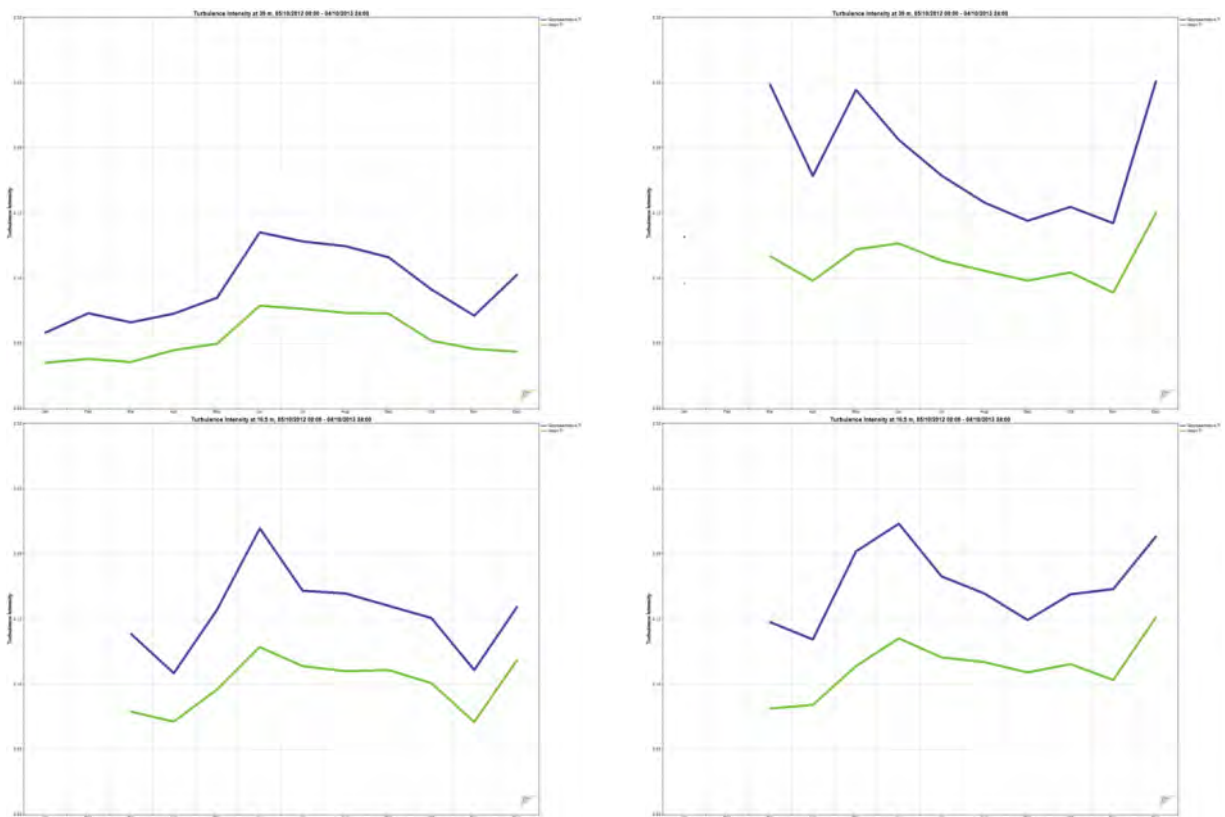


Figure 9-4 - Mean (green) and representative (purple) TI by month

During the summer months, when this site would have been snow-free, solar heating of the ground would have resulted in a less stable atmosphere around the met mast, with turbulent mixing reducing wind shear, as noted in section 8. During the winter the snow would have reflected much of the sunlight, producing for a less turbulent

wind regime. Figure 9-4 and Figure 9-3 show the stability-related turbulence regime reflected in the monthly and the mean diurnal data.

After quality control U1, the R.M. Young propeller anemometer typically reported lower TI than any of the NRG cup anemometers. This was true regardless of boom orientation or sensor height. This type of anemometer is less susceptible to the influence off-horizontal flows on its reported 10-minute standard deviation than a cup anemometer. This may be partly because of its axis orientation and blade design, but may also be because it has a longer distance constant than the cup anemometers (2.7 m vs. 2.36 m). The distance constant relates to the length of fluid flow which must pass to influence the response of an anemometer²⁶. Realistically, the R.M. Young sensor does not report TI in an equivalent fashion to the NRG cups; the readings are probably not directly comparable.

	U1	U2	U3	U4
Data points in 15 m/s bin	528	16	150	93
Mean TI at 15 m/s	0.05	0.07	0.08	0.09
Representative TI at 15 m/s	0.08	0.1	0.1	0.11
IEC3 turbulence category	C	C	C	C

Figure 9-5 - Bulk TI statistics by sensor

²⁶<http://www.renewableenergysystems.com/sublayouts/C2ECFSpecificationGlossary.aspx?pid=SPEC-I:5966%20G:7%20S:43>

9.2 TI at the Hub Height

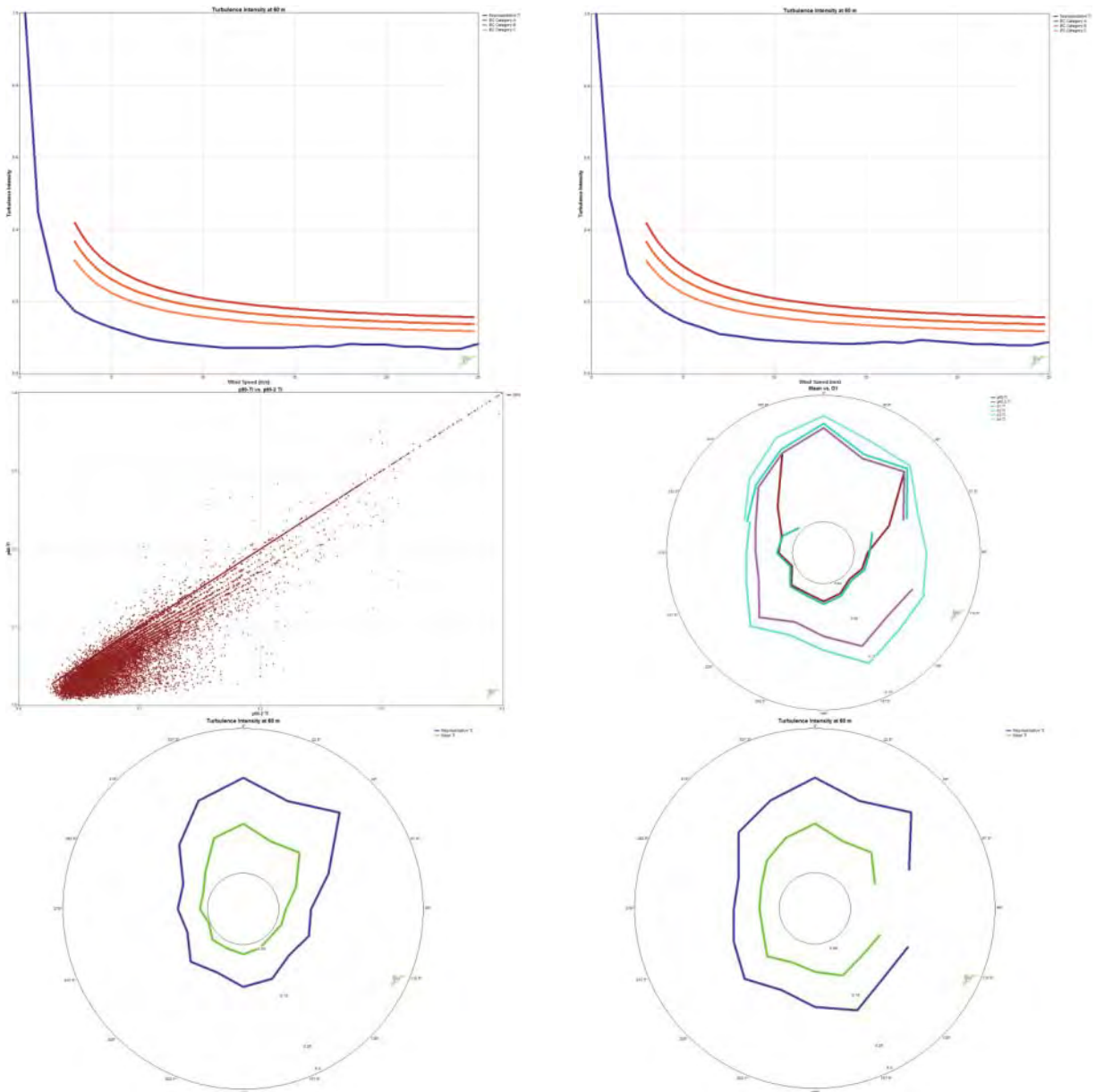


Figure 9-6 - Hub Height TI (HH-TI) characteristics

Top: Representative HH-TI vs. wind speed with U1-SD (R.M. Young); and with U3-SD

Middle Left: HH-TI with U1-SD vs. HH-TI with U3-SD

Middle Right: HH-TI rose with U1-SD (brown), with U3-SD (purple)

Bottom: Representative and mean HH-TI roses with U1-SD and with U3-SD

Turbulence intensity at the hub height is represented by a surrogate ratio of the 39 m sensor level standard deviation to the extrapolated hub height wind speed at 60 m. This TI value should uphold the principle that TI and turbulent mixing generally decreases with height as eddies dissipate as they dissipate in the boundary layer; further away from the influence of solar heating on the ground, the air should be less turbulent.

For this assessment, hub height TI results have been presented with U1-SD used in the calculations, as well as with U3-SD replacing U1-SD. Regardless, the TI class of the site is still well within the C category.

Quantity	Value	Quantity	Value
Data points in 15 m/s bin	773	Data points in 15 m/s bin	535
Mean TI at 15 m/s	0.045	Mean TI at 15 m/s	0.061
Representative TI at 15 m/s	0.073	Representative TI at 15 m/s	0.084
IEC3 turbulence category	C	IEC3 turbulence category	C

Figure 9-7 - Hub height TI statistics with U1-SD (left) and with U3-SD (right)

It is clear from the bottom-left graphic in Figure 9-8 that turbulence intensity changes in unison with the temperature at the site.

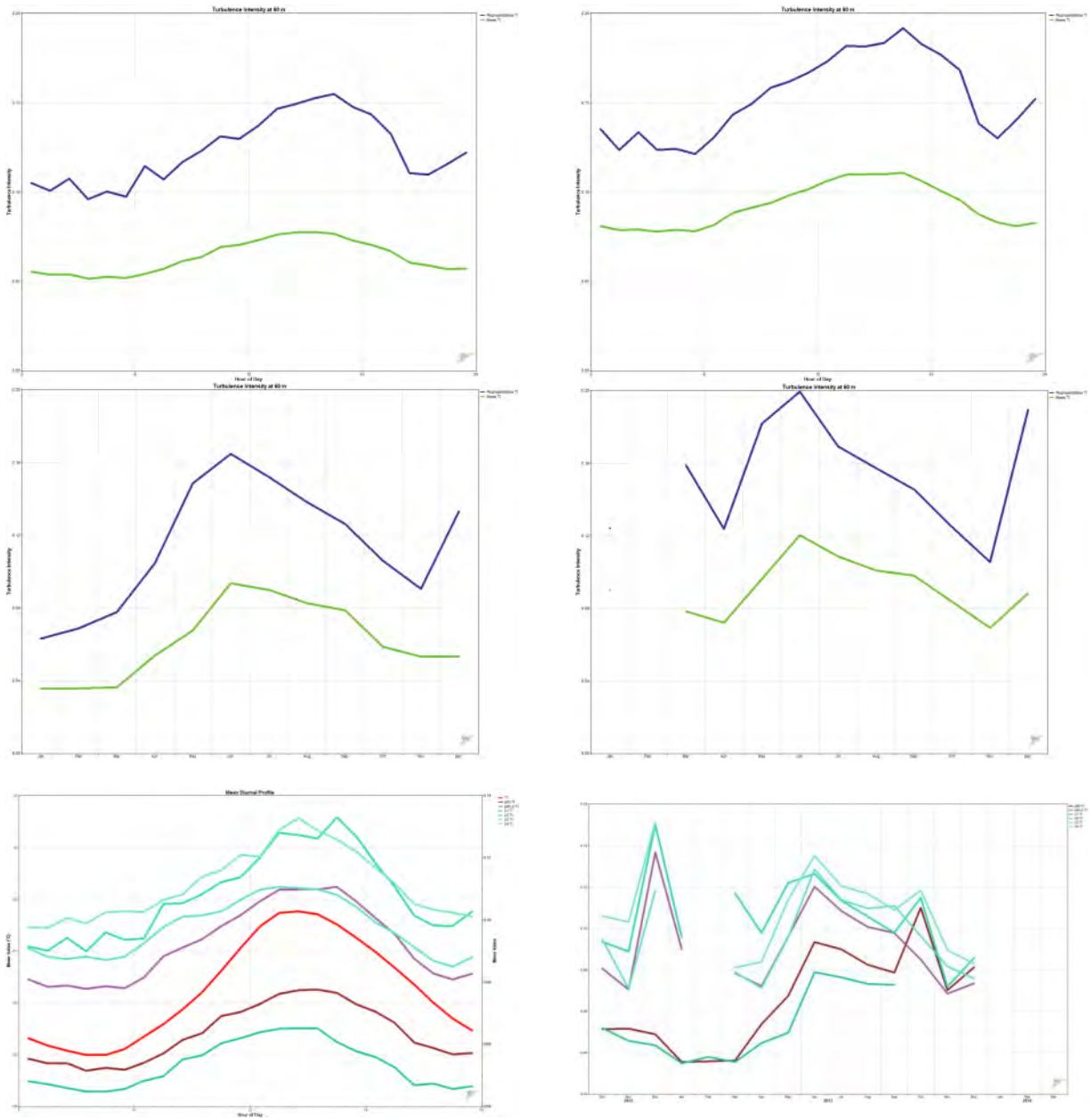


Figure 9-8 - Hub Height TI (HH-TI) characteristics

Top: Representative and mean diurnal HH-TI with U1-SD (R.M. Young); and with U3-SD

Middle: Representative and mean monthly HH-TI with U1-SD; and with U3-SD

Bottom Left: Diurnal TI for U1, U2, U3, U4; and hub height with U1-SD (brown) and with U3-SD (purple)

Bottom Right: Monthly TI for U1, U2, U3, U4; and hub height with U1-SD (brown) and with U3-SD (purple)

10 Climatological Adjustment

10.1 The Long-Term Reference Data Set

Environment Canada (EC) operates the Trail Valley climate monitoring station, 24 km southeast of Storm Hills, and 45 km north and east of Inuvik. The station has a heated Vaisala ultrasonic anemometer which would commonly be mounted 10 m above the ground, though Figure 10-3 shows it was difficult to confirm that. Regardless, the positioning of the station is less than ideal for use in industrial wind resource monitoring as it is fairly close to the ground and so likely heavily influenced by shear, veering or backing of the wind with respect to the 60 m target height, and thermal turbulence in the summer.

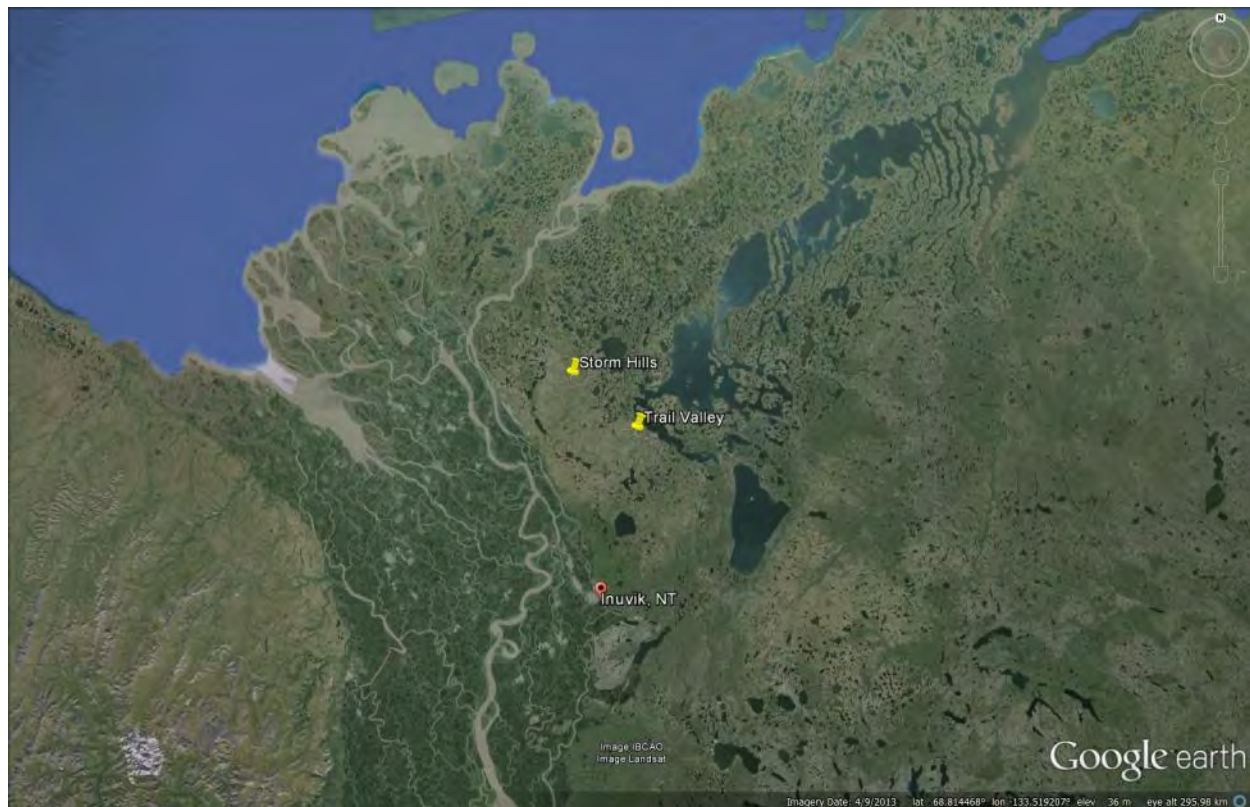


Figure 10-1 - Storm Hills and Trail Valley referenced to Inuvik, NT

The reference data set was reported in 1hr time steps, and consisted of the following useful variables:

- R-U1: the average horizontal wind speed recorded in the two minutes at the end of each observation hour (i.e. average from hr:58:00 to hr:59:59).

From 2000-Jan-01 the wind speed data was measured in knots rounded, and then converted to km/h and reported as rounded to the nearest whole-numbered value. However, as of 2013-Dec-12 the station started both measuring and reporting wind speeds rounded to the nearest km/hr, without converting from knots. This latter data was ignored as it was outside the time period concurrent with the target data. Interestingly, 2013-Dec-12 is the same day the R.M. Young sensor was damaged at Storm Hills.

- R-D1: the average wind direction referenced to true north and recorded in the two minutes at the end of each observation hour. The data was recorded in 10 degree bins from 10° to 360°. A value of 0° was a flag for calm winds.
- R-T1 : average temperature in °C (likely recorded in the two minutes at the end of each observation hour)

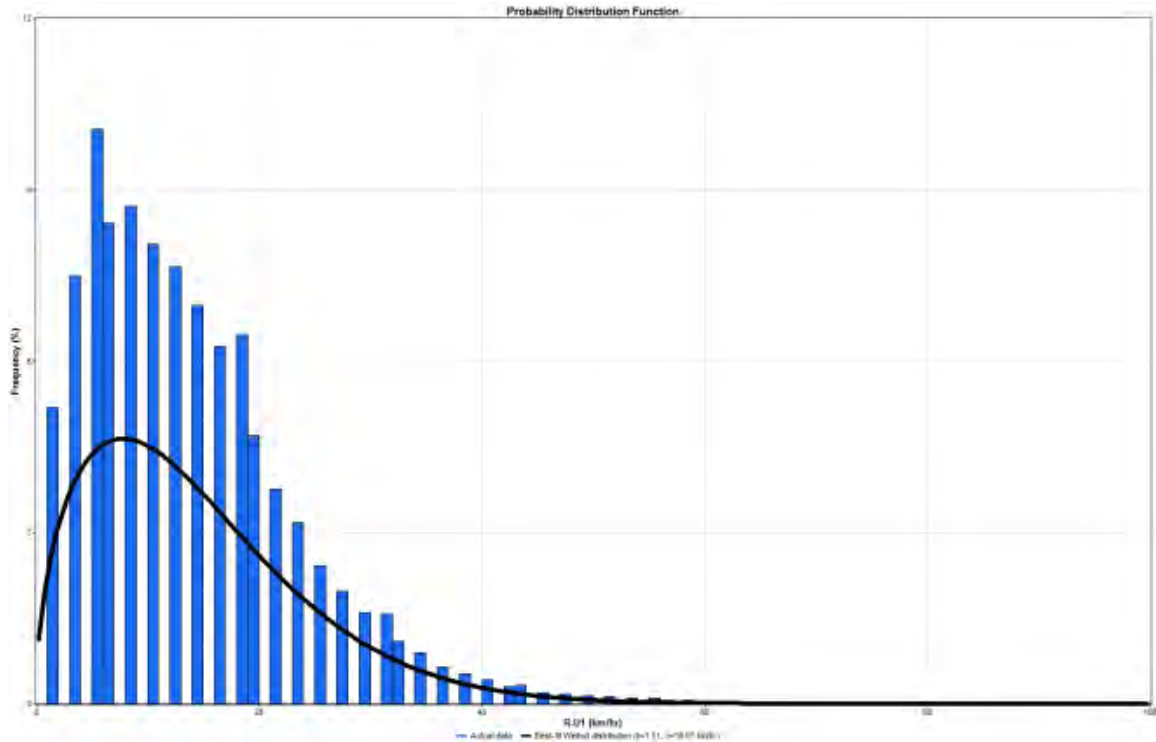


Figure 10-2 - EC Trail Valley quality-controlled reference wind speed frequency histogram, with 1km/hr wind speed binning

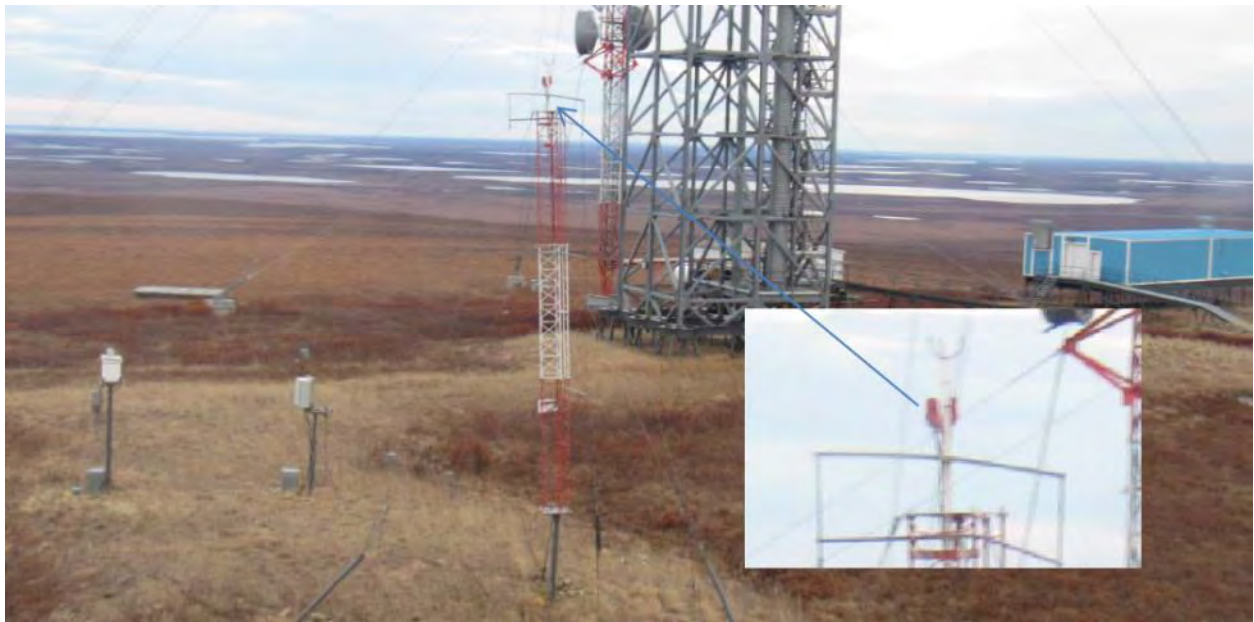


Figure 10-3 - The ultrasonic anemometer with the nearby structure in background

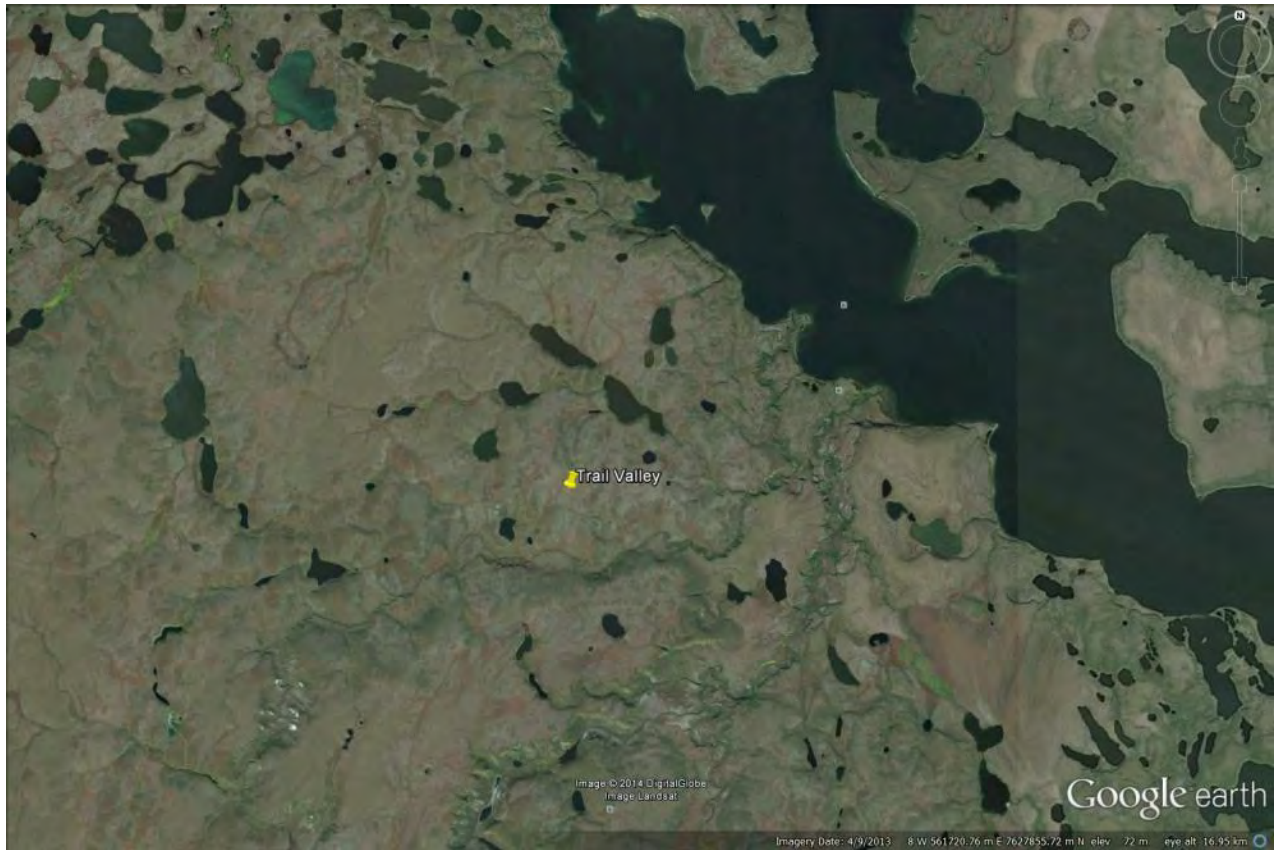


Figure 10-4 - Satellite imagery of the region surrounding the EC reference data source

In close proximity to the ultrasonic sensor mount is a much larger tower which would certainly cause wind shading when upwind of the EC sensor. Water bodies in Figure 10-3 and Figure 10-4 suggest it is to the north-northwest of the EC anemometer.

10.2 Comparison of the Concurrent Target and Raw Reference Data Sets

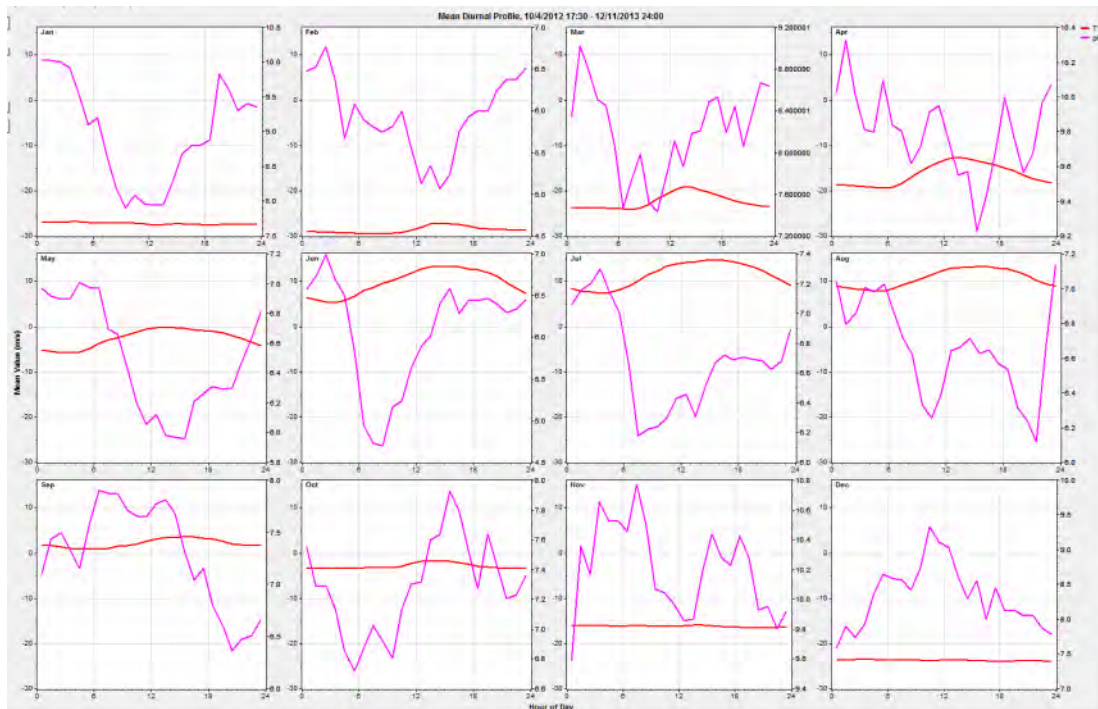


Figure 10-5 - Storm Hills target data hourly wind speed averages by month, with temperature 2012-Oct-04 to 2013-Dec-11

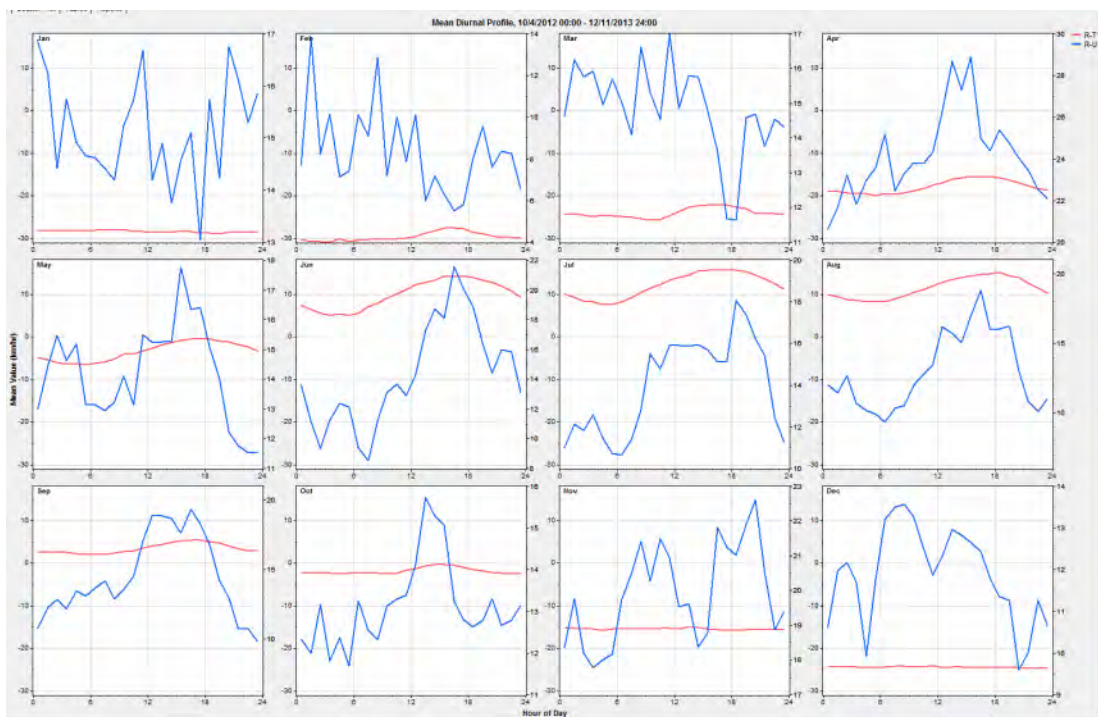


Figure 10-6 - Trail Valley reference data hourly wind speed averages by month, with temperature 2012-Oct-04 to 2013-Dec-11

The two sites show similar mid-to-late day speed profiles by month. However, being close to the surface, the Trail Valley reference data (Figure 10-6) did not show any nocturnal speed-up during the summer (May to August), rather it slowed down in the evening when the sun was lower in the sky (or set), and there would have been increased stability and shear in the lower boundary layer.



Figure 10-7 - Target (left) and un-quality controlled reference (right) wind direction frequency roses 2012-Oct-04 to 2013-Dec-11

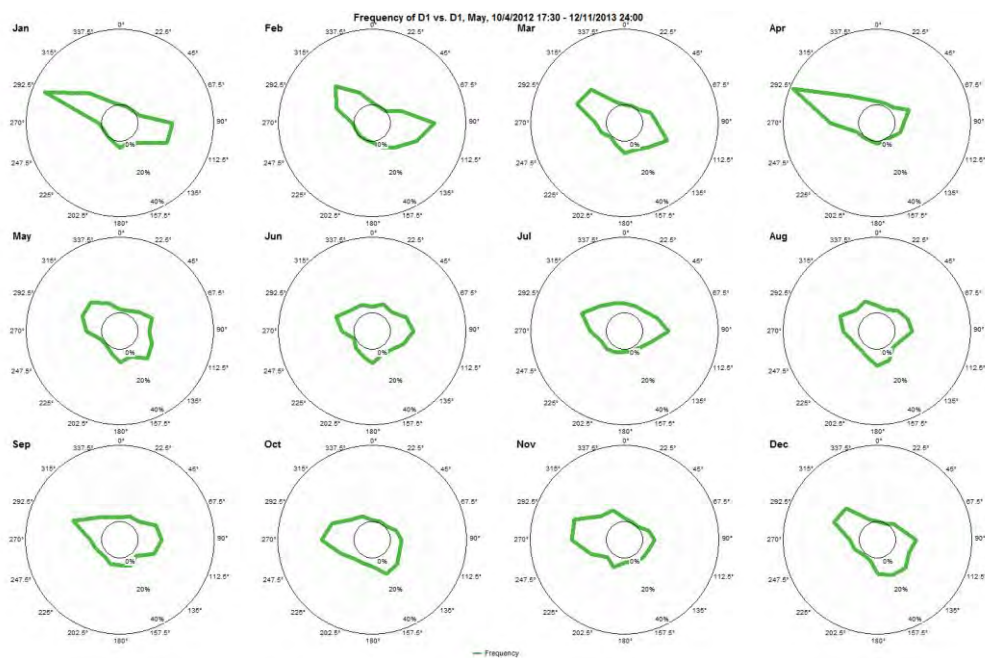


Figure 10-8 - Storm Hills target data, wind direction frequency roses by month 2012-Oct-04 to 2013-Dec-11

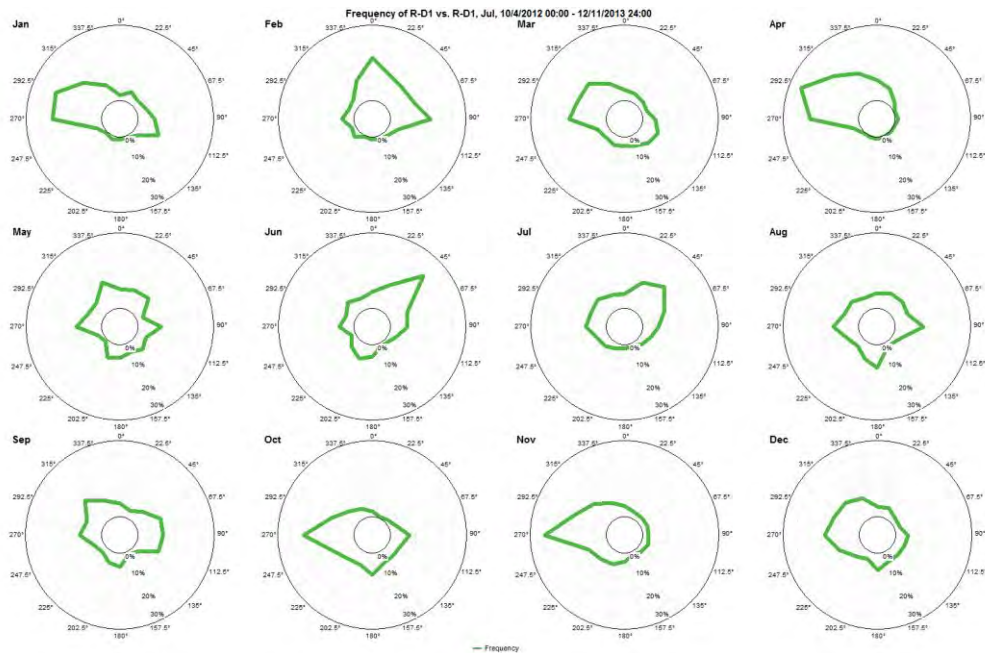


Figure 10-9 - Trail Valley target data, wind direction frequency roses by month
2012-Oct-04 to 2013-Dec-11

The monthly average wind frequency roses showed similarities during the winter months (September to April), with the exception of February. The summer months showed a significant north-northeasterly component at the EC reference site; the same direction where the sensor would be shaded by the upwind structure. This wind may be a lake breeze caused by solar radiation-induced temperature gradients between the land and the large water body to the northwest of the Trail valley site. The Storm Hills site may also see such an effect from the same water body, but because of its location, the winds would be westerly.

This analysis suggests that data from the summer months may reduce the quality of any overall correlation between the concurrent target and reference data sets.

10.3 Quality Control of the Reference Data

The EC reference data set was collected in a significantly different fashion to the target at Storm Hills. The direction data was of relatively low precision, and there was no redundant sensor at the site, so only a simple quality control process was applied to the sonic anemometer.

The anemometer wind speed data was left scaled in km/hr. If the wind direction was reported as zero (calm), then all sensor data was discarded, and if the sonic anemometer reported zero wind speed, then all sensor data was discarded.

As well, the proximity of the larger tower warranted the removal of all data reporting winds from sectors centered around the north-northwest. The range of sectors potentially affected was unclear, but it was decided that all data winds reported from within 45° of 22.5° true should be removed. This was also convenient given that the summer months at the reference site were shown in section 10.2 to have components from this direction which were likely uncorrelated to the measurements at Storm Hills.

Figure 10-2 and Figure 10-10 show the results from the reference data quality control. The conversion from knot measurements to rounded km/hr values makes the EC reference wind speed histogram appear with bin breaks and a giant spike; the Weibull fit statistics in the chart should be ignored.

The red circle in the chart at the top-right of Figure 10-10 shows that after quality control there were a significant number of concurrent data points where the winds at the target site were from northeasterly to southeasterly directions, while the reference site experienced winds from the west to the northwest. This discrepancy can be seen as a distinguishing feature between the two sites in the wind rose comparison chart. There were relatively stronger westerly and northwesterly components in the reference wind rose, while the target wind rose had stronger components from all easterly directions. Clearly the winds at the time steps circled in red were uncorrelated and so could have adversely affected the correlation used in the final climatological adjustment.

Comparison of Figure 10-8 and Figure 10-9 suggest that the uncorrelated events may have occurred between October and April. As well, when the comparison time-step is increased, the effect of the uncorrelated direction data points is reduced, which is reflected in the table in Figure 10-11 showing that the linear least-squares R^2 value improves with larger steps.

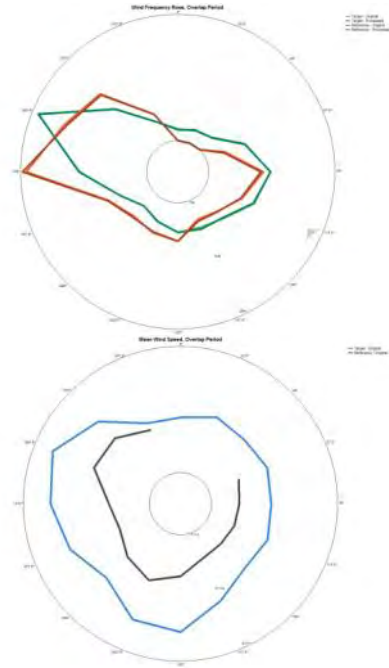
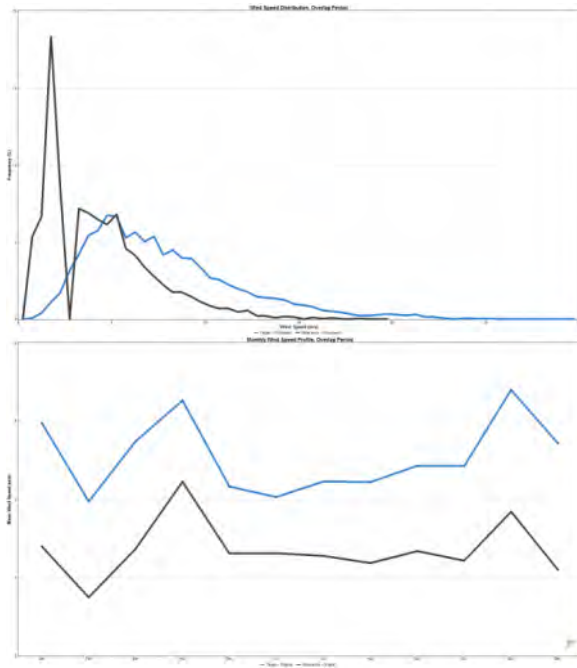
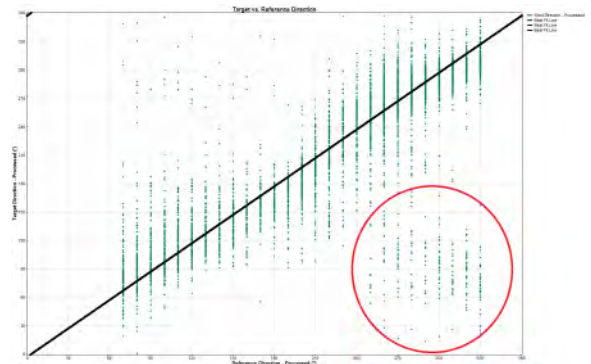
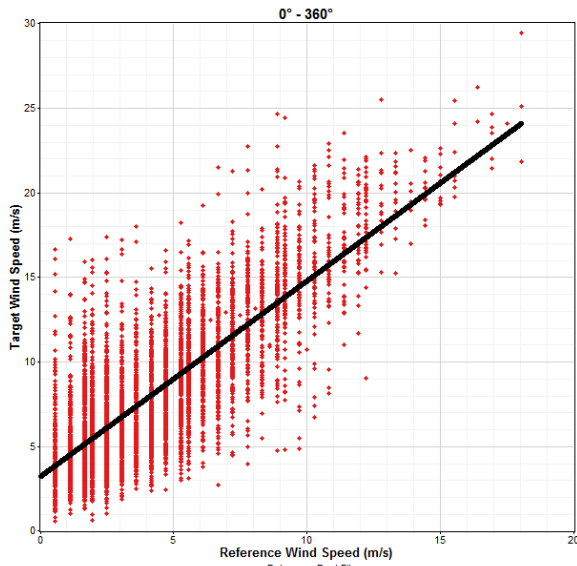


Figure 10-10- Quality-controlled 1-hour linear least-squares data set comparison between target and reference data sets
single direction sector bin

Overlap period 2012-Oct-04 to 2013-Dec-12

Top: speed and direction target vs. reference scatter plots

Middle: target (blue, green) and reference (black, orange) speed frequency profile and frequency roses

Bottom: monthly and sectorized wind speeds

10.4 Measure-Correlate-Predict (MCP) Process

Linear Least Squares (unforced) - 1 Direction Sector						
Correlation Step	1 hour	3 hours	4 hours	8 hours	12 hours	24 hours
Distance to reference site	23.6 km SE	23.6 km SE	23.6 km SE	23.6 km SE	23.6 km SE	23.6 km SE
Start of overlap	10/4/2012 17:00	10/4/2012 15:00	10/4/2012 16:00	10/4/2012 16:00	10/4/2012 12:00	10/4/2012 0:00
End of overlap	3/1/2014 0:00	3/1/2014 0:00	3/1/2014 0:00	3/1/2014 0:00	3/1/2014 0:00	3/1/2014 0:00
Overlap duration	17 months	17 months	17 months	17 months	17 months	17 months
Concurrent time steps	5,884	1,984	1,291	627	402	188
R2 - speed	0.623	0.668	0.673	0.698	0.729	0.76
R2 - direction	0.799	0.821	0.866	0.893	0.92	0.954

Figure 10-11 - Preliminary linear least-squares correlation statistics

The data sets differed in their collection and averaging periods: the Storm Hills target data was made up of 10-minute average values which were then averaged for correlation purposes to 1-hour values at the shortest; while the reference data were 2-minute averages taken at the end of every hour. Windographer offset the EC reference data set backwards in time by 40 minutes to maximize correlation potential. This likely accounted for differences owing to the relative proximity of the sites, as well as to account for the different sampling and averaging techniques.

Figure 10-11 compares some basic correlation statistics for various comparison time steps where a simple single-sector linear least-squares correlation regime was used. It was decided that 24 hour time-step was too long a period, as it would not capture any of the nocturnal wind shear effects noted in the shear analysis. 3-4 hours was a reasonable time-step in order to smooth out the sampling from in the EC reference data set. The 8 and 12-hour comparison periods offered small sample sizes and were thought less likely to capture diurnal variations in the final analysis. The one hour time-step data set was retained for use with a robust matrix time-series correlation algorithm offered by Windographer.

The bi-polar nature of the wind frequency roses for both the quality-controlled reference and target data sets, and the generally good R^2 values of the direction correlations in Figure 10-11 implied that sector-wise binning of the data was not necessary. However, the correlation statistics for a linear least-squares correlation regime using 4-sector binning is offered in Appendix Figure 11-39. Using 4-sector binning, R^2 values for the important wind sectors (135° - 315°) were extremely good for winds from the western sector, but not so good from the eastern or southern sectors, regardless of the correlation time step.

After further analysis, it was decided to work with only one wind direction sector for correlation between the wind speed data sets. However, for wind direction correlation 12 sectors were used in the 1-hour comparisons, and 4 sectors were used for the 3-hour and 4-hour comparisons.

A number of correlation algorithms were tested against one another for each of the 1, 3, and 4-hr comparison time steps. Ultimately, in all three cases, a matrix time-series correlation algorithm was employed²⁷. In each of those algorithms the target and reference wind speed data sets were binned in 1 m/s and 5 km/hr (1.39 m/s) sets respectively. The improvement in the shape of the reference data set histogram with this binning scheme can be seen in Figure 10-12.

²⁷Windographer 3.2.5 documentation: Matrix Time-series Algorithm

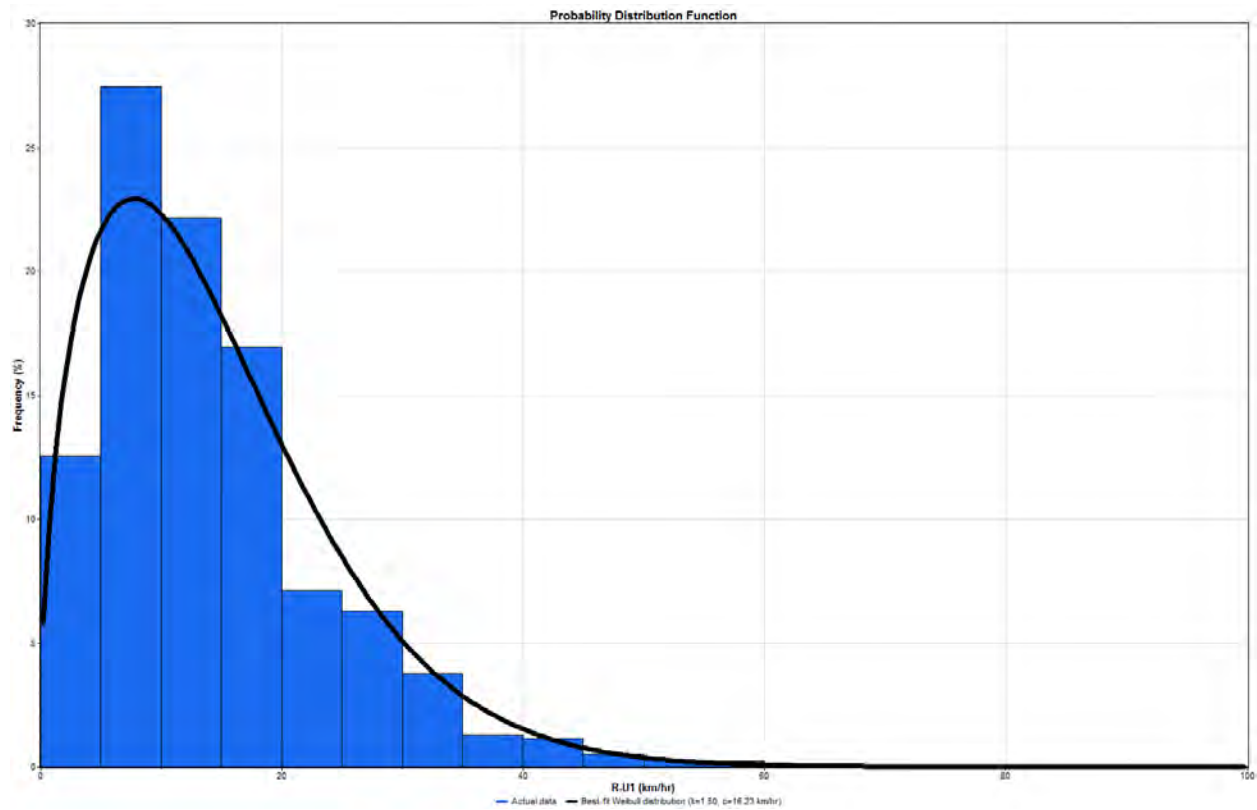


Figure 10-12 - EC Trail Valley reference histogram, with 5 km/hr wind speed bins

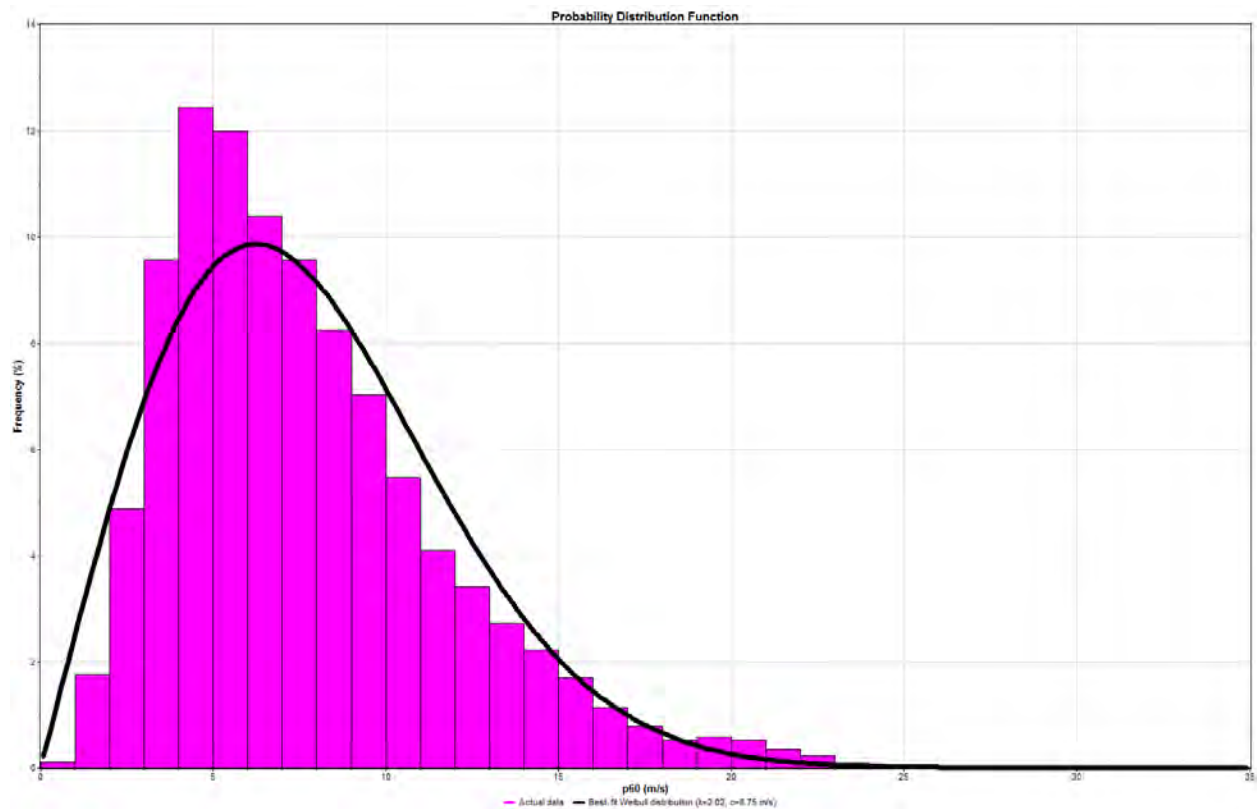


Figure 10-13 - Storm Hills target histogram, with 1 m/s wind speed bins

Figure 10-14 shows the results of correlation algorithm testing for linear least-squares and matrix time-series techniques. In all, three tests were employed: the first alternated between five hour periods of data correlation of the target and reference sets, followed by a five hour synthesis of the target data set and analysis of the resulting error statistics; the second and third tests used ten and fifteen-hour alternating periods in the same fashion.

The 1-hour comparison time-step correlation was found best suited to a matrix time-series algorithm employing an intermediate-stage analysis technique which binned data using a moving average of values covering three hours worth of time-steps. The 3-hour and 4-hour comparison steps used the same algorithm, but with an intermediate-stage that binned data using 9-hour and 12-hour moving averages respectively. The synthesis testing error statistics quoted in Figure 10-14 are: the mean bias error (MBE); the mean absolute error (MAE); the root mean-squared error (RMSE); and the error in the frequency distribution (DISE).

Synthesis Test	Error Statistics	1-hr time-step		3-hr time-step		4-hr time-step	
		LLS	MTS 3-hr	LLS	MTS 9-hr	LLS	MTS 12-hr
Alternating 5-hr	MBE (%)	0.201	0.691				
	MAE (%)	24.1	17.2				
	RMSE (%)	31.2	23.5				
	DISE (%)	30.8	5.4				
Alternating 10-hr	MBE (%)	-1.9	-2.5	0.0465	0.423		
	MAE (%)	23.6	19.8	21.6	18		
	RMSE (%)	30.6	26.7	28	24		
	DISE (%)	26.1	4.29	23.6	8.56		
Alternating 15-hr	MBE (%)	0.224	0.328	0.0576	0.457	-1.91	-1.46
	MAE (%)	23.9	22.4	22.3	21.4	20.7	19.6
	RMSE (%)	31	29.4	29.2	28.2	27.4	25.6
	DISE (%)	30.5	5.72	16.6	6.27	23.7	11.9

Figure 10-14 - MCP testing and error statistics; linear least-squares vs. matrix time-series algorithms

The correlation statistics for the wind direction comparisons can be found in Appendix 11.4. It should be noted that the MCP process may have been improved if the quality control of the reference data set had included a data selection step which excluded a time steps when the wind direction was not reasonably well correlated with the target wind direction. This was an oversight on the part of the analyst and could have been done with a scatter plot analysis but time did not allow for any modification to the analysis.

10.5 Characterizing the Long-Term Wind Climate

The final summary of the three correlation schemes are highlighted in the figures below.

Examination of Figure 10-10 and the summary figures in this section suggest the wind regime during the period of data collection was not normal from a climatological perspective. Both the target and reference data sets show a significantly different month-by-month wind speed profile recorded during the overlap period than the reference set shows over the long-term.

The testing statistics (Figure 10-14) showed little difference in efficacy between the three matrix time-series MCP schemes employed. The mean of monthly-mean (MoMM) long-term wind speeds at 60 m were estimated to be 7.87 m/s, 7.73 m/s and 7.96 m/s for the 1-hour, 3-hour, and 4-hour comparison time-steps respectively, though a thorough uncertainty analysis should be carried out at some point because the synthesis error statistics previously quoted are significant; the by-product of a less-than ideal reference data set. The three-hour time-step MCP statistics were quoted in the executive summary.

	Target Original	Target Processed	Final
Start time	10/4/2012 17:30	10/4/2012 17:00	1/1/2000 0:00
End time	3/7/2014 0:00	3/7/2014 0:00	3/7/2014 0:00
Duration	17 months	17 months	14 years
Time step	10 minutes	60 minutes	60 minutes
Time steps - speed	47,312	7,999	67,503
Time steps - direction	57,045	7,999	68,884
Mean speed @ 60 m	7.725 m/s	7.705 m/s	7.831 m/s
MoMM spd. @ 60 m	7.670 m/s	7.649 m/s	7.871 m/s
Min. speed @ 60 m	0.223 m/s	0.575 m/s	0.269 m/s
Max. speed @ 60 m	32.169 m/s	29.413 m/s	37.996 m/s
Weibull k @ 60 m	2.02	2.039	2.187
Weibull c @ 60 m	8.750 m/s	8.732 m/s	8.868 m/s
Mean WPD @ 60 m	602 W/m2	540 W/m2	528 W/m2
Mean dir. @ 39 m	274.6°	279.0°	244.9°

Figure 10-15- 1-hour comparison time-step MCP statistics

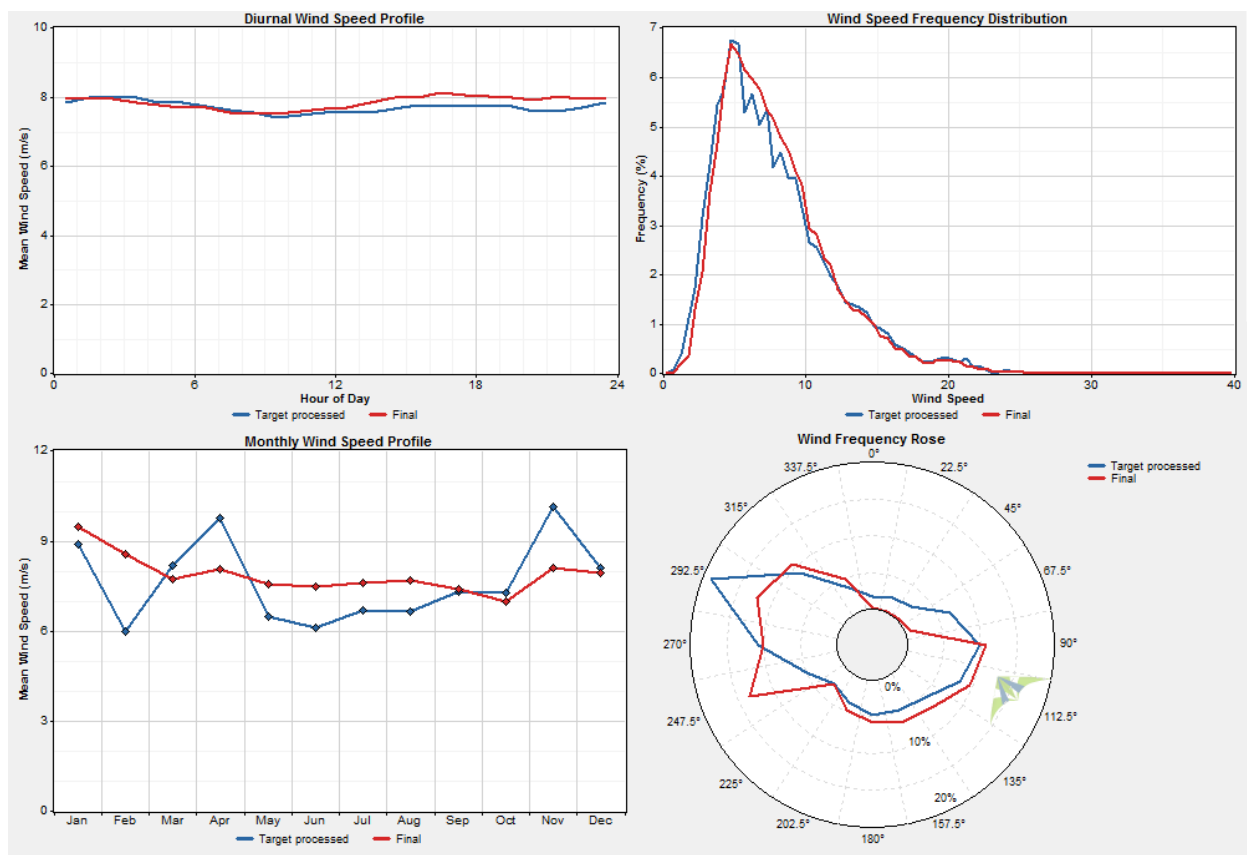


Figure 10-16 - Summary charts for the 1-hour comparison time-step MCP results
Target data set processed to 1-hour (blue), and the final synthesized target data set (red)

Top: diurnal profiles; wind speed frequency profile
Bottom: monthly wind speed profile; wind frequency roses

	Target Original	Target Processed	Final
Start time	10/4/2012 17:30	10/4/2012 15:00	1/1/2000 0:00
End time	3/7/2014 0:00	3/7/2014 0:00	3/7/2014 0:00
Duration	17 months	17 months	14 years
Time step	10 minutes	3 hours	3 hours
Time steps - speed	47,312	2,673	22,756
Time steps - direction	57,045	2,673	22,756
Mean speed @ 60 m	7.725 m/s	7.703 m/s	7.685 m/s
MoMM spd. @ 60 m	7.670 m/s	7.646 m/s	7.730 m/s
Min. speed @ 60 m	0.223 m/s	1.066 m/s	1.066 m/s
Max. speed @ 60 m	32.169 m/s	25.227 m/s	34.075 m/s
Weibull k @ 60 m	2.02	2.072	2.185
Weibull c @ 60 m	8.750 m/s	8.729 m/s	8.703 m/s
Mean WPD @ 60 m	602 W/m2	531 W/m2	503 W/m2
Mean dir. @ 39 m	274.6°	278.5°	244.9°

Figure 10-17 - 3-hour comparison time-step MCP statistics

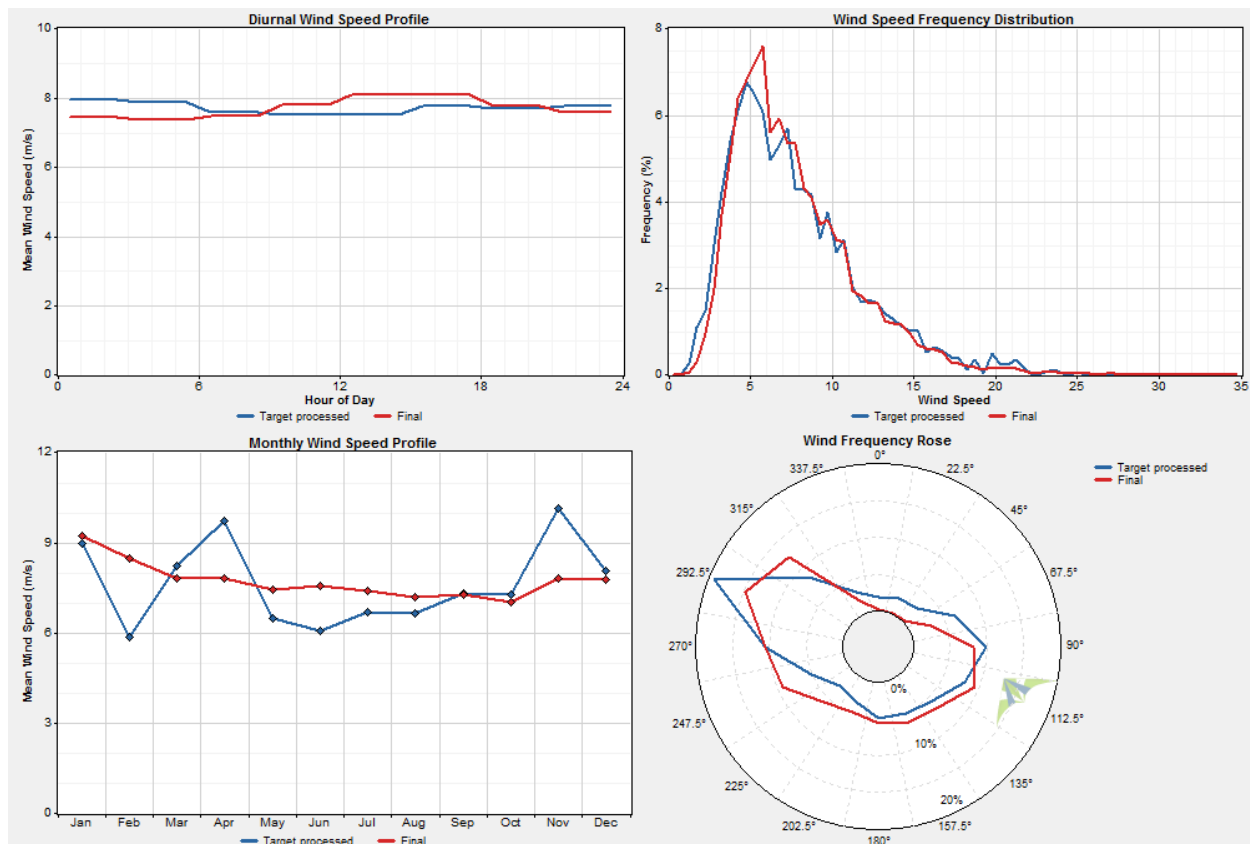


Figure 10-18 - Summary charts for the 3-hour comparison time-step MCP results
Target data set processed to 3-hours (blue), and the final synthesized target data set (red)

Top: diurnal profiles; wind speed frequency profile
Bottom: monthly wind speed profile; wind frequency roses

	Target Original	Target Processed	Final
Start time	10/4/2012 17:30	10/4/2012 16:00	1/1/2000 0:00
End time	3/7/2014 0:00	3/7/2014 0:00	3/7/2014 0:00
Duration	17 months	17 months	14 years
Time step	10 minutes	4 hours	4 hours
Time steps - speed	47,312	1,889	15,533
Time steps - direction	57,045	1,889	15,533
Mean speed @ 60 m	7.725 m/s	7.823 m/s	7.901 m/s
MoMM spd. @ 60 m	7.670 m/s	7.772 m/s	7.960 m/s
Min. speed @ 60 m	0.223 m/s	1.249 m/s	1.209 m/s
Max. speed @ 60 m	32.169 m/s	24.220 m/s	34.686 m/s
Weibull k @ 60 m	2.02	2.117	2.21
Weibull c @ 60 m	8.750 m/s	8.866 m/s	8.946 m/s
Mean WPD @ 60 m	602 W/m2	544 W/m2	538 W/m2
Mean dir. @ 39 m	274.6°	278.2°	243.0°

Figure 10-19 -- 4-hour comparison time-step MCP statistics

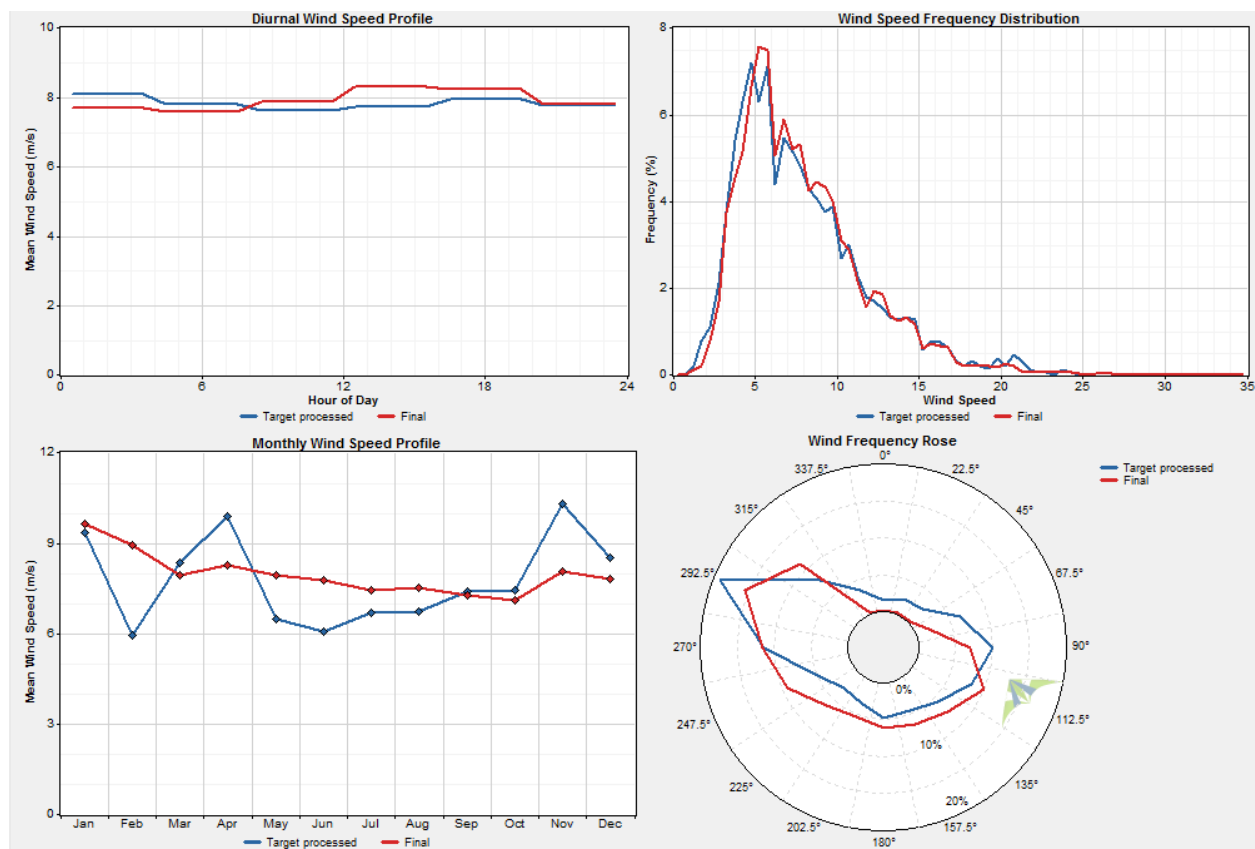


Figure 10-20 - Summary charts for the 4-hour comparison time-step MCP results
Target data set processed to 4-hours (blue), and the final synthesized target data set (red)

Top: diurnal profiles; wind speed frequency profile
Bottom: monthly wind speed profile; wind frequency roses

10.5.1 3-Hour Time-Step MCP Climatological Adjustment Results

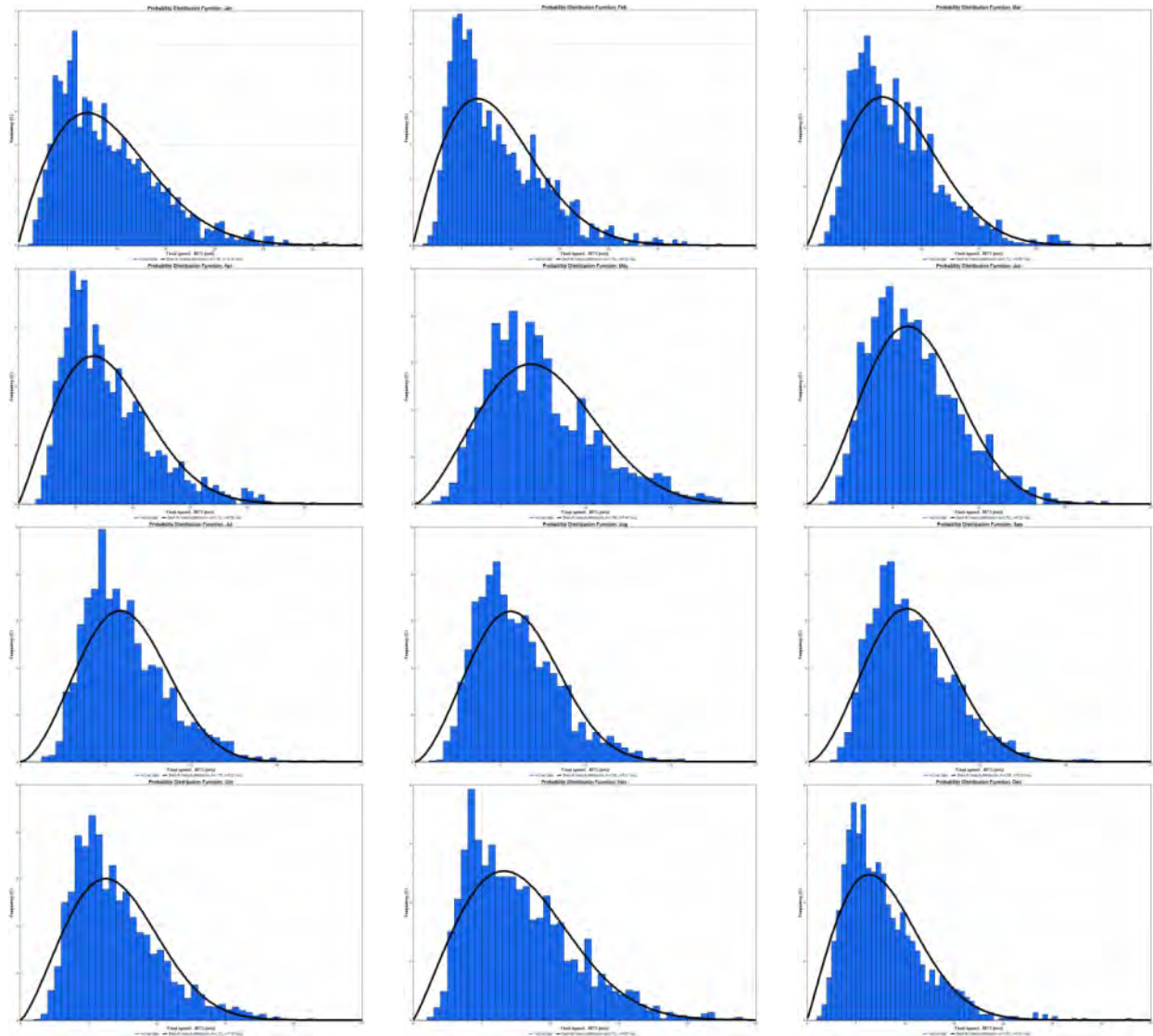


Figure 10-21 - 3-hour comparison time step MCP results
Monthly wind speed histograms

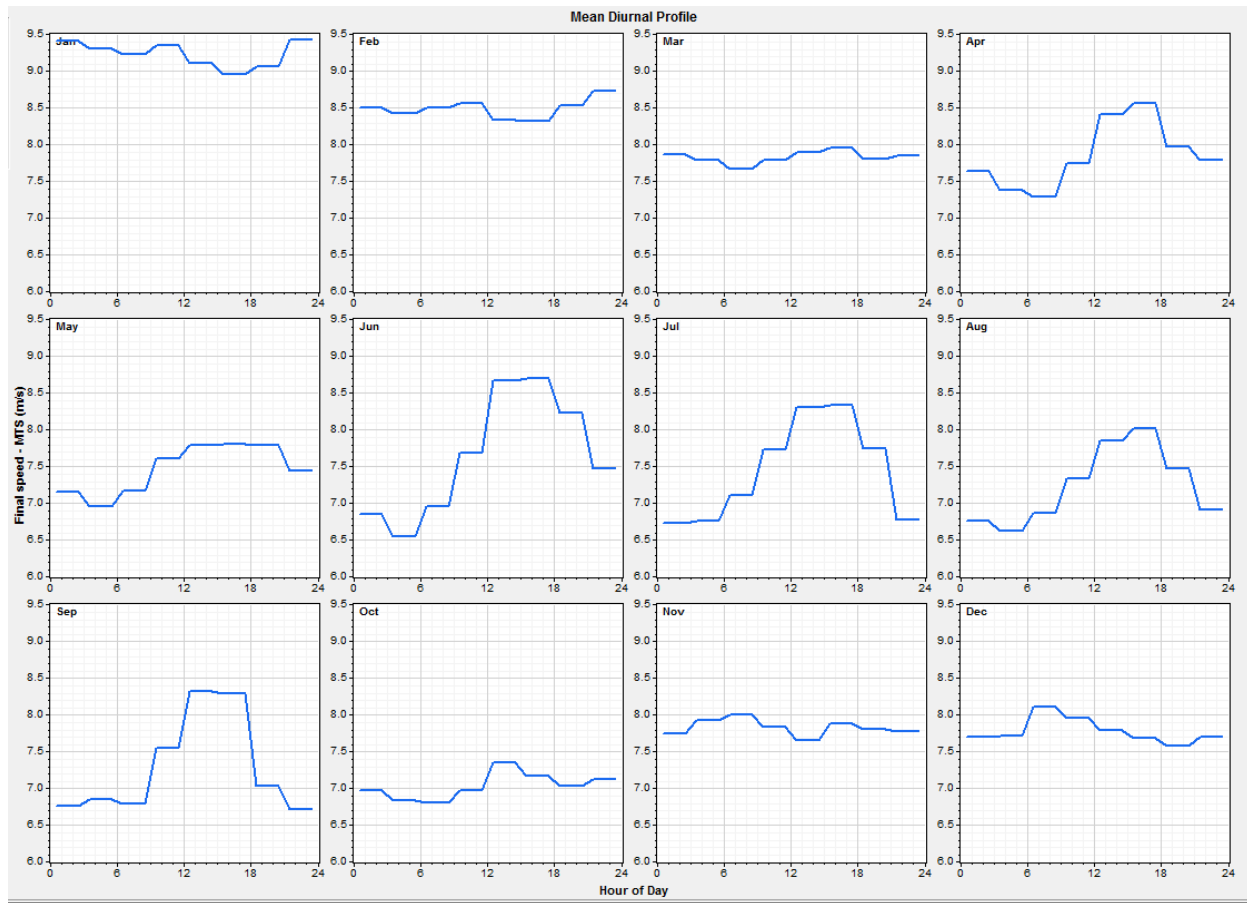


Figure 10-22 - 3-hour comparison time step MCP results
Diurnal wind speed profile

The diurnal wind speed profiles in Figure 10-22 reveal that the reference data set effectively washed out the overnight jet recorded at the Storm Hills target site. A matrix time-series correlation algorithm should preserve diurnal patterns in the target data set, but this didn't happen for any of the three comparison time-steps studied.

The previously noted quality control issues related to the reference data set reporting un-correlated wind directions implies that the wind frequency roses in Figure 10-23 may present results that are the consequence of data which should have been removed. Best practice would be to assume the standard wind frequency roses computed with the Storm Hills data is valid; a fairly good assumption.

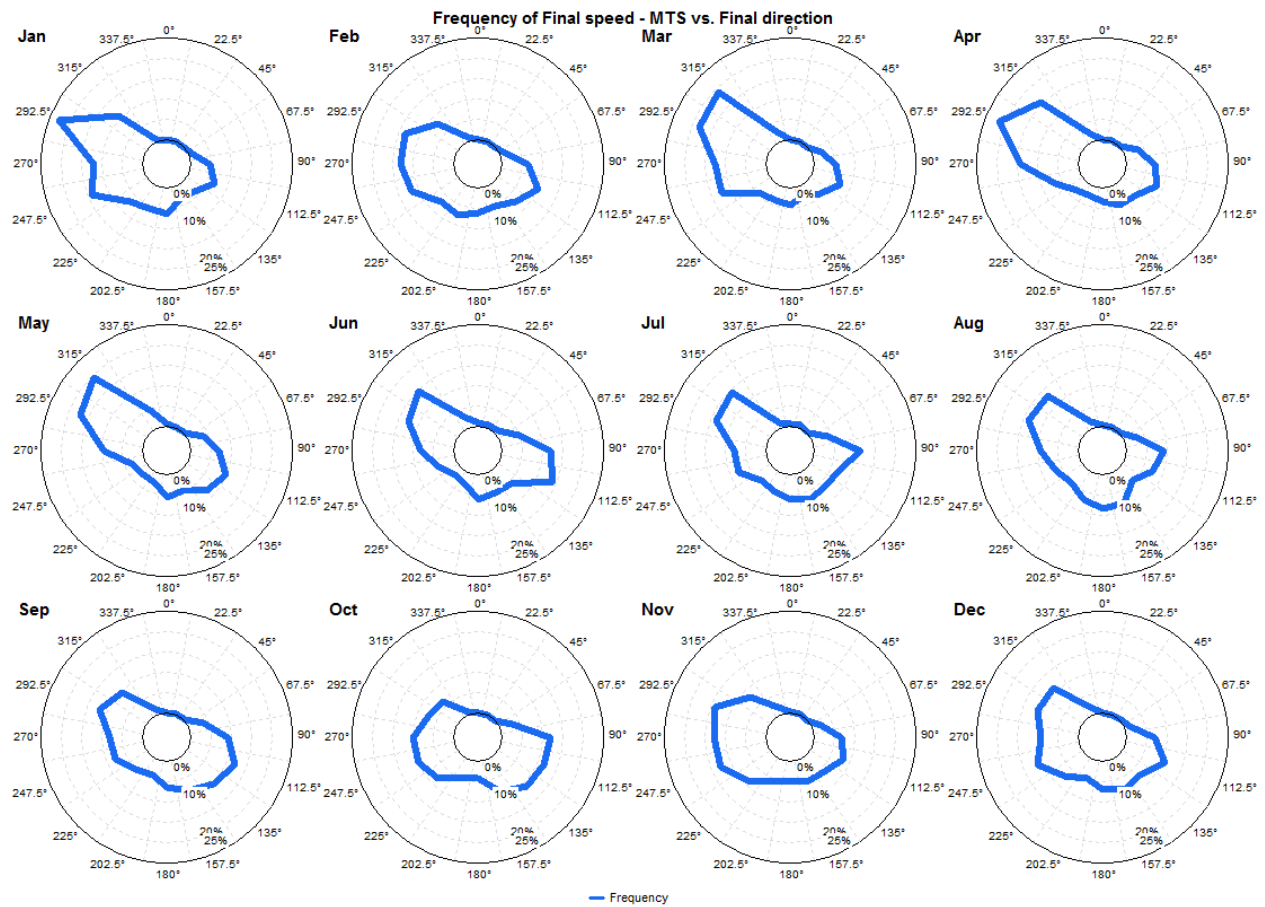


Figure 10-23 - 3-hour comparison time step MCP results
Monthly wind direction frequency roses

11 Appendices

11.1 Data Recovery Rates By Month and Hour of Day

11.1.1 Physical Sensors (data to 2013-Dec-12)

Hour	Jan	Feb	Mar	Apr	May	Jun	Jul	Aug	Sep	Oct	Nov	Dec	All
00:00 - 01:00	27.151	28.869	55.856	70.556	59.677	60	59.677	52.688	60	31.897	26.111	24.194	41.184
01:00 - 02:00	27.419	29.167	55.405	70.556	58.065	60	58.065	48.387	60	32.759	22.222	26.344	40.669
02:00 - 03:00	27.419	28.274	56.306	68.889	58.065	61.667	66.667	44.624	61.111	29.31	22.778	26.882	40.734
03:00 - 04:00	27.419	29.167	54.505	60	55.376	66.111	80.645	52.151	58.333	30.747	23.889	25.269	41.506
04:00 - 05:00	28.495	32.143	54.505	58.333	56.989	58.333	75.806	61.29	56.667	35.057	22.5	25	41.956
05:00 - 06:00	30.376	30.06	52.703	60.556	63.441	60	70.968	68.28	51.111	37.356	23.333	25	42.6
06:00 - 07:00	30.645	29.167	52.252	63.889	66.667	53.889	77.957	69.355	48.889	35.345	24.444	26.344	42.954
07:00 - 08:00	32.796	30.357	47.748	65.556	65.591	46.111	76.344	67.742	49.444	38.793	21.944	26.344	42.535
08:00 - 09:00	34.14	30.06	43.694	71.111	64.516	54.444	70.43	66.129	55	37.356	20.833	25.806	42.632
09:00 - 10:00	32.258	30.357	45.045	71.111	63.441	55	63.978	64.516	58.333	37.931	22.778	22.849	42.149
10:00 - 11:00	30.108	31.548	40.541	72.222	58.065	54.444	62.903	65.591	55.556	38.793	24.722	21.505	41.409
11:00 - 12:00	30.914	31.845	45.045	76.667	65.591	58.333	60.753	65.591	53.333	37.069	25.556	23.387	42.664
12:00 - 13:00	31.183	32.143	50.45	72.222	66.129	55.556	65.054	59.14	55.556	37.931	26.667	20.161	42.568
13:00 - 14:00	32.258	33.631	58.559	77.222	65.054	52.778	56.452	58.602	56.667	37.644	26.667	21.774	43.179
14:00 - 15:00	33.065	31.548	60.811	72.778	65.591	54.444	51.075	58.602	55.556	37.356	25.556	21.774	42.535
15:00 - 16:00	31.72	31.845	64.414	77.778	67.204	52.778	52.151	55.914	48.333	36.782	26.667	22.043	42.535
16:00 - 17:00	31.72	29.762	63.514	79.444	63.978	50	48.925	50.538	47.778	36.782	28.056	23.387	41.763
17:00 - 18:00	32.258	26.19	64.414	75	64.516	57.222	46.237	46.774	48.889	34.758	26.389	22.043	40.791
18:00 - 19:00	31.183	25	63.063	75.556	67.742	59.444	53.226	47.849	50	35.593	23.333	25	41.426
19:00 - 20:00	27.688	26.488	53.153	76.667	70.43	56.667	51.075	46.237	53.333	33.898	23.889	24.731	40.334
20:00 - 21:00	28.763	29.464	51.802	75.556	61.29	49.444	44.624	45.161	51.111	32.768	22.5	23.118	38.6
21:00 - 22:00	30.645	27.976	55.856	75	62.903	56.667	49.462	51.613	58.889	29.379	20.833	21.774	39.82
22:00 - 23:00	28.763	28.571	52.252	76.667	63.441	56.111	50.538	56.989	56.667	30.508	22.5	23.118	40.238
23:00 - 24:00	27.688	28.274	56.757	67.778	66.129	54.444	51.075	57.527	56.111	30.791	26.389	23.118	40.462

Figure 11-1 - Anemometer U1 Post-QC diurnal data recovery rates (%) by month

Hour	Jan	Feb	Mar	Apr	May	Jun	Jul	Aug	Sep	Oct	Nov	Dec	All
00:00 - 01:00	1.075	0	2.703	11.667	19.355	29.444	40.86	34.409	21.667	8.046	9.444	7.796	12.548
01:00 - 02:00	1.613	0	2.252	6.111	21.505	25	31.72	38.172	19.444	8.333	8.333	5.645	11.326
02:00 - 03:00	1.613	0	2.252	10	20.968	22.778	35.484	37.097	17.222	8.333	8.056	4.032	11.197
03:00 - 04:00	1.075	0	0.45	17.778	16.667	19.444	24.731	35.484	23.333	9.77	10	3.495	10.94
04:00 - 05:00	1.613	0	1.351	14.444	20.968	21.111	23.118	31.183	20.556	10.345	10.833	5.376	11.1
05:00 - 06:00	1.613	0	3.604	11.111	20.968	17.778	21.505	26.882	16.667	8.333	8.333	6.183	9.878
06:00 - 07:00	1.075	0	4.054	8.333	20.968	15	20.43	25.269	19.444	10.92	8.333	6.72	9.878
07:00 - 08:00	1.613	0	4.505	14.444	20.43	16.667	24.194	24.194	18.889	4.023	9.167	4.839	9.62
08:00 - 09:00	1.344	0	2.703	18.889	19.355	16.667	19.355	18.817	18.333	3.448	7.778	4.839	8.784
09:00 - 10:00	1.613	0	4.955	18.333	20.968	17.778	25.806	15.054	18.889	3.161	9.444	4.839	9.459
10:00 - 11:00	2.419	0	5.856	23.333	19.355	17.222	30.645	17.742	19.444	4.598	8.889	4.032	10.264
11:00 - 12:00	3.226	0	5.405	23.889	19.355	17.778	34.409	22.581	23.333	4.598	6.944	4.032	10.907
12:00 - 13:00	2.957	0	4.505	17.222	22.581	21.667	26.344	25.269	22.778	6.609	5.833	5.914	10.811
13:00 - 14:00	2.688	0	3.153	13.333	27.957	21.667	37.097	25.806	21.667	7.759	6.389	7.796	11.808
14:00 - 15:00	0.538	0	0.45	17.222	27.957	22.778	39.247	27.957	26.111	8.621	9.722	9.14	12.806
15:00 - 16:00	0.538	0	0	20.556	25.806	29.444	41.398	33.333	24.444	8.621	10	8.065	13.481
16:00 - 17:00	0	0	0	18.333	25.806	37.222	46.774	36.559	22.778	7.759	10	8.065	14.06
17:00 - 18:00	1.075	0	0	17.778	26.344	34.444	48.925	34.409	25.556	7.977	9.167	6.72	13.95
18:00 - 19:00	1.613	0	0	20.556	26.344	38.333	51.613	38.71	27.222	9.322	10.833	5.108	15.061
19:00 - 20:00	0.806	0	0	27.222	25.269	39.444	49.462	41.935	28.333	9.04	11.944	6.452	15.735
20:00 - 21:00	1.344	0	0	31.111	27.419	41.111	46.237	39.247	32.222	8.475	10.833	8.065	16.121
21:00 - 22:00	1.613	0	0	30.556	31.183	37.222	48.925	36.022	27.778	9.04	9.722	6.989	15.639
22:00 - 23:00	1.613	0	0	29.444	31.183	31.111	46.237	36.022	24.444	8.475	6.944	6.989	14.483
23:00 - 24:00	1.613	0	0	16.667	26.344	25	47.312	31.72	23.333	9.605	8.056	6.989	13.102

Figure 11-2 - Anemometer U2 Post-QC diurnal data recovery rates (%) by month

Hour	Jan	Feb	Mar	Apr	May	Jun	Jul	Aug	Sep	Oct	Nov	Dec	All
00:00 - 01:00	0	0	3.153	47.222	40.323	36.111	31.183	36.559	40	41.667	33.611	5.914	23.102
01:00 - 02:00	0	0	4.505	42.778	37.097	39.444	33.333	32.258	49.444	40.23	33.889	3.763	22.973
02:00 - 03:00	0	0	3.153	41.111	43.011	36.667	35.484	34.946	42.222	41.379	35.278	3.763	23.134
03:00 - 04:00	0	0	7.207	43.889	44.624	45	44.624	40.323	42.222	41.379	34.167	5.108	25.064
04:00 - 05:00	0	0	6.306	52.222	39.247	48.889	52.688	53.226	47.222	45.402	34.167	4.57	27.317
05:00 - 06:00	0	0	6.306	54.444	40.86	51.667	51.613	53.763	43.333	44.253	36.111	4.839	27.574
06:00 - 07:00	0	0	4.955	53.889	44.624	50	53.226	58.602	40.556	43.966	35.833	4.839	27.735
07:00 - 08:00	0	0	3.153	52.222	40.86	49.444	47.312	57.527	37.778	45.69	34.167	2.957	26.448
08:00 - 09:00	0	0	3.604	52.222	44.086	52.222	47.849	59.677	38.333	47.414	39.722	2.957	27.864
09:00 - 10:00	0	0	5.856	50	41.398	51.667	40.323	53.763	41.667	49.713	39.444	2.957	27.317
10:00 - 11:00	0	0	6.306	52.222	37.634	49.444	36.022	50	36.667	43.966	35.556	2.151	25.161
11:00 - 12:00	0	0	8.108	46.111	41.935	53.333	33.871	52.688	37.222	42.529	35.556	4.032	25.547
12:00 - 13:00	0	0	5.405	42.222	43.011	44.444	40.86	48.387	30.556	41.379	34.167	1.882	23.906
13:00 - 14:00	0	0	3.604	45	45.161	48.889	34.409	50.538	36.667	41.092	37.222	1.882	24.743
14:00 - 15:00	0	0	6.306	41.111	46.237	41.111	34.409	47.849	32.778	43.966	37.5	2.957	24.421
15:00 - 16:00	0	0	4.955	47.778	45.161	37.778	34.946	44.624	38.889	40.517	37.778	2.151	24.196
16:00 - 17:00	0	0	6.306	43.333	40.86	32.222	31.183	39.247	28.889	39.08	37.5	1.613	22.072
17:00 - 18:00	0	0	6.757	44.444	40.323	28.889	29.57	38.172	32.222	38.746	35	2.419	21.761
18:00 - 19:00	0	0	4.505	39.444	40.86	29.444	23.656	37.097	35	43.22	35.278	2.688	21.708
19:00 - 20:00	0	0	5.856	37.222	43.548	31.111	25.806	34.946	31.111	38.983	34.444	2.151	21.066
20:00 - 21:00	0	0	14.414	43.889	38.71	23.889	25.269	36.559	23.889	46.893	31.389	3.226	21.676
21:00 - 22:00	0	0	13.514	43.889	32.258	27.778	25.269	38.71	30.556	48.023	32.778	3.763	22.319
22:00 - 23:00	0	0	7.658	41.111	38.71	28.333	25.806	39.785	32.222	45.763	36.944	4.839	22.704
23:00 - 24:00	0	0	4.054	41.667	43.548	30	24.194	47.312	36.111	43.503	37.222	4.839	23.218

Figure 11-3 - Anemometer U3 Post-QC diurnal data recovery rates (%) by month

Hour	Jan	Feb	Mar	Apr	May	Jun	Jul	Aug	Sep	Oct	Nov	Dec	All
00:00 - 01:00	0	0	4.505	43.889	43.011	48.889	67.742	45.161	41.111	17.816	24.722	1.613	22.458
01:00 - 02:00	0	0	9.009	46.667	41.935	56.111	65.591	53.226	45.556	19.253	24.722	0.269	23.906
02:00 - 03:00	0	0	10.36	50.556	40.86	53.333	59.14	46.774	41.667	18.391	24.722	0	22.876
03:00 - 04:00	0	0	8.559	39.444	35.484	47.222	55.914	49.462	47.778	22.126	22.778	1.344	22.104
04:00 - 05:00	0	0	8.559	39.444	36.022	38.333	45.699	47.312	47.222	18.966	22.222	1.613	20.463
05:00 - 06:00	0	0	3.604	40.556	38.172	33.333	47.849	42.473	46.111	15.805	21.389	1.613	19.337
06:00 - 07:00	0	0	4.955	38.889	33.871	27.222	42.473	41.398	47.778	16.954	25	1.075	18.919
07:00 - 08:00	0	0	6.306	34.444	36.559	32.222	50	43.011	41.667	14.368	22.5	1.613	18.887
08:00 - 09:00	0	0	7.207	36.667	37.097	35	53.763	37.097	43.889	13.793	21.944	1.613	19.144
09:00 - 10:00	0	0	8.559	38.889	36.022	40	59.677	32.258	42.778	13.506	20	1.613	19.337
10:00 - 11:00	0	0	3.604	40.556	34.946	41.667	64.516	36.559	49.444	13.218	21.111	1.613	20.142
11:00 - 12:00	0	0	2.252	41.667	34.946	45	70.968	38.172	47.778	12.644	21.944	3.226	20.914
12:00 - 13:00	0	0	1.802	50.556	31.183	51.111	62.903	40.86	52.222	14.655	23.333	3.226	21.847
13:00 - 14:00	0	0	3.604	48.889	44.624	52.222	69.355	38.172	59.444	11.494	19.444	2.151	22.458
14:00 - 15:00	0	0	3.153	47.778	44.086	53.333	63.978	41.935	52.222	13.218	18.333	4.301	22.201
15:00 - 16:00	0	0	3.153	53.333	47.312	55	64.516	52.151	55.556	15.805	20.278	3.763	24.099
16:00 - 17:00	0	0	3.604	55	45.699	58.889	66.667	60.215	64.444	16.379	20.833	3.226	25.547
17:00 - 18:00	0	0	4.054	55	43.548	63.333	67.742	60.215	63.889	18.519	21.389	2.688	25.972
18:00 - 19:00	0	0	2.703	54.444	38.172	59.444	69.892	61.29	61.111	20.621	21.944	1.344	25.466
19:00 - 20:00	0	0	3.604	59.444	46.774	62.778	71.505	55.914	56.667	23.729	21.667	1.613	26.397
20:00 - 21:00	0	0	3.604	53.333	50	67.778	66.667	52.151	64.444	21.469	23.611	1.613	26.429
21:00 - 22:00	0	0	6.306	55	49.462	64.444	69.355	47.849	58.889	16.102	23.333	1.344	25.401
22:00 - 23:00	0	0	5.856	52.778	45.161	64.444	66.667	47.312	52.778	18.079	21.111	0	24.245
23:00 - 24:00	0	0	8.559	55	44.086	53.333	68.817	43.011	41.111	19.774	24.444	0	23.635

Figure 11-4 - Anemometer U4 Post-QC diurnal data recovery rates (%) by month

Hour	Jan	Feb	Mar	Apr	May	Jun	Jul	Aug	Sep	Oct	Nov	Dec	All
00:00 - 01:00	44.355	37.5	76.126	93.333	96.774	93.889	100	92.473	87.222	90.805	95	61.29	76.512
01:00 - 02:00	43.817	35.119	77.928	93.889	93.548	96.667	100	95.161	89.444	86.207	91.944	60.215	75.611
02:00 - 03:00	43.548	33.036	78.829	96.667	91.935	96.667	100	91.398	91.111	86.494	91.111	59.946	75.257
03:00 - 04:00	40.591	37.5	81.081	96.667	90.323	95	100	91.935	93.333	89.655	88.333	59.677	75.515
04:00 - 05:00	40.054	41.071	76.577	98.889	90.323	91.667	100	93.548	93.333	93.103	90.556	56.452	75.804
05:00 - 06:00	40.591	40.774	72.973	100	90.323	90	100	92.473	91.111	91.954	91.111	59.409	75.644
06:00 - 07:00	42.473	39.286	74.775	100	90.323	90	100	93.548	90	92.529	92.778	62.634	76.48
07:00 - 08:00	43.548	39.286	75.225	100	90.323	90	100	93.548	90	95.402	94.722	62.634	77.188
08:00 - 09:00	42.473	38.69	75.676	100	90.323	90	97.849	90.86	90	96.552	95.556	61.29	76.802
09:00 - 10:00	42.204	35.119	77.928	100	89.785	93.333	96.774	87.634	86.667	95.69	95.278	59.409	75.901
10:00 - 11:00	41.129	35.714	74.324	100	87.097	93.333	96.774	87.097	88.889	94.253	94.167	58.065	75.064
11:00 - 12:00	40.591	37.5	72.973	100	93.548	93.333	96.774	87.634	86.667	94.54	93.333	60.484	75.611
12:00 - 13:00	43.548	41.667	72.072	100	96.774	93.333	96.774	87.097	86.667	94.54	93.889	61.828	76.737
13:00 - 14:00	43.548	41.071	75.225	99.444	100	96.667	96.774	89.785	87.222	91.092	93.889	59.409	76.77
14:00 - 15:00	42.742	41.071	77.928	96.667	100	93.333	92.473	91.398	88.889	92.241	93.333	60.753	76.673
15:00 - 16:00	41.935	40.179	81.081	100	100	93.333	94.624	93.548	91.111	90.23	93.333	59.14	76.866
16:00 - 17:00	42.742	38.095	77.477	100	100	93.333	96.774	93.548	90	88.793	93.333	60.484	76.544
17:00 - 18:00	42.742	33.333	75.676	100	100	93.333	96.774	91.935	90	90.028	92.5	60.753	75.892
18:00 - 19:00	41.667	36.607	77.027	100	100	93.333	96.774	91.398	91.667	93.22	92.5	62.903	76.911
19:00 - 20:00	41.129	39.286	78.378	100	100	96.111	97.312	93.548	90	92.09	92.5	61.022	77.103
20:00 - 21:00	40.323	41.071	80.631	100	100	96.667	96.774	93.548	92.222	92.655	94.444	58.333	77.457
21:00 - 22:00	41.398	39.583	81.081	99.444	98.387	96.667	96.774	96.774	93.333	95.763	96.111	59.677	78.292
22:00 - 23:00	43.817	37.5	78.378	96.667	96.774	96.667	96.774	96.774	88.333	96.61	93.333	58.871	77.296
23:00 - 24:00	46.237	36.607	77.928	93.889	96.774	93.889	97.312	96.774	83.889	93.22	95	57.258	76.525

Figure 11-5 - Vane D1 Post-QC diurnal data recovery rates (%), by month

11.1.2 Derived Variables (data to 2013-Dec-12)

Hour	Jan	Feb	Mar	Apr	May	Jun	Jul	Aug	Sep	Oct	Nov	Dec	All
00:00 - 01:00	28.226	28.869	58.108	77.222	75.806	84.444	90.86	84.409	74.444	39.655	35	31.989	51.673
01:00 - 02:00	29.032	29.167	57.658	73.889	75.269	82.778	81.72	83.871	73.889	40.517	30.556	31.989	50.418
02:00 - 03:00	29.032	28.274	58.559	76.111	75.269	83.889	89.247	78.495	74.444	37.644	30.833	30.914	50.322
03:00 - 04:00	28.495	29.167	54.955	71.667	68.817	81.667	97.312	80.645	74.444	40.517	32.778	28.763	50.225
04:00 - 05:00	30.108	32.143	55.856	69.444	72.581	76.667	91.935	89.785	70.556	45.115	32.778	30.376	51.319
05:00 - 06:00	31.989	30.06	55.405	67.778	78.495	75.556	87.634	88.172	60.556	45.402	31.667	31.183	50.547
06:00 - 07:00	31.72	29.167	55.856	67.778	80.108	66.111	95.699	86.022	61.667	46.264	32.778	33.065	50.869
07:00 - 08:00	34.409	30.357	52.252	72.778	78.495	61.111	92.473	82.796	61.667	42.816	30	31.183	49.646
08:00 - 09:00	35.484	30.06	46.396	80	74.731	66.667	86.022	76.882	66.667	40.805	27.778	30.645	48.842
09:00 - 10:00	33.871	30.357	49.55	81.111	77.957	65.556	82.796	76.882	70	41.092	32.222	27.688	49.292
10:00 - 11:00	32.527	31.548	46.396	85.556	75.269	68.333	88.172	77.957	68.333	43.391	33.611	25.538	49.743
11:00 - 12:00	34.14	31.845	50.45	88.889	80.645	68.889	88.71	83.333	70.556	41.667	32.5	27.419	51.19
12:00 - 13:00	34.14	32.143	54.955	85	83.333	65	87.634	77.419	72.222	42.816	32.5	26.075	50.901
13:00 - 14:00	34.946	33.631	61.261	85.556	86.559	70.556	87.097	77.419	72.778	44.54	33.056	29.57	52.831
14:00 - 15:00	33.602	31.548	61.261	86.111	85.484	71.111	84.409	84.946	75	45.977	34.444	30.914	53.346
15:00 - 16:00	32.258	31.845	64.414	94.444	88.172	73.889	87.097	84.409	66.667	45.115	35.556	30.108	53.829
16:00 - 17:00	31.72	29.762	63.514	93.333	88.71	78.889	86.022	80.645	64.444	44.253	38.056	31.452	53.668
17:00 - 18:00	33.333	26.19	64.414	90	86.559	81.111	88.172	79.032	65.556	42.735	35.278	28.763	52.62
18:00 - 19:00	32.796	25	63.063	91.667	86.559	85.556	94.086	82.258	72.778	44.915	32.778	30.108	53.757
19:00 - 20:00	28.495	26.488	53.153	91.111	87.097	83.889	90.323	81.183	71.667	42.938	33.611	31.183	52.248
20:00 - 21:00	30.108	29.464	51.802	92.778	82.796	78.333	87.634	79.57	72.778	41.243	31.111	31.183	51.509
21:00 - 22:00	32.258	27.976	55.856	91.111	86.559	83.333	88.172	85.484	77.778	38.418	28.611	28.763	52.087
22:00 - 23:00	30.376	28.571	52.252	90	89.247	82.222	86.022	89.247	71.667	38.983	28.056	30.108	51.606
23:00 - 24:00	29.301	28.274	56.757	78.889	91.398	77.778	86.022	86.559	70	40.395	33.889	30.108	51.574

Figure 11-6 - Derived variable UT diurnal calculable rates (%) by month

Hour	Jan	Feb	Mar	Apr	May	Jun	Jul	Aug	Sep	Oct	Nov	Dec	All
00:00 - 01:00	0	0	7.207	83.333	76.882	82.222	96.237	81.72	78.889	55.747	54.722	7.258	43.372
01:00 - 02:00	0	0	10.36	84.444	76.344	87.778	94.624	84.946	85.556	57.184	53.056	3.763	43.983
02:00 - 03:00	0	0	11.261	85	78.495	86.667	91.935	78.495	82.222	58.046	57.222	3.763	43.983
03:00 - 04:00	0	0	13.964	81.111	77.419	85.556	93.011	83.871	87.222	59.195	52.778	6.452	44.434
04:00 - 05:00	0	0	13.514	83.889	72.581	77.778	91.935	92.473	88.889	61.207	53.611	6.183	44.659
05:00 - 06:00	0	0	9.91	88.333	75.269	80	93.011	90.323	79.444	59.483	53.333	6.452	44.144
06:00 - 07:00	0	0	8.559	89.444	76.344	72.222	93.011	91.398	80.556	58.621	56.111	5.376	43.951
07:00 - 08:00	0	0	9.459	83.333	75.269	78.333	95.699	91.935	75	56.322	54.167	4.57	43.243
08:00 - 09:00	0	0	9.91	82.222	77.957	80	93.548	87.097	73.333	58.908	56.667	3.495	43.404
09:00 - 10:00	0	0	11.261	81.667	73.118	84.444	91.398	80.108	78.333	58.908	56.944	4.032	43.275
10:00 - 11:00	0	0	7.207	86.111	70.43	85	94.086	82.258	77.222	54.31	56.389	3.226	42.664
11:00 - 12:00	0	0	9.009	83.333	71.505	86.111	96.774	87.634	75	52.011	55.833	5.645	43.082
12:00 - 13:00	0	0	7.207	88.889	69.892	86.667	96.237	83.871	73.889	53.736	55.833	4.839	42.986
13:00 - 14:00	0	0	6.757	83.333	82.796	91.667	95.161	86.559	81.667	50.862	55	4.032	43.726
14:00 - 15:00	0	0	6.757	81.111	84.409	87.222	91.398	89.247	77.222	54.598	54.722	7.258	43.887
15:00 - 16:00	0	0	5.856	89.444	82.258	87.222	92.473	92.473	81.111	53.448	56.389	5.914	44.562
16:00 - 17:00	0	0	6.757	90	82.258	86.667	93.548	91.935	81.111	50	57.5	4.839	44.273
17:00 - 18:00	0	0	7.658	90	80.108	86.667	93.011	90.323	83.889	52.422	55.556	4.57	44.262
18:00 - 19:00	0	0	4.955	83.333	76.344	84.444	91.935	90.323	83.889	59.322	56.667	3.495	44.059
19:00 - 20:00	0	0	7.207	87.222	86.022	83.889	93.548	88.172	78.333	55.367	55.278	3.763	44.059
20:00 - 21:00	0	0	14.414	87.778	84.409	86.667	88.172	84.409	83.889	60.734	54.444	4.839	45.087
21:00 - 22:00	0	0	14.414	91.667	76.882	85.556	94.086	84.946	81.667	61.864	55.278	5.108	45.311
22:00 - 23:00	0	0	11.712	88.889	82.258	86.111	91.935	85.484	77.222	61.864	55.556	4.839	44.958
23:00 - 24:00	0	0	11.261	84.444	81.72	81.667	89.785	89.247	75	61.299	57.222	4.839	44.477

Figure 11-7 - Derived variable UB diurnal calculable rates (%) by month

11.2 Wind Roses - Validated Sensor Data

11.2.1 Frequency of Wind Occurrence by Sector, and Month (data to 2013-Dec-12)

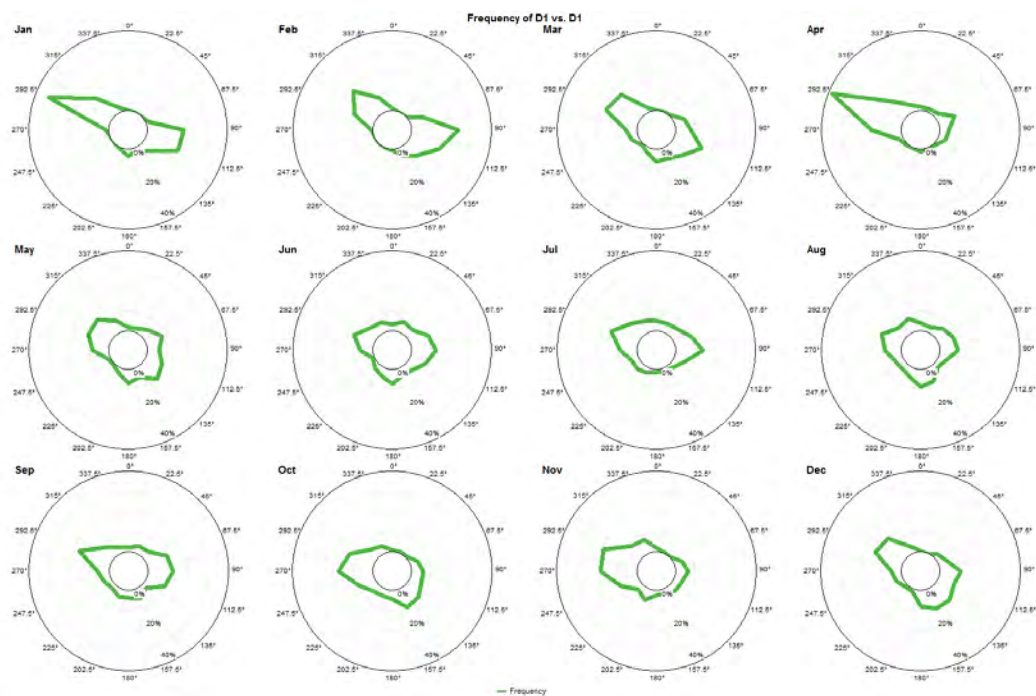


Figure 11-8

11.2.2 Frequency of Wind Occurrence by Sector, and Hour (data to 2013-Dec-12)

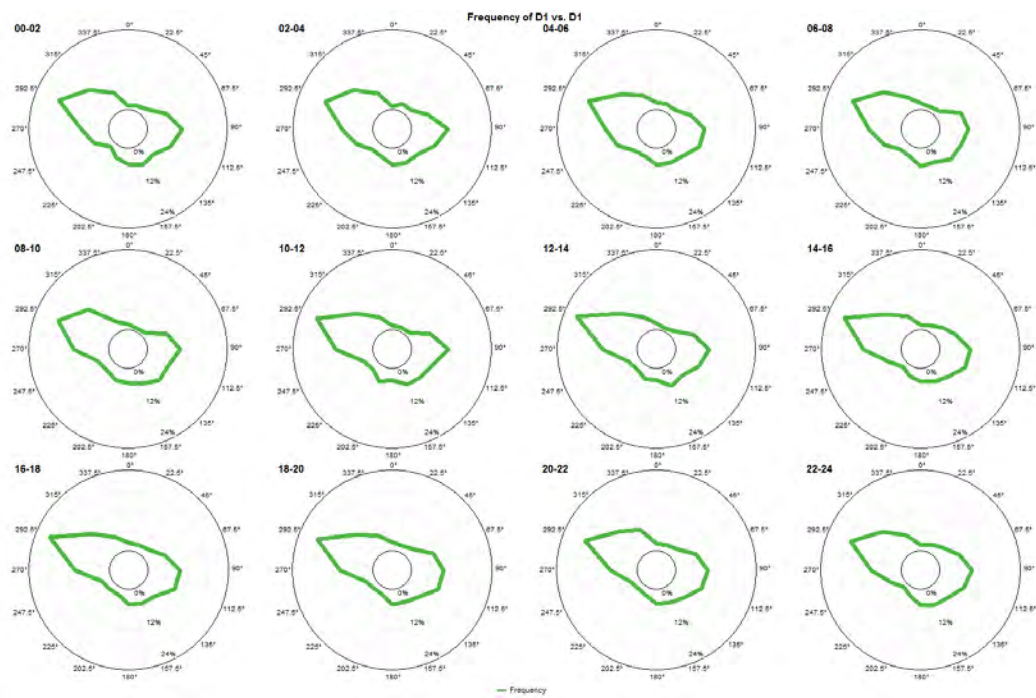


Figure 11-9

11.2.3 Frequency of Wind Occurrence by Sector, Month, and Hour (data to 2013-Dec-12)

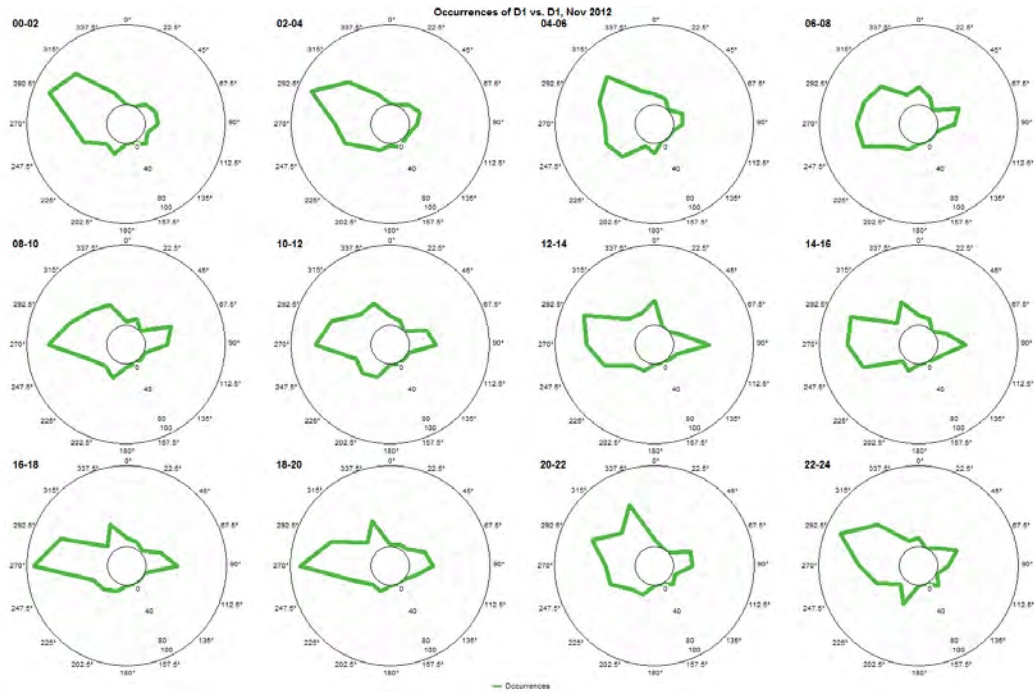


Figure 11-10 - 2012-Nov

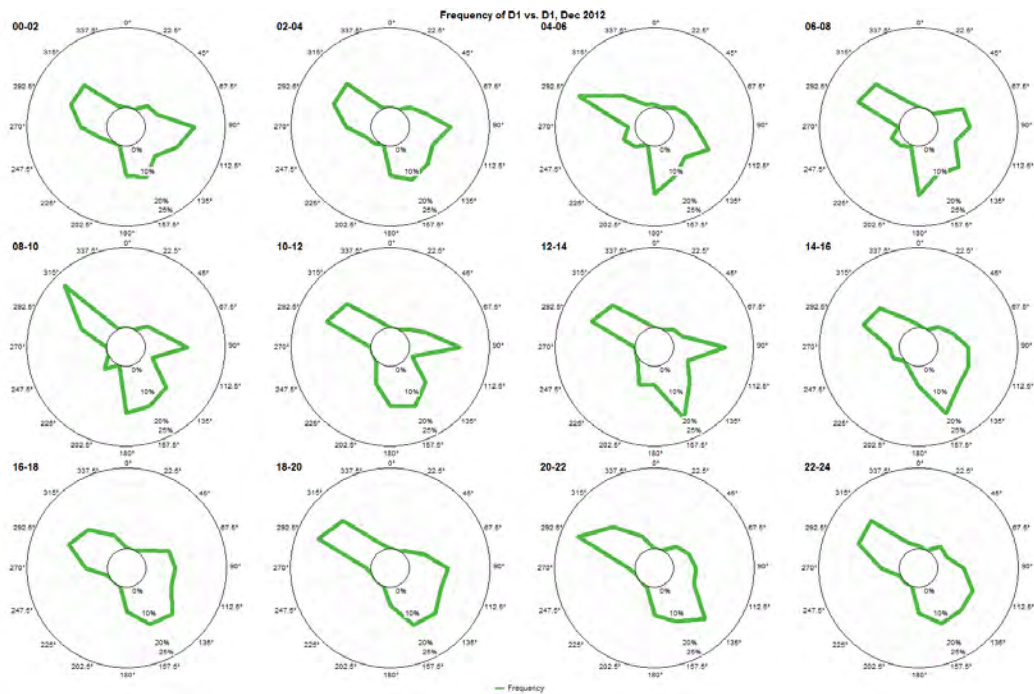


Figure 11-11 – 2012-Dec

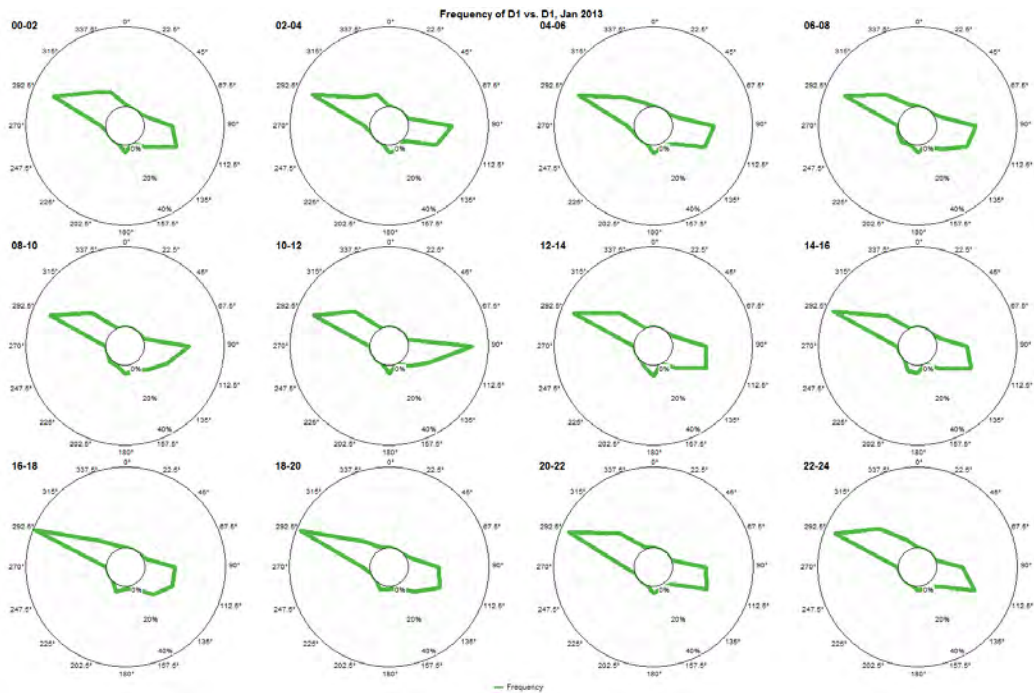


Figure 11-12 – 2013-Jan

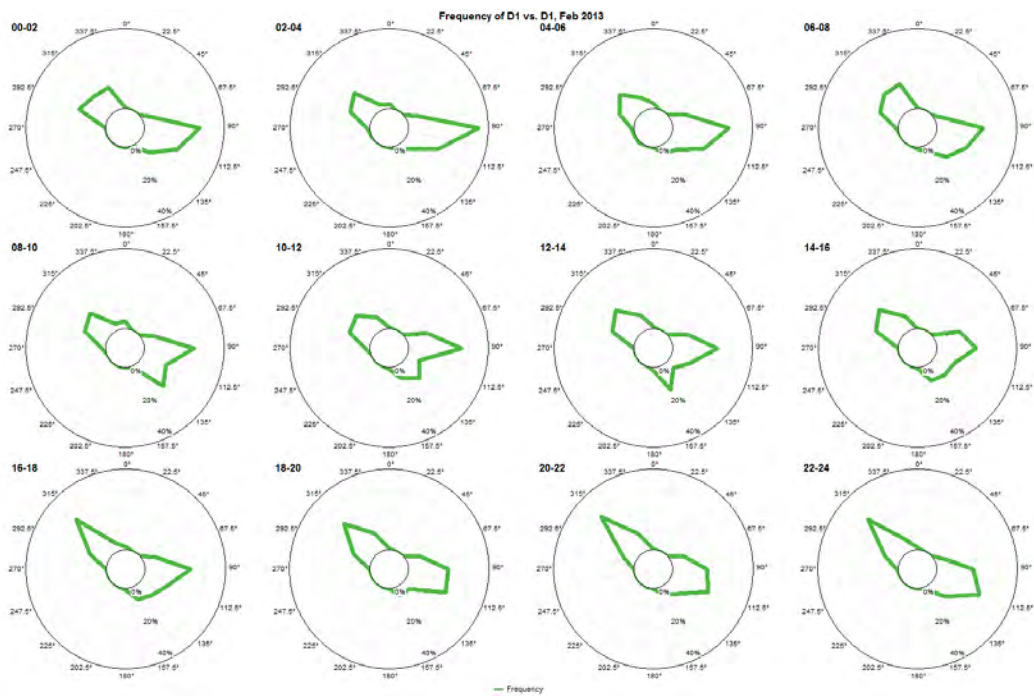


Figure 11-13 – 2013-Feb

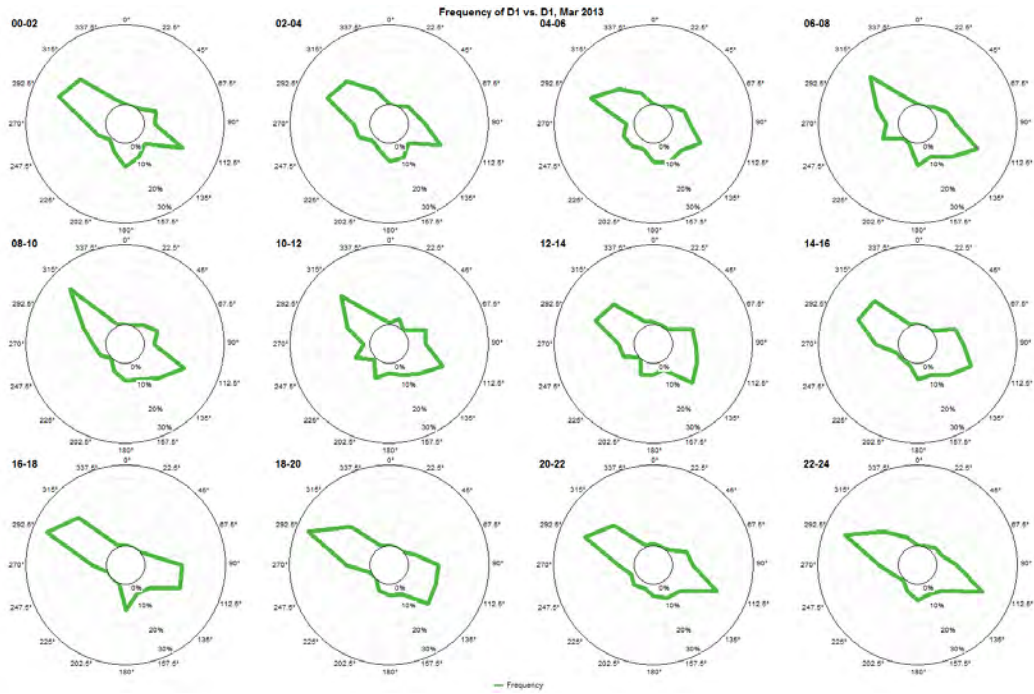


Figure 11-14 – 2013-Mar

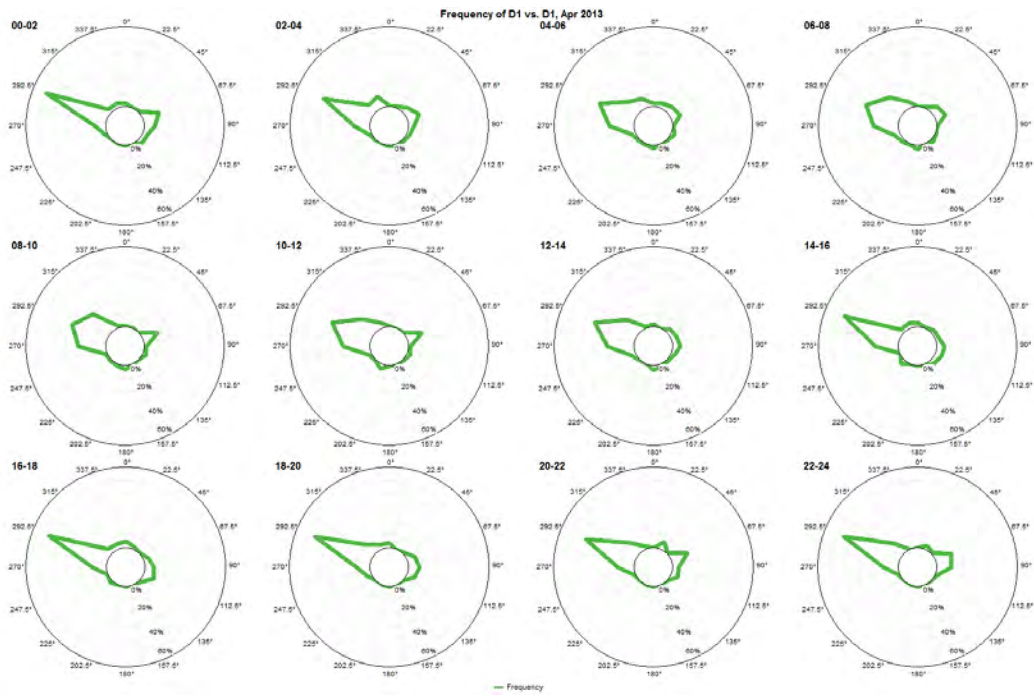


Figure 11-15 - 2013-Apr

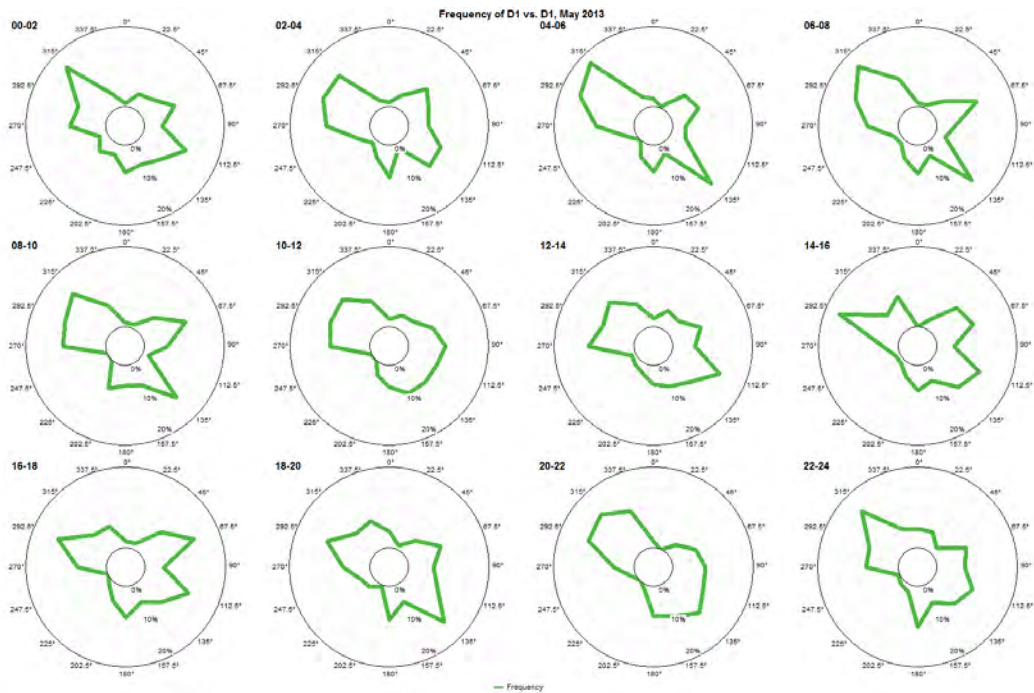


Figure 11-16 – 2013-May

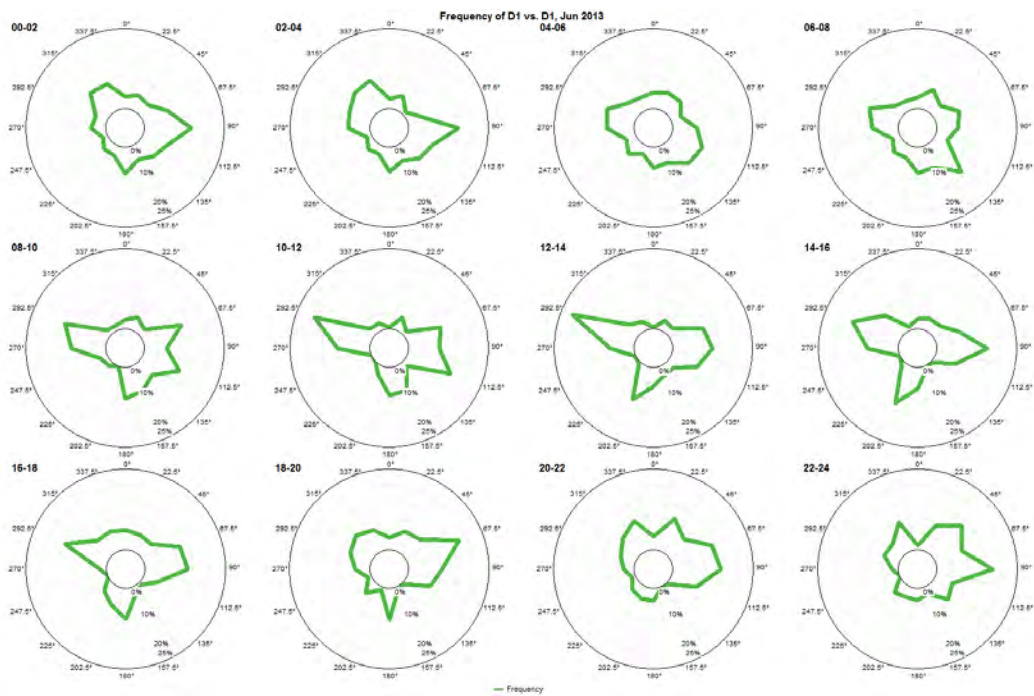


Figure 11-17 – 2013-Jun

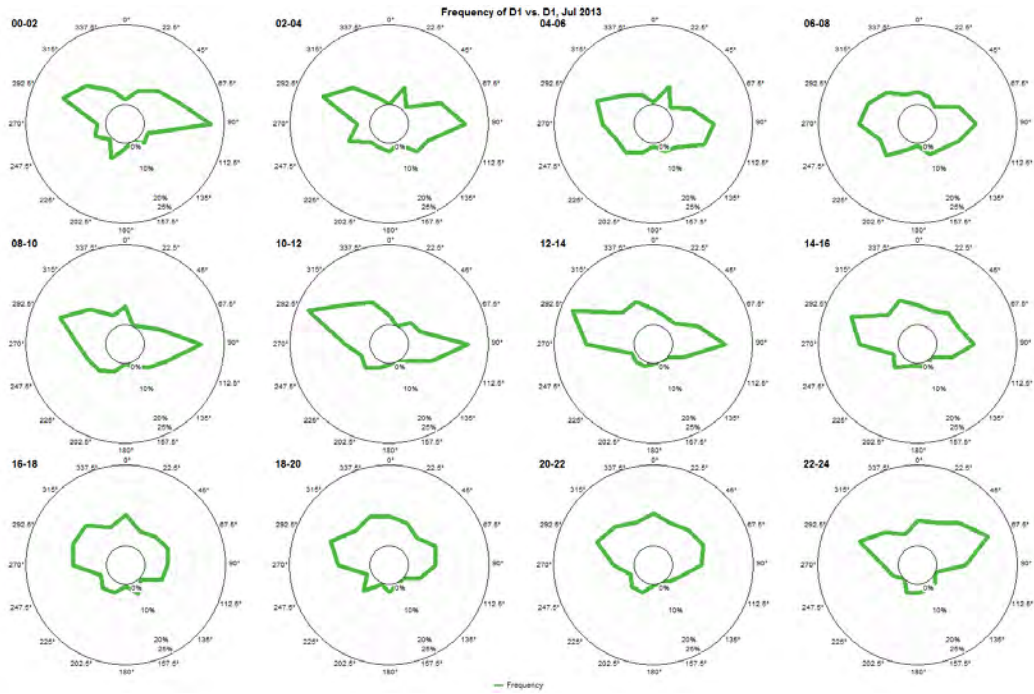


Figure 11-18 – 2013-Jul

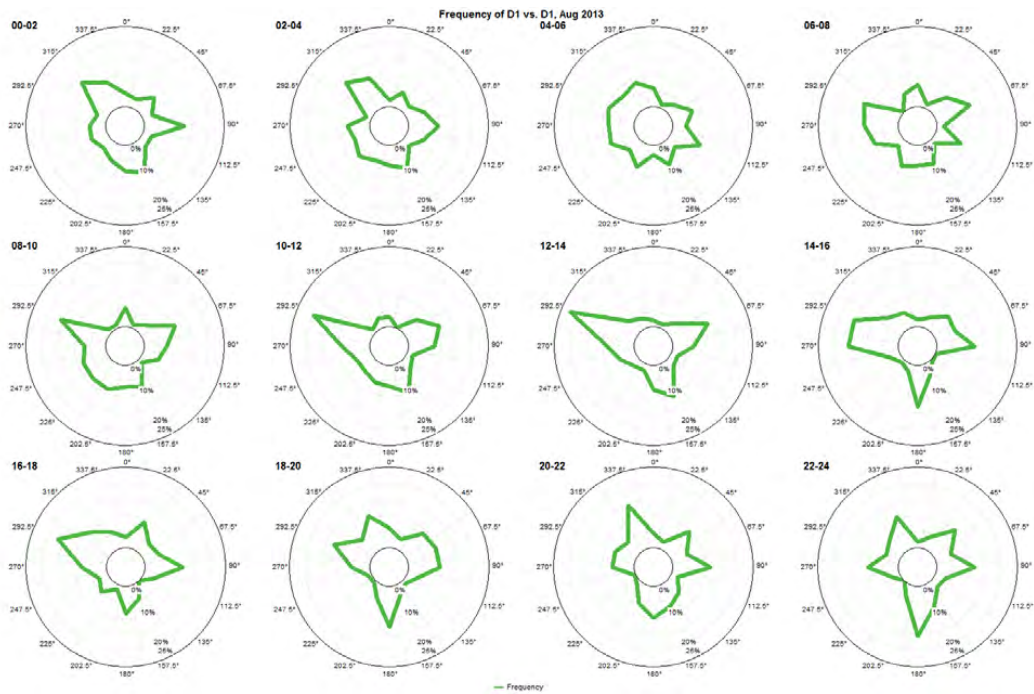


Figure 11-19 – 2013-Aug

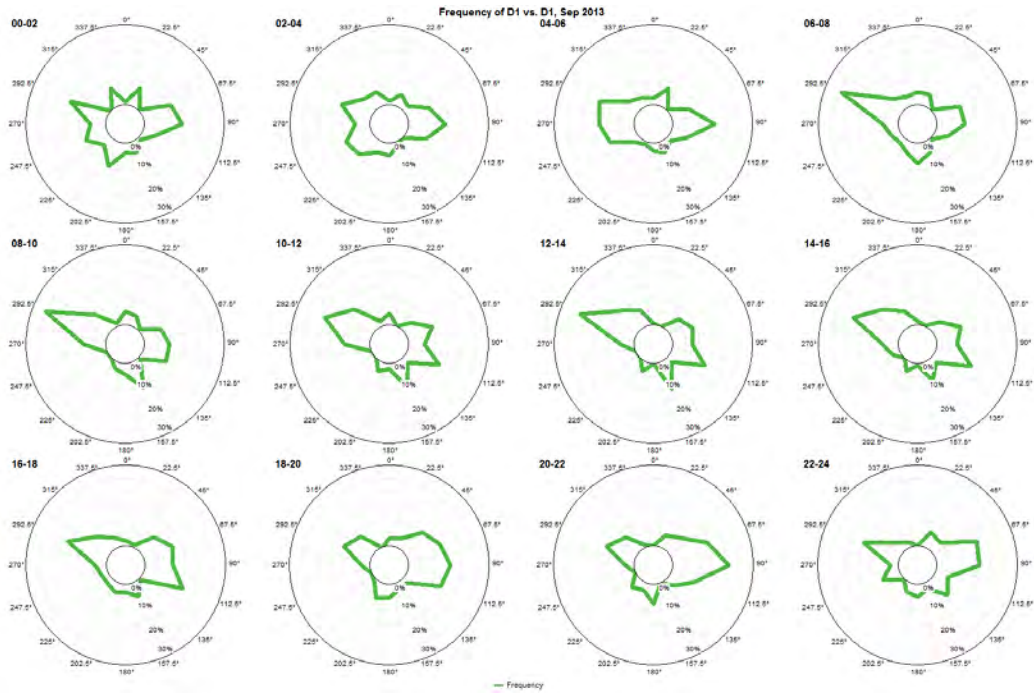


Figure 11-20 – 2013-Sep

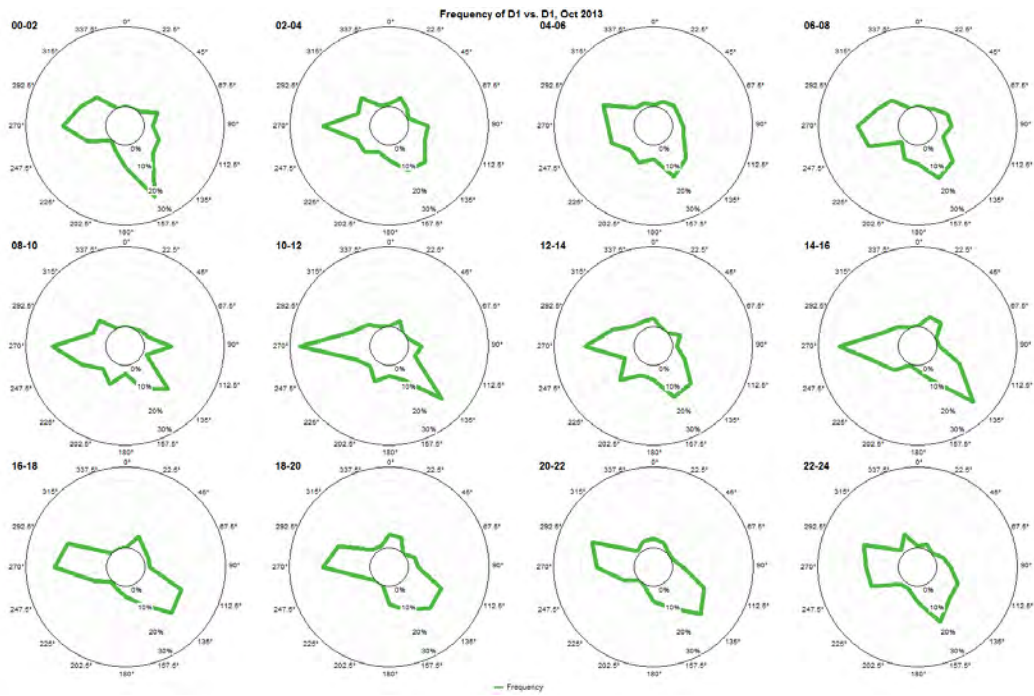


Figure 11-21 – 2013-Oct

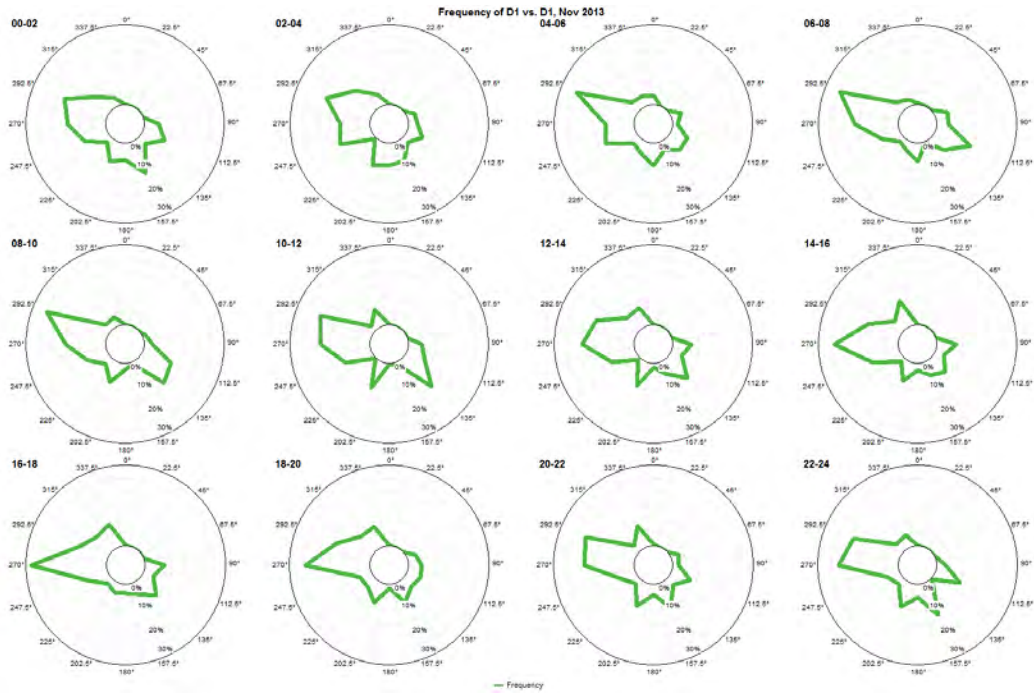


Figure 11-22 – 2013-Nov

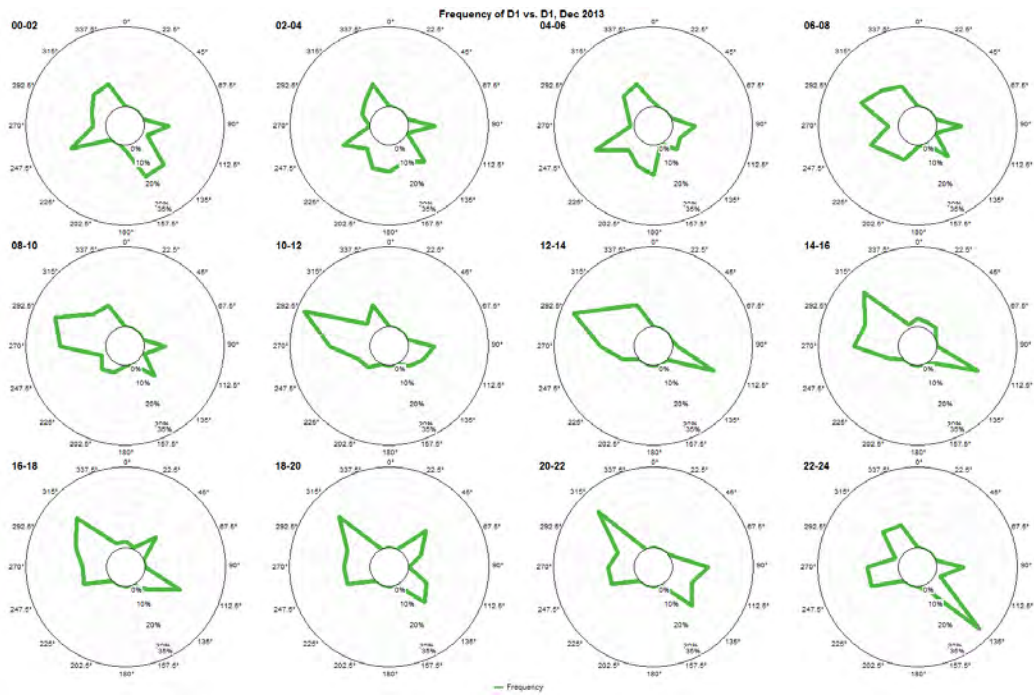


Figure 11-23 – 2013-Dec

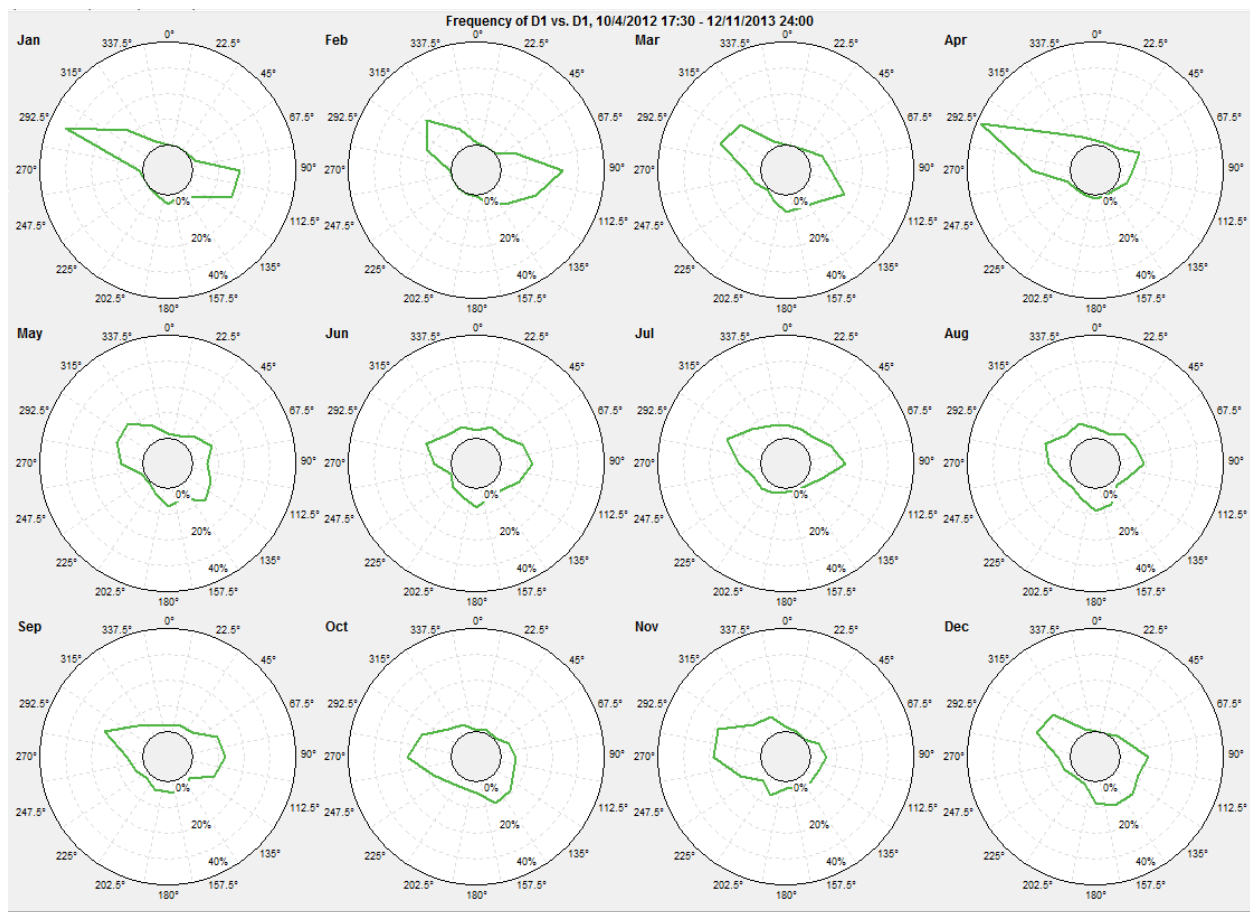


Figure 11-24 - Monthly wind frequency roses

11.3 Wind Shear: The Physical Sensors

11.3.1 Shear: South-Southwest-Oriented Sensors U1 & U3

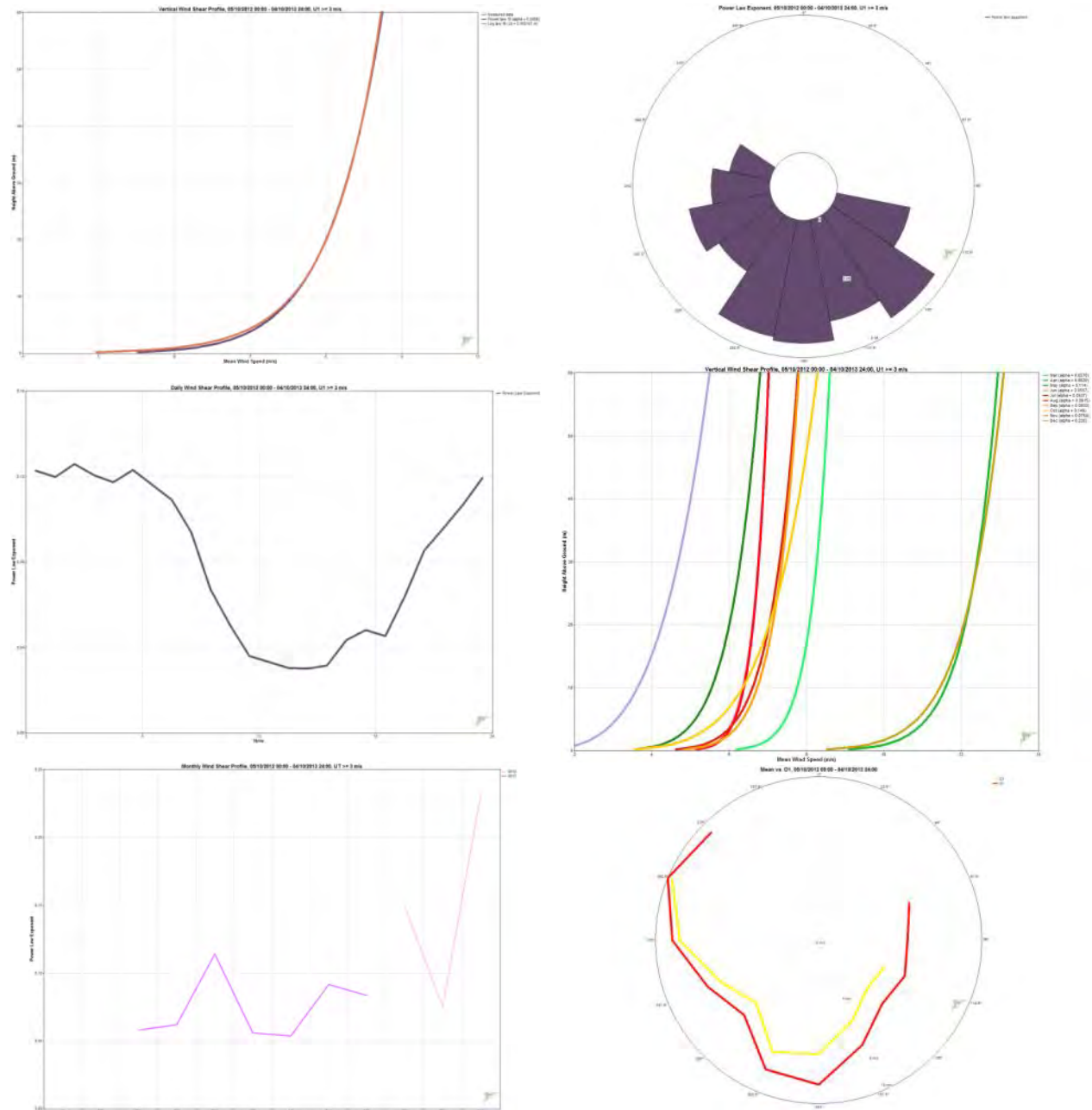
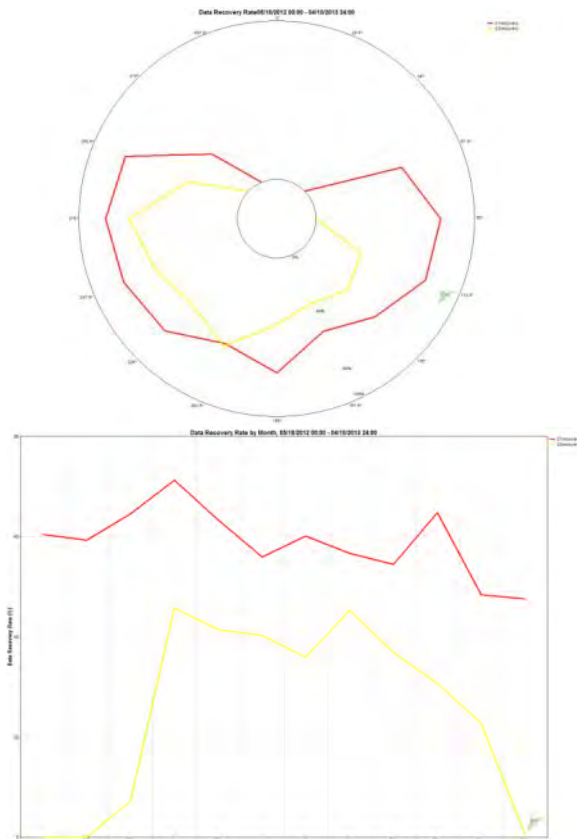


Figure 11-25 - Characteristic shear charts, where $U1 > 3\text{m/s}$
 $\alpha = 0.081$, $z_0 = 0.00011$

Top: wind speed profile to 60 m; shear exponent by sector;
 Middle: diurnal shear exponent profile; monthly wind speed profiles;
 Bottom: monthly shear exponent; $U1$, $U3$ wind speed roses



Direction Sector	Time Steps	Power Law Exp
348.75° - 11.25°	0	
11.25° - 33.75°	0	
33.75° - 56.25°	0	
56.25° - 78.75°	0	
78.75° - 101.25°	0	
101.25° - 123.75°	1,158	0.088
123.75° - 146.25°	911	0.145
146.25° - 168.75°	501	0.121
168.75° - 191.25°	996	0.143
191.25° - 213.75°	580	0.139
213.75° - 236.25°	542	0.08
236.25° - 258.75°	856	0.097
258.75° - 281.25°	2,594	0.069
281.25° - 303.75°	3,056	0.049
303.75° - 326.25°	0	
326.25° - 348.75°	0	
	11194	

Month	Time Steps	Power Law Exp
Jan	0	
Feb	0	
Mar	260	0.058
Apr	1,705	0.062
May	1,559	0.114
Jun	1,385	0.056
Jul	1,399	0.054
Aug	1,741	0.091
Sep	1,189	0.083
Oct	1,040	0.149
Nov	911	0.075
Dec	5	0.232
	11194	

Figure 11-26- U1 and U3 recovery rates and shear exponent calculable occurrences, by sector and month, where U1 > 3 m/s

	Jan	Feb	Mar	Apr	May	Jun	Jul	Aug	Sep	Oct	Nov	Dec	
U1	0	0	260	1,705	1,559	1,385	1,399	1,741	1,189	1,040	911	5	11194
U3			7,986	12,615	6,478	6,858	6,863	7,48	7,532	7,769	12,686	4,972	
Power Law Exp			0.058	0.062	0.114	0.056	0.054	0.091	0.083	0.149	0.075	0.232	
													All
00:00 - 01:00			0.064	0.07	0.11	0.154	0.107	0.199	0.114	0.175	0.129		0.123
01:00 - 02:00			0.054	0.082	0.125	0.165	0.108	0.165	0.108	0.164	0.1		0.12
02:00 - 03:00			0.025	0.087	0.144	0.202	0.112	0.15	0.109	0.164	0.091		0.126
03:00 - 04:00			0.181	0.086	0.133	0.14	0.109	0.12	0.121	0.198	0.096		0.121
04:00 - 05:00			0.214	0.083	0.148	0.133	0.121	0.136	0.096	0.163	0.074		0.117
05:00 - 06:00			0.282	0.079	0.152	0.119	0.146	0.155	0.122	0.156	0.072		0.123
06:00 - 07:00			0.122	0.071	0.18	0.093	0.124	0.153	0.113	0.16	0.061		0.116
07:00 - 08:00			0.121	0.062	0.173	0.055	0.081	0.159	0.108	0.157	0.092		0.109
08:00 - 09:00			0.077	0.053	0.199	0.008	0.025	0.141	0.121	0.172	0.072		0.094
09:00 - 10:00			-0.034	0.061	0.131	-0.01	0.019	0.062	0.093	0.156	0.061		0.067
10:00 - 11:00			-0.086	0.073	0.076	-0.024	-0.002	0.017	0.059	0.149	0.077		0.05
11:00 - 12:00			0.019	0.056	0.055	-0.033	-0.001	0.007	0.037	0.107	0.066		0.036
12:00 - 13:00			-0.018	0.052	0.047	-0.025	-0.001	0.009	0.014	0.113	0.066		0.033
13:00 - 14:00			-0.053	0.047	0.032	-0.023	-0.008	0.007	0.011	0.126	0.076		0.03
14:00 - 15:00			0.057	0.024	0.04	-0.025	-0.005	0.014	0.002	0.117	0.082		0.03
15:00 - 16:00			0.09	0.021	0.028	-0.016	-0.01	0.016	0.037	0.096	0.086		0.031
16:00 - 17:00			0.062	0.043	0.075	-0.01	-0.011	0.019	0.013	0.113	0.071		0.043
17:00 - 18:00			0.046	0.05	0.129	-0.012	0.001	0.024	0.009	0.132	0.052		0.048
18:00 - 19:00			0.035	0.059	0.108	-0.012	-0.003	0.021	0.038	0.137	0.032		0.045
19:00 - 20:00			0.078	0.065	0.102	0	0.009	0.05	0.084	0.178	0.047		0.064
20:00 - 21:00			0.043	0.064	0.143	0.033	0.019	0.115	0.117	0.164	0.082		0.085
21:00 - 22:00			0.107	0.069	0.118	0.092	0.041	0.132	0.135	0.154	0.08	0.181	0.096
22:00 - 23:00			-0.025	0.069	0.15	0.135	0.091	0.164	0.112	0.147	0.08	0.316	0.107
23:00 - 24:00			0.042	0.07	0.155	0.169	0.081	0.173	0.129	0.159	0.08	0.154	0.12

Figure 11-27 - Heat chart of shear exponent by month and hour of day, where U1 > 3 m/s

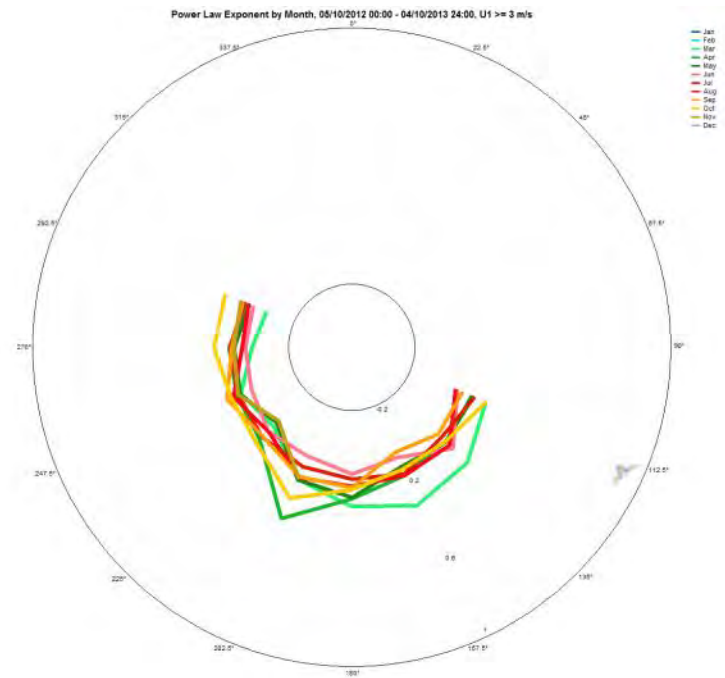


Figure 11-28 - Shear exponent by month and sector, where $U_1 > 3$ m/s

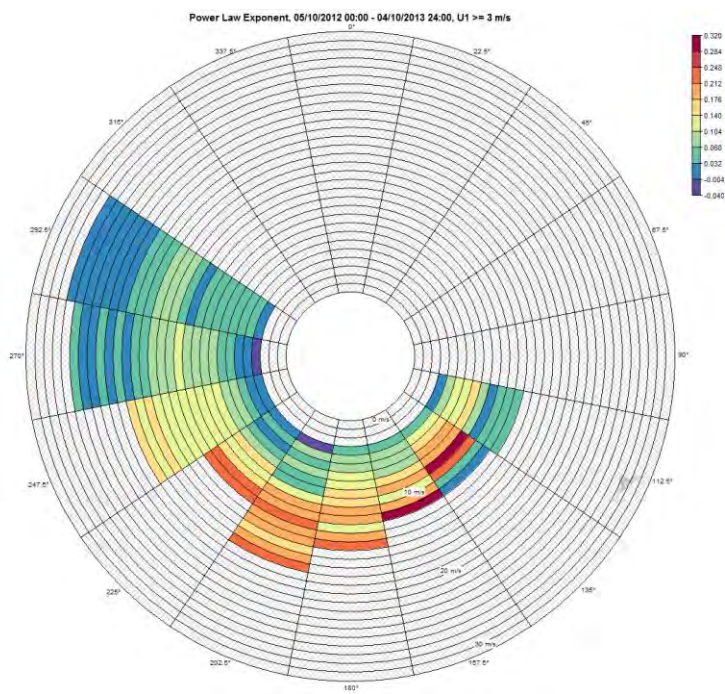
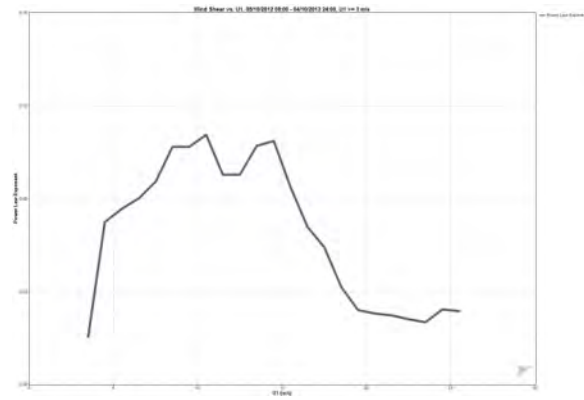
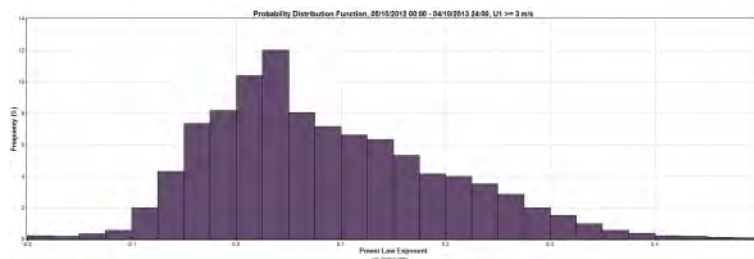


Figure 11-29 - Shear exponent (colour) by sector and U_1 wind speed bin, where $U_1 > 3$ m/s



11-30 - Shear exponent by U1, where U1 > 3 m/s



11-31 - Shearexponent frequency distribution, where U1 > 3 m/s

11.3.2 Shear:North-Northeast-Oriented Sensors U2 & U4

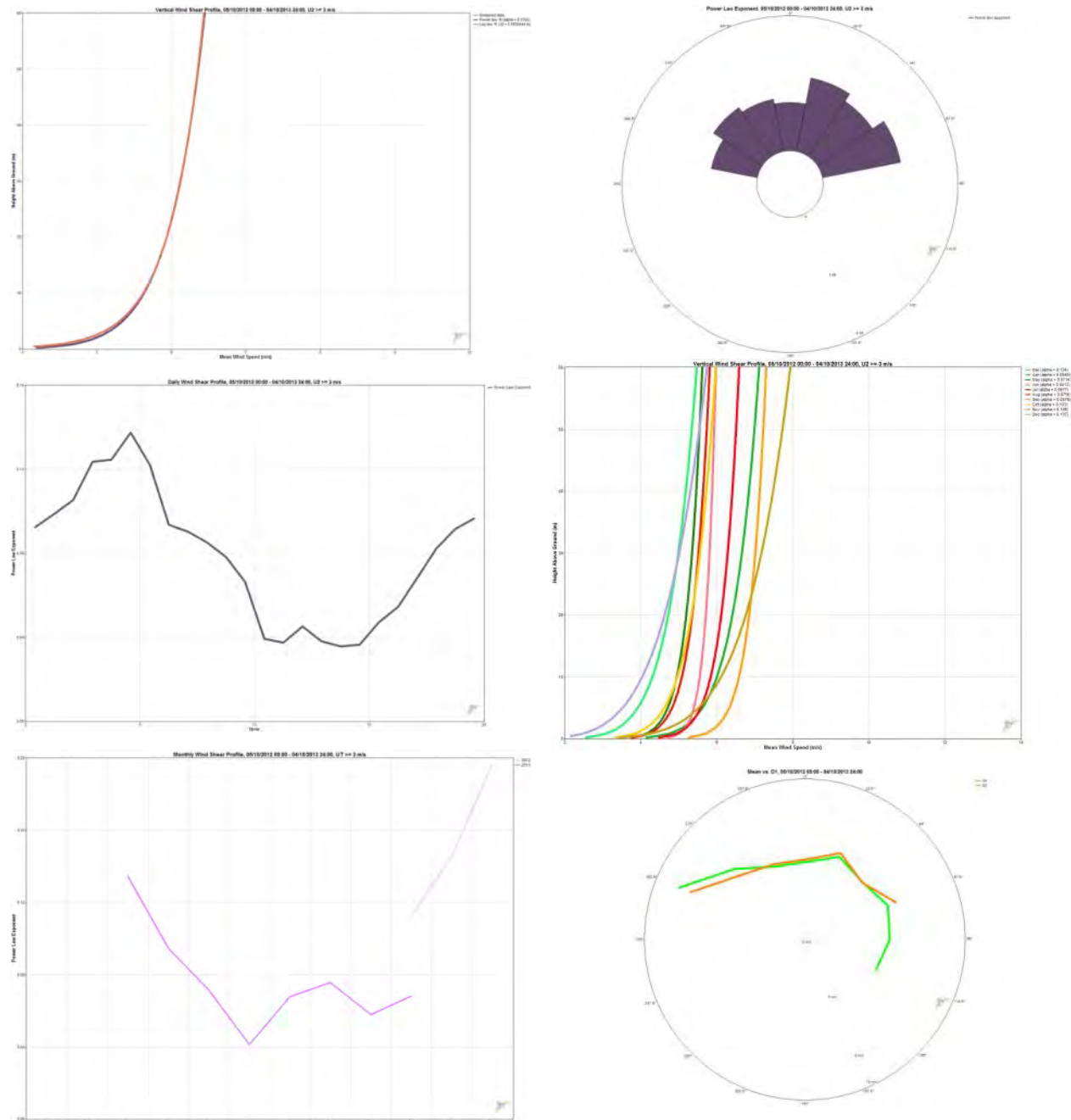
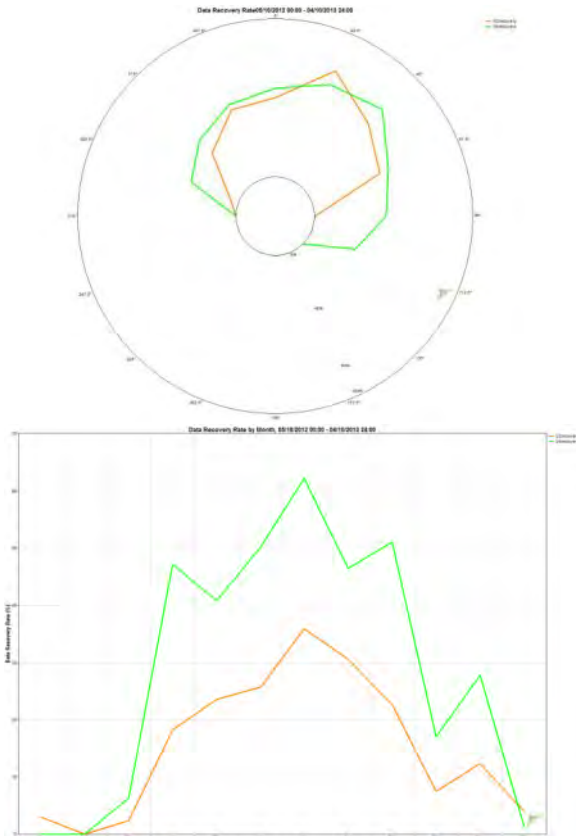


Figure 11-32 - Characteristic shear charts, where $U2 > 3 \text{ m/s}$

$$\alpha = 0.0755, z_0 = 0.00004$$

Top: wind speed profile to 60 m; shear exponent by sector;
 Middle: diurnal shear exponent profile; monthly wind speed profiles;
 Bottom: monthly shear exponent; $U2$, $U4$ wind speed roses



Direction Sector		Power Law Exp
348.75° - 11.25°	489	0.058
11.25° - 33.75°	766	0.089
33.75° - 56.25°	724	0.079
56.25° - 78.75°	1,429	0.095
78.75° - 101.25°	0	
101.25° - 123.75°	0	
123.75° - 146.25°	0	
146.25° - 168.75°	0	
168.75° - 191.25°	0	
191.25° - 213.75°	0	
213.75° - 236.25°	0	
236.25° - 258.75°	0	
258.75° - 281.25°	0	
281.25° - 303.75°	493	0.056
303.75° - 326.25°	1,407	0.07
326.25° - 348.75°	1,167	0.063
	6475	

Month	Time Steps	Power Law Exp
Jan	0	
Feb	0	
Mar	51	0.134
Apr	525	0.095
May	813	0.071
Jun	884	0.041
Jul	1,429	0.068
Aug	1,170	0.076
Sep	858	0.058
Oct	245	0.103
Nov	494	0.146
Dec	6	0.197
	6475	

Figure 11-33 - U2 and U4 recovery rates and shear exponent calculable occurrences, by sector and month, where U2 > 3 m/s

	Jan	Feb	Mar	Apr	May	Jun	Jul	Aug	Sep	Oct	Nov	Dec	
	0	0	51	525	813	884	1,429	1,170	858	245	494	6	6475
U2			5.166	6.843	5.45	5.876	6.404	5.63	7.121	5.711	7.452	5.275	
U4			4.602	6.308	5.126	5.671	6.042	5.276	6.775	5.226	6.574	4.453	
Power Law Exp			0.134	0.095	0.071	0.041	0.068	0.076	0.058	0.103	0.146	0.197	
													All
00:00 - 01:00			0.068	0.072	0.055	0.014	0.126	0.133	0.083	0.111	0.096		0.092
01:00 - 02:00			0.289	0.06	0.064	0.066	0.123	0.12	0.063	0.135	0.119		0.099
02:00 - 03:00			0.21	0.153	0.095	0.053	0.118	0.102	0.086	0.133	0.139		0.105
03:00 - 04:00			0.337	0.169	0.205	0.072	0.101	0.137	0.073	0.239	0.134		0.123
04:00 - 05:00			0.226	0.184	0.123	0.058	0.085	0.152	0.081	0.168	0.194		0.125
05:00 - 06:00			0.198	0.214	0.13	0.124	0.087	0.138	0.095	0.039	0.231	0.204	0.137
06:00 - 07:00			0.109	0.272	0.096	0.06	0.098	0.115	0.09	0.081	0.193		0.122
07:00 - 08:00			0.113	0.2	0.064	0.107	0.066	0.095	0.091	0.151	0.099		0.093
08:00 - 09:00			0.131	0.252	0.094	0.047	0.043	0.045	0.071	0.186	0.105		0.09
09:00 - 10:00			0.204	0.172	0.106	0.024	0.036	0.014	0.063	0.204	0.136		0.085
10:00 - 11:00			0.061	0.167	0.119	0.021	0.038	0.018	0.06	0.035	0.138		0.078
11:00 - 12:00			0.108	0.135	0.114	0.018	0.037	0.027	0.043	0.097	0.191		0.066
12:00 - 13:00			-0.168	0.136	0.072	0.018	0.028	0.016	0.033	0.052	0.063		0.039
13:00 - 14:00			-0.185	0.059	0.068	0.027	0.024	0.035	0.006	0.051	0.14		0.037
14:00 - 15:00				0.052	0.049	0.027	0.037	0.03	0.009	0.071	0.136		0.045
15:00 - 16:00				0.05	0.021	0.025	0.021	0.027	0.016	0.066	0.15		0.038
16:00 - 17:00				0.042	0.006	0.024	0.032	0.033	0.011	0.059	0.178		0.036
17:00 - 18:00				0.022	0.015	0.026	0.033	0.036	0.026	0.069	0.139		0.036
18:00 - 19:00				0.034	0.031	0.026	0.048	0.047	0.036	0.106	0.129		0.047
19:00 - 20:00				0.04	0.033	0.03	0.047	0.048	0.063	0.109	0.21		0.054
20:00 - 21:00				0.04	0.059	0.039	0.061	0.076	0.073	0.105	0.17		0.068
21:00 - 22:00				0.047	0.074	0.068	0.089	0.105	0.079	0.133	0.109		0.082
22:00 - 23:00				0.054	0.064	0.083	0.115	0.116	0.078	0.126	0.14		0.092
23:00 - 24:00				0.029	0.06	0.064	0.121	0.111	0.1	0.135	0.143		0.097

Figure 11-34 - Heat chart of shear exponent by month and hour of day, where U2 > 3 m/s

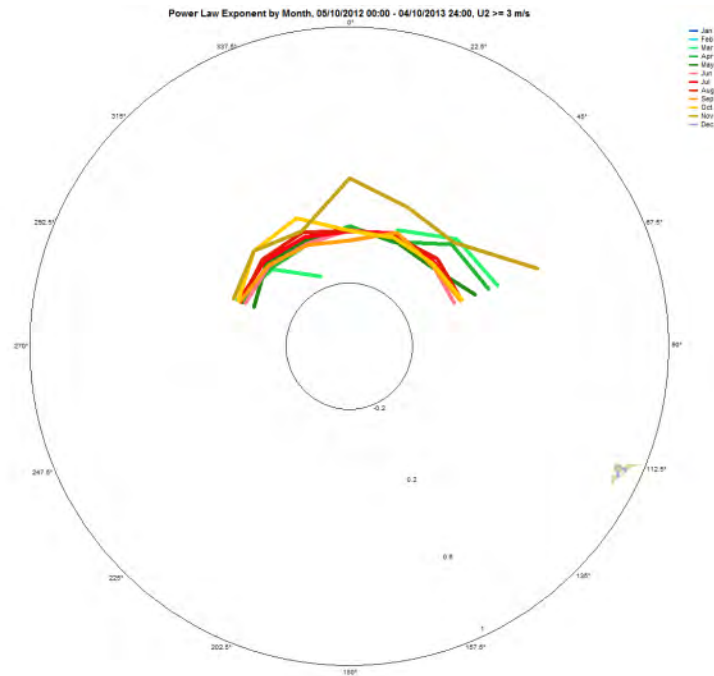


Figure 11-35 - Shear exponent by month and sector, where $U_2 > 3$ m/s

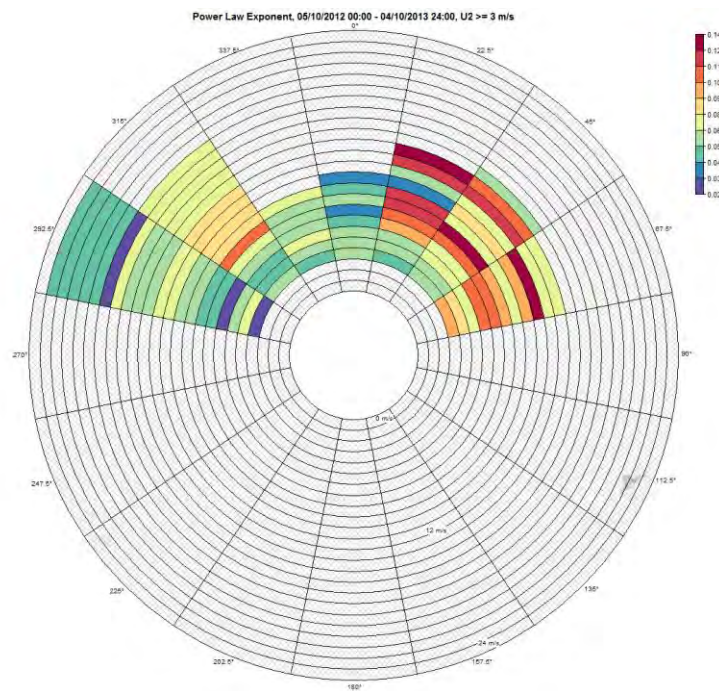


Figure 11-36 - Shear exponent by month and sector, where $U_2 > 3$ m/s

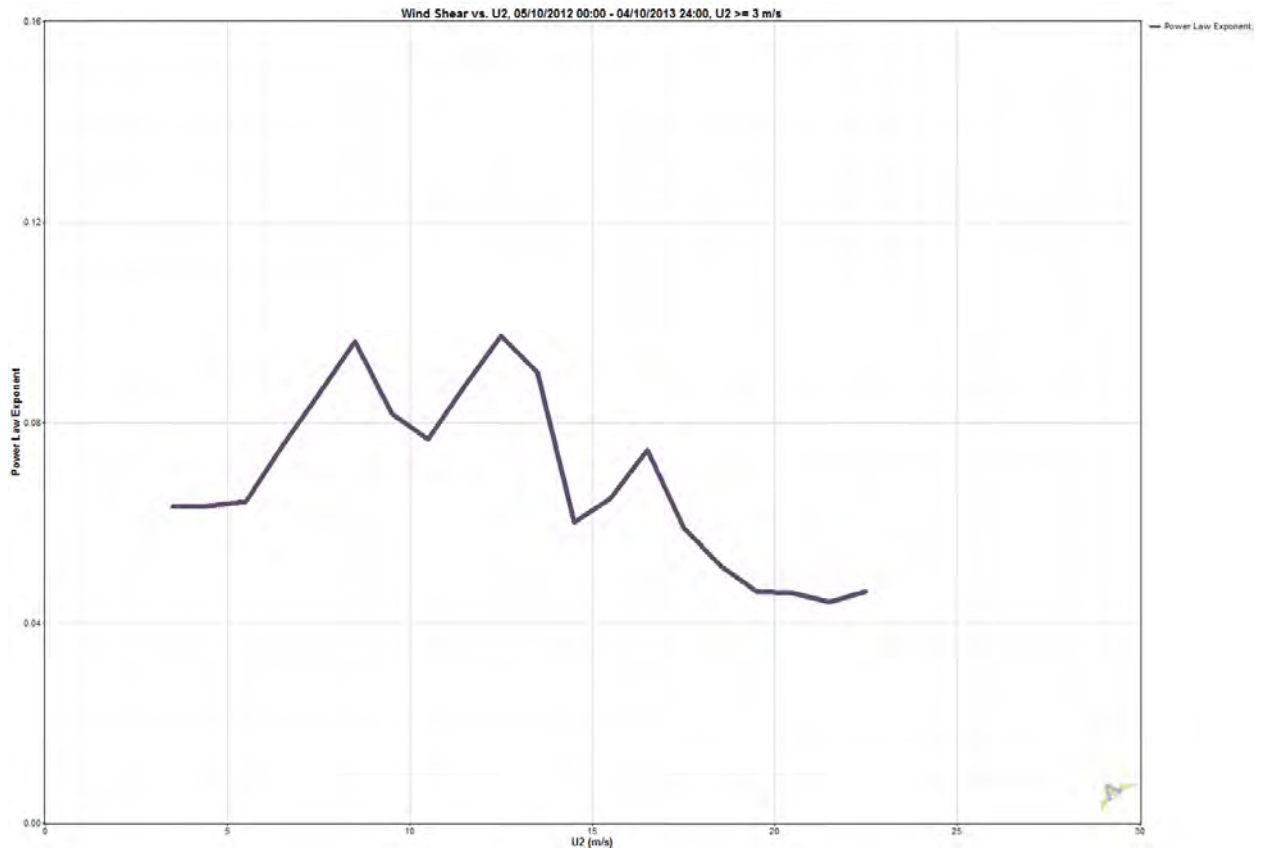


Figure 11-37 - Shear exponent by U2, where U2 \geq 3 m/s

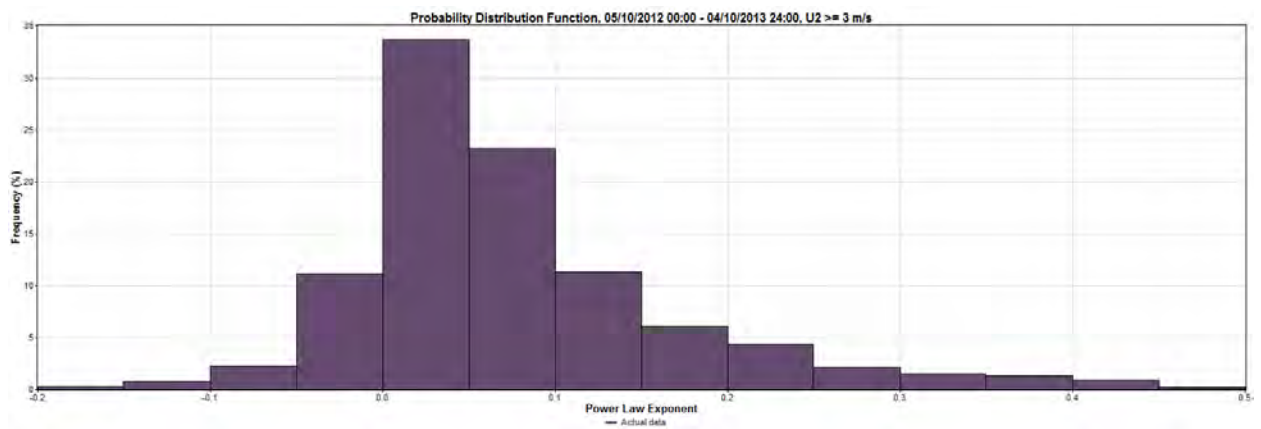


Figure 11-38 - Shear exponent frequency distribution, where U2 \geq 3 m/s

11.4 Measure-Correlate-Predict Data

	Forced				Unforced		
	Time Steps	Best-fit Intercept (m/s)	Slope	R2	Time Steps	Slope	R2
315° - 45°	587	2.211	1.198	0.809	587	1.481	0.747
45° - 135°	1,195	4.733	0.6	0.134	1,195	1.877	-0.653
135° - 225°	1,139	4.851	0.774	0.295	1,139	1.637	-0.201
225° - 315°	2,963	2.627	1.305	0.723	2,963	1.687	0.639
All	5,884			0.529	5,884		0.225
1 hour							
315° - 45°	166	2.266	1.196	0.841	166	1.483	0.776
45° - 135°	381	4.418	0.685	0.163	381	1.89	-0.461
135° - 225°	392	4.784	0.85	0.32	392	1.74	-0.145
225° - 315°	1,045	2.175	1.386	0.78	1,045	1.711	0.722
All	1,984			0.576	1,984		0.328
3 hours							
315° - 45°	81	2.208	1.203	0.869	81	1.462	0.818
45° - 135°	232	4.409	0.72	0.18	232	1.904	-0.405
135° - 225°	263	5.152	0.782	0.271	263	1.756	-0.28
225° - 315°	715	2.152	1.397	0.784	715	1.712	0.732
All	1,291			0.576	1,291		0.327
4 hours							
315° - 45°	31	2.291	1.215	0.917	31	1.461	0.867
45° - 135°	108	5.188	0.583	0.108	108	2.012	-0.648
135° - 225°	139	4.556	0.88	0.331	139	1.769	-0.104
225° - 315°	349	1.908	1.45	0.812	349	1.733	0.773
All	627			0.589	627		0.338
8 hours							
315° - 45°	19	2.415	1.192	0.921	19	1.473	0.861
45° - 135°	61	3.793	0.935	0.286	61	1.973	-0.122
135° - 225°	83	5.299	0.807	0.311	83	1.835	-0.332
225° - 315°	239	1.962	1.448	0.84	239	1.746	0.795
All	402			0.65	402		0.426
12 hours							
315° - 45°	6	2.622	1.322	0.76	6	1.766	0.654
45° - 135°	24	4.099	0.84	0.162	24	2.002	-0.173
135° - 225°	50	4.395	0.84	0.305	50	1.819	-0.188
225° - 315°	108	1.954	1.464	0.866	108	1.764	0.823
All	188			0.63	188		0.429
24 hours							

Figure 11-39 - 4-sector linear least-squares correlation statistics for various correlation time steps, with both forced and unforced target intercepts

Sector	Data	Mean	Mean
	Points	Veer (°)	Direction (°)
345° - 15°	0	-2.779	-2.779
15° - 45°	0	-2.779	27.221
45° - 75°	188	13.003	73.003
75° - 105°	519	8.588	98.588
105° - 135°	488	3.614	123.614
135° - 165°	277	-4.860	145.140
165° - 195°	351	-17.361	162.639
195° - 225°	511	-13.057	196.943
225° - 255°	517	-1.298	238.702
255° - 285°	1,145	-2.117	267.883
285° - 315°	1,301	-4.631	295.369
315° - 345°	587	-3.042	326.958
All	5,884	-2.779	

Figure 11-40 - Direction correlation data; 1-hr comparison time-step, 12 sectors
 $R^2 = 0.777$

Sector	Data	Mean	Mean
	Points	Veer (°)	Direction (°)
345° - 15°	0	-2.779	-2.779
15° - 45°	0	-2.779	27.221
45° - 75°	188	13.003	73.003
75° - 105°	519	8.588	98.588
105° - 135°	488	3.614	123.614
135° - 165°	277	-4.860	145.140
165° - 195°	351	-17.361	162.639
195° - 225°	511	-13.057	196.943
225° - 255°	517	-1.298	238.702
255° - 285°	1,145	-2.117	267.883
285° - 315°	1,301	-4.631	295.369
315° - 345°	587	-3.042	326.958
All	5,884	-2.779	

Figure 11-41 - Direction correlation data; 3-hr comparison time-step, 4 sectors
 $R^2 = 0.799$

Sector	Data	Mean	Mean
	Points	Veer (°)	Direction (°)
315° - 45°	81	-4.817	-4.817
45° - 135°	232	6.502	96.502
135° - 225°	263	-13.643	166.357
225° - 315°	715	-1.640	268.360
All	1,291	-2.821	

Figure 11-42 - Direction correlation data; 4-hr comparison time-step, 4 sectors
 $R^2 = 0.861$